Investigating the roles of cytoplasmic proteins talin and kindlin3 in integrin LFA-1 activation

Li Yan Feng

School of Biological Sciences

A thesis submitted to Nanyang Technological University
in fulfilment of the requirement for the degree of
Doctor of Philosophy

2009

Investigating the roles of cytoplasmic proteins talin and kindlin3 in integrin LFA-1 activation

A Thesis for the Degree of Doctor of Philosophy

at Nanyang Technological University

Li Yan Feng

Supervised by Dr. Tan Suet Mien

School of Biological Sciences

Nanyang Technological University

Abstract

The integrin αLβ2 (LFA-1, CD11a/CD18) mediates leukocyte adhesion and migration that are required for a functional immune system. It is known that inside-out signaling triggers αLβ2 conformational changes, which affect its ligand-binding affinity. At least three αLβ2 affinity states (low, intermediate, and high) were described. Talin is a four-point-one ezrin radixin moesin (FERM)-domain containing cytoplasmic protein that connects αLβ2 to the actin filament. The talin head domain is also known to activate αLβ2 ligand binding. However, it remains to be determined whether talin promotes an intermediate or high affinity αLβ2. In the first part of this study using transfectants and T cells, we showed that talin induced an intermediate affinity αLβ2 that adhered constitutively to its ligand intercellular adhesion molecule (ICAM)-1 but not ICAM-3. Adhesion to ICAM-3 was induced when an additional exogenous activating agent was included. Similar profiles were observed with soluble ICAMs. In addition, the intermediate affinity αLβ2 induced by talin allowed adhesion and migration of T cells on immobilized ICAMs.

Kindlins are also FERM-domain containing proteins that have been reported to regulate integrin function. In the second part of this study, we showed that kindlin3 co-activates αLβ2 together with talin, and that its pleckstrin homology (PH) domain and F3 subdomain are required in the process. Interestingly, kindlin3-overexpressed T cells showed reduced migration on ICAM-1. Immunofluorescence staining suggest that kindlin3 and talin both localize at the leading edge of migratory T cells. It remains to be determined how kindlin3 reduces the migration of T cells. It would also be interesting to investigate at the molecular level the cooperativity of kindlin3 and talin in the regulation of αLβ2 function.

Acknowledgements

I wish to thank my supervisor Dr. Tan Suet Mien, not only for his patience and guidance, but also for providing me with an interesting project.

I am grateful to Prof. Law S.K.A., who provided us several integrin plasmids and monoclonal antibodies for the project.

I appreciate the help from Dr. Puan Kia Joo for providing us the peripheral blood T lymphocytes and T lymphoblasts.

I wish to thank my labmates Zhi Hong, Xiao Yan, Rhoda, Man Li, Ming Long, Cheng Ming, Feng Chen, Manisha, and Adeline for their helpful suggestions and assistance. Special thanks to Dr. Tang Ren Hong for his guidance at the beginning of my study. Without their support, my project would not be successful.

Finally, I am indebted to my parents, brother, and friends. They provided me selfless help and encouragement during the course of my Ph.D study.

Contents

Abbreviations

bp	base pair(s)
BSA	bovine serum albumin
CD	cluster of differentiation
cDNA	complementary DNA
C-terminal	carboxy terminal
DMSO	dimethyl sulphoxide
dNTP	deoxyribonucleotide triphosphate
DNA	deoxyribonucleic acid
DTT	dithiothreitol
E.coli	*Escherichia coli*
ECL	enhanced chemiluminescence
ECM	extracellular matrix
EDTA	ethylene-diamine-tetra acetic acid
EGTA	ethylene-glycol-bis (β-aminoethylether)-tetra acetic acid
EM	electron microscope
Fc	fragment crystallization (of Ig)
FACS	fluorescence activated cell sorter
FBS	fetal bovine serum
FERM	four-point-one ezrin radixin moesin
FITC	fluorescein isothiocyanate
FRET	fluorescence resonance energy transfer

HA	hemagglutinin
HEPES	N-[2-hydroxyethy] piperazine-N'-[2-ethanesulfonic acid]
HRP	horse radish peroxidase
ICAM	intercellular adhesion molecule
Ig	immunoglobulin
IP	immunoprecipitation
kDa	kilodaltons
I domain	inserted domain
I-EGF	integrin epidermal growth factor-like
Ig	immunoglobulin
mAb	monoclonal antibody
MCS	multi-cloning site
NMR	nuclear magnetic resonance
OD	optical density
PBS	phosphate buffered saline
PBTLs	peripheral blood T lymphocytes
PCR	polymerase chain reaction
PIP2	Phosphatidylinositol (4,5)-bisphosphate
PIP3	Phosphatidylinositol (3,4,5)-trisphosphate
PS	positive selection
PSI	plexins, semaphorins, and integrins
SDS-PAGE	sodium dodecyl sulphate polyacrylamide gel electrophoresis
TM	transmembrane domain

Tris	Tris (hydroxymethyl)-aminoethane
UV	ultraviolet
v/v	volume per volume
w/v	weight per volume
βTD	β tail domain

The single-letter and triplet codes for amino acid residues are used. Restriction enzymes are referred to by their three-letter names derived from that of the source microorganism. Other abbreviations are defined in the text where first encountered.

Chapter 1 Introduction

1.1 Overview

Integrins are a family of cell surface adhesion molecules that are also signaling receptors (Hynes, 2002; Luo et al., 2007; Wegener and Campbell, 2008). They transmit signals bidirectionally across the plasma membrane by undergoing extensive structural rearrangements. By regulating cell-cell and cell-matrix contacts, integrins participate in numerous biological processes including angiogenesis, inflammation, hemostasis, and cell fate determination (Springer and Wang, 2004; Streuli, 2009).

In humans, there are 18 different integrin α subunits and 8 different β subunits, forming 24 specific α/β integrin heterodimers (Hynes, 1992) (Fig. 1.1). Each integrin may have more than one ligand, and many integrins bind to common ligands (Plow et al., 2000; Springer, 1994) (Fig. 1.2). The major ligands for integrins are the extracellular matrix (ECM) proteins (fibronectin, collagen, and laminins) and the cell surface proteins intercellular adhesion molecules (ICAMs) and vascular cell-adhesion molecules (VCAMs) (Ley et al., 2007).

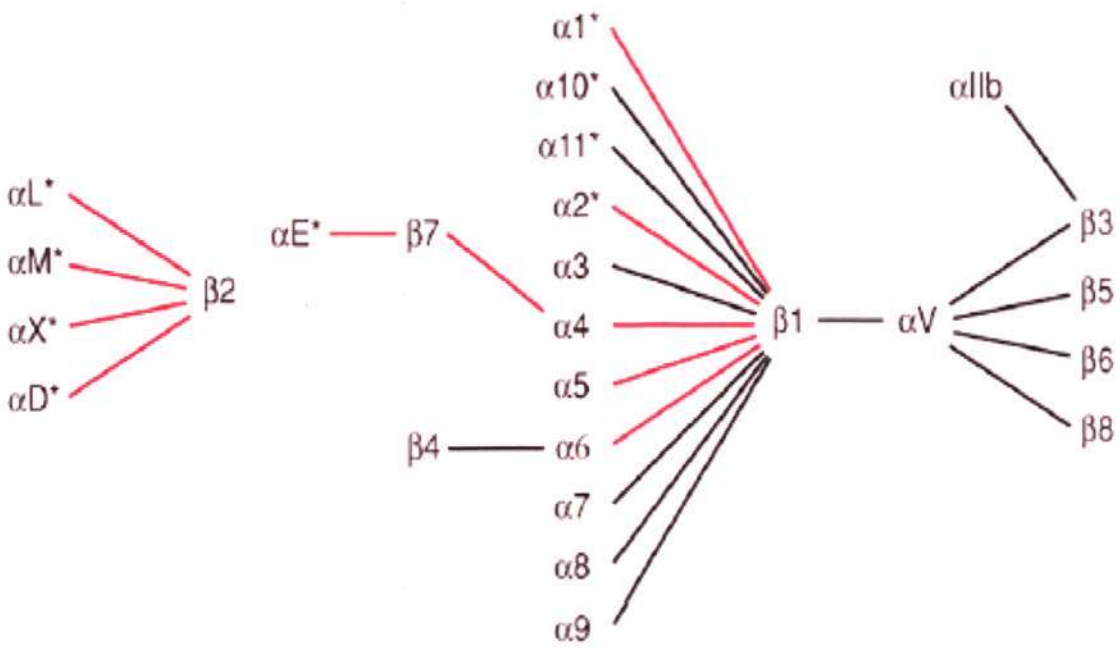

Fig. 1.1 The human integrin superfamily. Integrins are formed by specific non-covalent association of different α and β subunits (indicated by solid lines). A single subunit can pair with more than one partner subunit in some cases, for example, the β1 subunit can pair with 12 different α subunits. The α subunits with an additional I (inserted)-domain are marked with asterisks. Integrins that are expressed in immune cells are shown with red connecting lines (from Luo et al., 2007).

Integrin extracellular ligands

Ligand	Integrin
Adenovirus penton base protein	$\alpha_v\beta_3$, $\alpha_v\beta_5$
Bone sialoprotein	$\alpha_v\beta_3$, $\alpha_v\beta_5$
Borrelia burgdorferi	$\alpha_{IIb}\beta_3$
Candida albicans	$\alpha_M\beta_2$
Collagens	$\alpha_1\beta_1$, $\alpha_2\beta_1$, $\alpha_{11}\beta_1$, $\alpha_{Ib}\beta_3$
Denatured collagen	$\alpha_5\beta_1$, $\alpha_v\beta_3$, $\alpha_{IIb}\beta_3$
Cytotactin/tenascin-C	$\alpha_8\beta_1$, $\alpha_9\beta_1$, $\alpha_v\beta_3$, $\alpha_v\beta_6$
Decorsin	$\alpha_{IIb}\beta_3$
Disintegrins	$\alpha_v\beta_3$, $\alpha_{IIb}\beta_3$
E cadherin	$\alpha_E\beta_7$
Echovirus 1	$\alpha_2\beta_1$
Epiligrin	$\alpha_3\beta_1$
Factor X	$\alpha_M\beta_2$
Fibronectin	$\alpha_2\beta_1$, $\alpha_3\beta_1$, $\alpha_4\beta_1$, $\alpha_4\beta_7$, $\alpha_5\beta_1$, $\alpha_8\beta_1$, $\alpha_v\beta_1$, $\alpha_v\beta_3$, $\alpha_v\beta_5$, $\alpha_v\beta_6$, $\alpha_v\beta_8$, $\alpha_{IIb}\beta_3$
Fibrinogen	$\alpha_5\beta_1$, $\alpha_M\beta_2$, $\alpha_v\beta_3$, $\alpha_x\beta_2$, $\alpha_{IIb}\beta_3$
HIV Tat protein	$\alpha_v\beta_3$, $\alpha_v\beta_5$
iC3b	$\alpha_M\beta_2$, $\alpha_x\beta_2$
ICAM-1	$\alpha_L\beta_2$, $\alpha_M\beta_2$
ICAM-2,3,4,5	$\alpha_L\beta_2$
Invasin	$\alpha_3\beta_1$, $\alpha_4\beta_1$, $\alpha_5\beta_1$, $\alpha_6\beta_1$
Laminin	$\alpha_1\beta_1$, $\alpha_2\beta_1$, $\alpha_6\beta_1$, $\alpha_7\beta_1$, $\alpha_6\beta_4$, $\alpha_v\beta_3$
MAdCAM-1	$\alpha_4\beta_7$
Matrix metalloproteinase-2	$\alpha_v\beta_3$
Neutrophil inhibitory factor	$\alpha_M\beta_2$
Osteopontin	$\alpha_v\beta_3$
Plasminogen	$\alpha_{IIb}\beta_3$
Prothrombin	$\alpha_v\beta_3$, $\alpha_{IIb}\beta_3$
Sperm fertilin	$\alpha_6\beta_1$
Thrombospondin	$\alpha_3\beta_1$, $\alpha_v\beta_3$, $\alpha_{IIb}\beta_3$
VCAM-1	$\alpha_4\beta_1$, $\alpha_4\beta_7$
Vitronectin	$\alpha_v\beta_1$, $\alpha_v\beta_3$, $\alpha_v\beta_5$, $\alpha_{IIb}\beta_3$
von Willebrand factor	$\alpha_v\beta_3$, $\alpha_{IIb}\beta_3$

Fig. 1.2 Integrin extracellular ligands (from Plow et al., 2000).

1.2 Overall conformation of an integrin

Each integrin subunit consists of a large extracellular domain, a single transmembrane domain, and a short cytoplasmic domain with the exception of the β4 subunit that has a large cytoplasmic domain consisting of 4 fibronectin type III repeats (de Pereda et al., 1999) (Fig. 1.3A). The α and β subunits associate with one another forming a receptor with a large globular "head" and two "stalks". The globular "head" is involved in ligand-binding, and the two extracellular "stalks" are connected to the transmembrane and cytoplasmic domains of the individual subunit. The ligand-binding function of an integrin is regulated by conformational changes. The seminal reports on the crystal structures of the integrins, αVβ3 and αIIbβ3, reveal an integrin with a bent conformation (Xiong et al., 2001; Xiong et al., 2002; Zhu et al., 2008). In this conformation, the "stalks" of both subunits are severely bent, bringing the globular "head" close to the plasma membrane, which will impede its binding to large ligands because of steric constraints. Conceivably, the projection of the globular "head" away from the plasma membrane will allow better accessibility to ligands, and this will require the unbending or extension of the integrin. The term "activation" is widely used in numerous reports describing the up-regulation of integrin ligand-binding affinity that is conformational-dependent (Takagi et al., 2003; Xiong et al., 2001; Xiong et al., 2002). The current paradigm of integrin activation involves the transition of an integrin from a bent conformation to an extended conformation (Xiao et al., 2004).

1.2.1 The extracellular domains of the integrin α subunit

The extracellular region of the integrin α subunit is linearly organized from the N- to C-terminus into distinct domains: a β-propeller, thigh, calf-1 and calf-2 domains (Takagi and Springer, 2002) (Fig. 1.3A). The region in the α subunit that is bent when an integrin

adopts a bent conformation is termed the genu (Xie et al., 2004; Xiong et al., 2001).

A prominent feature in the integrin α subunit is a seven-bladed β-propeller domain that is similar to the β-propeller domain found in the β subunit of the G proteins (Springer, 1997). Each of the seven blades (W1-W7) has four anti-parallel β-strands. Strands 1, 2, 3 and 4 are connected by successive hairpin turns, and strand 4 of one blade is connected to strand 1 of the next blade (Fig. 1.4). There are three Ca^{2+} binding sites found in the hairpin turns connecting strands 1 and 2 in blades 5-7 at the bottom of the propeller (Xiong et al., 2001). An additional site can be found in blade 4 of some integrin α subunits (Springer et al., 2000). The presence of calcium may stabilize the folding of the β-propeller (Xiong et al., 2001). Notably, 9 of the 18 human α subunits (α1, α2, α10, α11, αE , αL, αM, αX and αD) contain an additional domain that is inserted between blade 2 and blade 3 of the β-propeller, and it is referred to as the inserted (I)-domain. In integrins that do not have the I-domain, the β-propeller appears to directly participate in ligand recognition (Humphries, 2000). In integrins that contain the I-domain, the β-propeller can also contribute towards ligand-binding as in the αMβ2 (Yalamanchili et al., 2000), or it plays no direct role as in the αLβ2 (Shimaoka et al., 2001).

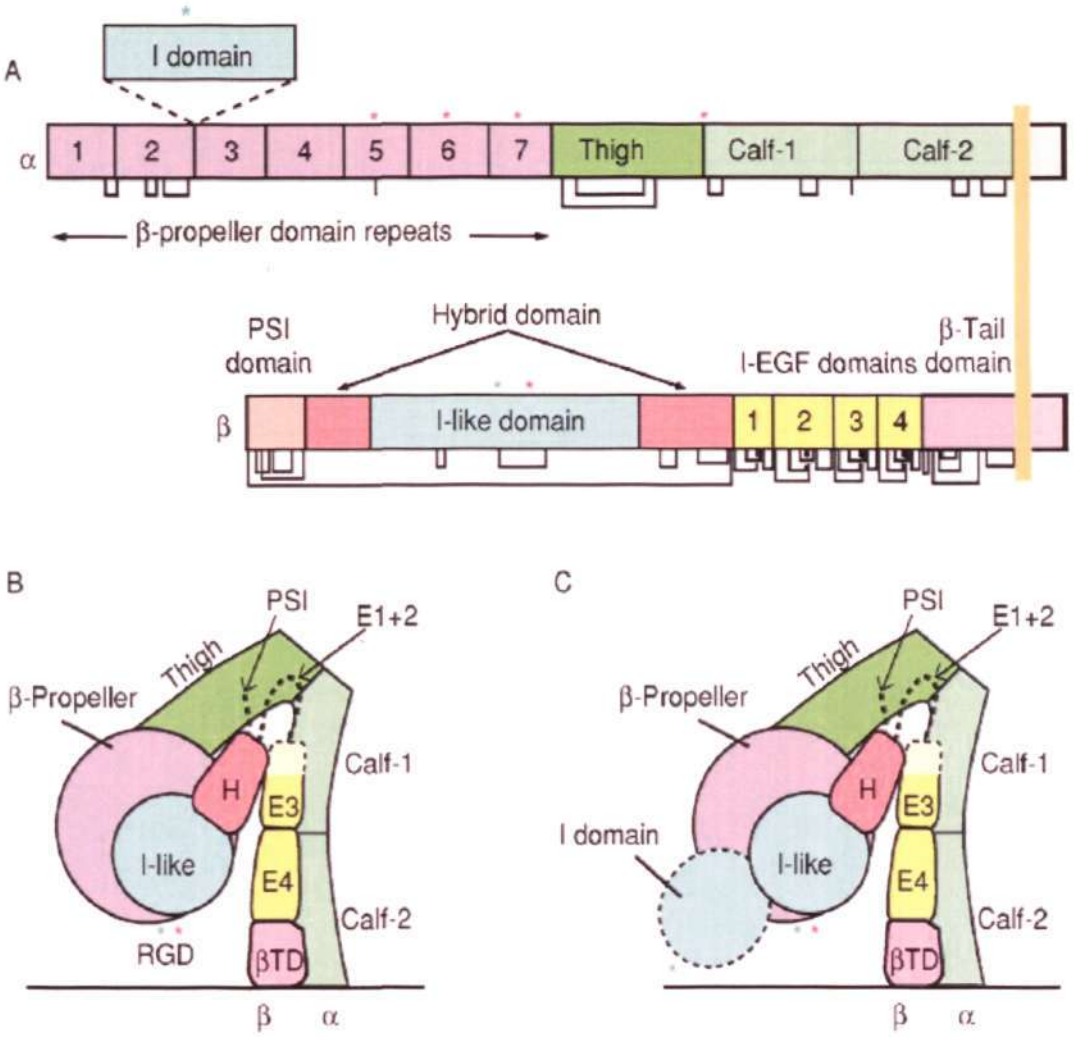

Fig. 1.3 Integrin domains organization. (A) Organization of domains within the primary structure of integrin. Depending on the α subunit, it may contain an I-domain insertion as denoted by the dotted line. Asterisks show Mg^{2+} (blue) and Ca^{2+} (red) binding sites. Lines below the diagrams show disulfide bonds. (B) Arrangement of domains of a bent integrin αVβ3. Each domain is color coded as in (A). (C) The structure in (B) with an I-domain added (from Springer et al., 2004).

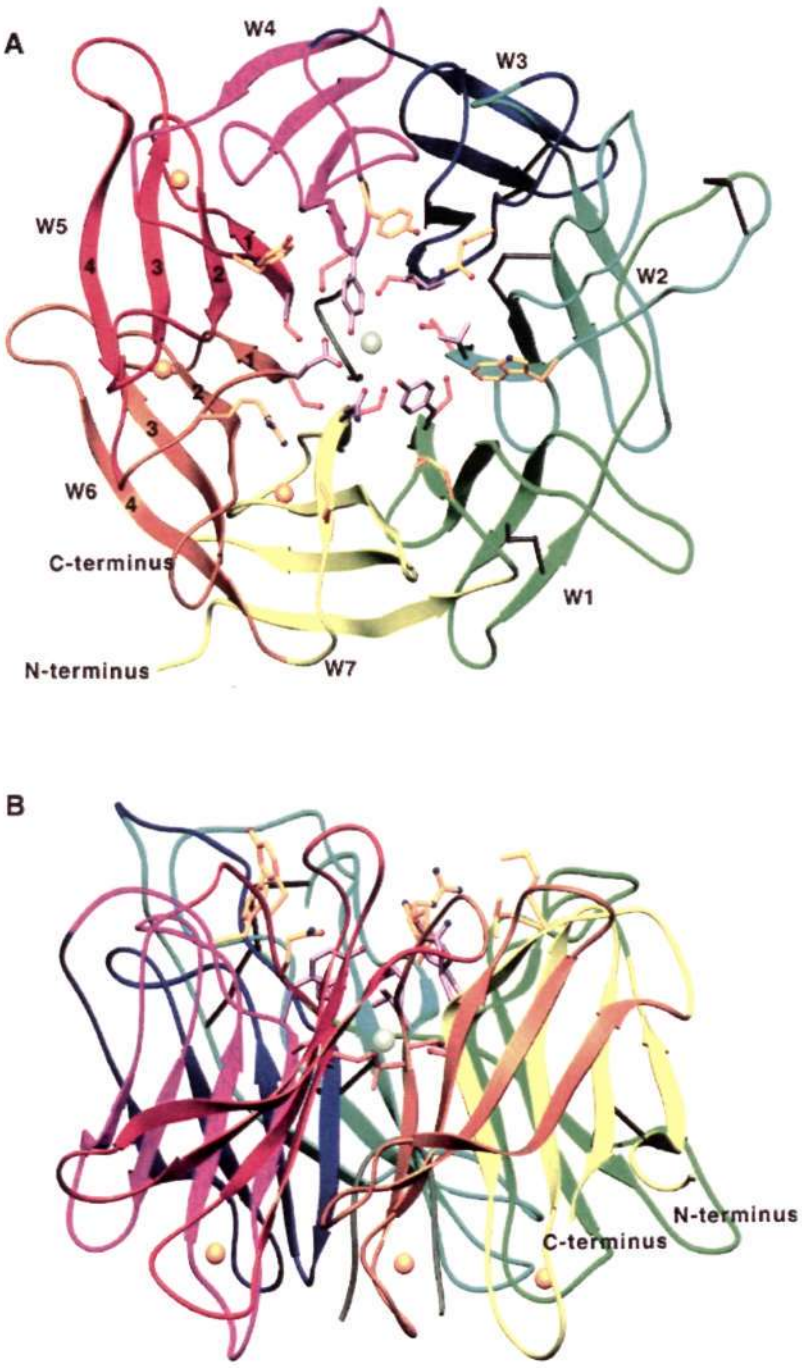

Fig. 1.4 The α subunit β-propeller. Ribbon diagrams of the model for the integrin α4 subunit β-propeller domain. Views are from the top (A) and side (B). Each blade of the β-propeller is shown in a different color and labelled W1-W7. The strands of each blade are labelled 1-4, from the center. A hypothetical polypeptide finger in the central cavity is gray. Cysteines in disulfides are black. Ca^{2+} ions and a hypothetical Mg^{2+} ion are gold and silver spheres, respectively (from Springer., 1997).

The I-domain, which is homologous to the von Willebrand factor A domain, is also referred to as the A domain, and it is composed of approximately 200 amino acids. The I-domain adopts the dinucleotide-binding or Rossmann fold, with a central hydrophobic β-sheet surrounded by a number of α-helices (Emsley et al., 1997; Lee et al., 1995b; Mould et al., 2003c) (Fig. 1.5). The I-domain is the major ligand-binding domain for those integrins containing an I-domain. Deletion of the I-domain in integrin αL abolished its binding to ligands ICAM-1 and -3 (Leitinger and Hogg, 2000; Yalamanchili et al., 2000), and an isolated recombinant αL I-domain, which was engineered into a high affinity conformation by a disulfide bond, was sufficient to bind ligands (Lu et al., 2001a).

Binding of the I-domain to ligand depends on divalent cation. The divalent cation coordination site, designated the metal ion-dependent adhesion site (MIDAS), is located on the upper surface of the I-domain, and it binds negatively charged residues in the ligand. The cation in the MIDAS is coordinated by the side-chains of five residues located in the β1-α1, α2-α3, and β4-α4 loops. The first loop provides three coordinating residues with the characteristic sequence, Asp-X-Ser-X-Ser or DXSXS in single amino acid code (X means any other amino acid). A Thr and an Asp coordinating residues are found in the second and third loops, respectively (Shimaoka et al., 2002).

Based on the crystal structures of the αM I-domain obtained in the presence of different metal ions, two conformations of the I-domain were observed (Lee et al., 1995a; Lee et al., 1995b) (Fig. 1.6). In one of these conformations, a Glu residue from an αM I-domain inserts into the MIDAS of another αM I-domain in the crystal. The five MIDAS residues, two water molecules, and the Glu side-chain complete the coordination sphere surrounding the central metal ion Mg^{2+}, and therefore may be viewed as a liganded

I-domain (Lee et al., 1995a; Lee et al., 1995b). This conformation is referred to as the open conformation. The other conformation, in the presence of Mn^{2+}, did not have an exogenous residue completing the coordination sphere, and was taken as the structure of an un-liganded I-domain (Lee et al., 1995a; Lee et al., 1995b). This conformation is known as the closed conformation. There are marked differences between the open and closed I-domain conformations in that the positions of the MIDAS residues and the number of water molecules are different. Importantly, the C-terminal helix of the αM I-domain in the open conformation showed approximately 10 Å downward shift when compared to that in the closed conformation, suggesting that ligand-binding of an I-domain will induce significant conformational changes that can be propagated to other regions of the integrin. Similar observations were made in the liganded integrin αL and α2 I-domains (Emsley et al., 1997; Emsley et al., 2000; Huth et al., 2000; Legge et al., 2000). The transition of the I-domain from a closed conformation to an open conformation is coupled with an increase in ligand-binding affinity. This was suggested using recombinant αL I-domain engineered into a closed, intermediate, or open conformation by the introduction of disulfide bond that stabilize the C-terminal helix (Shimaoka et al., 2003). The intermediate and open αL I-domain conformations showed 500- and 10,000-fold increase, respectively, in their affinity for ICAM-1 with respect to the closed conformation (Luo et al., 2007; Shimaoka et al., 2003).

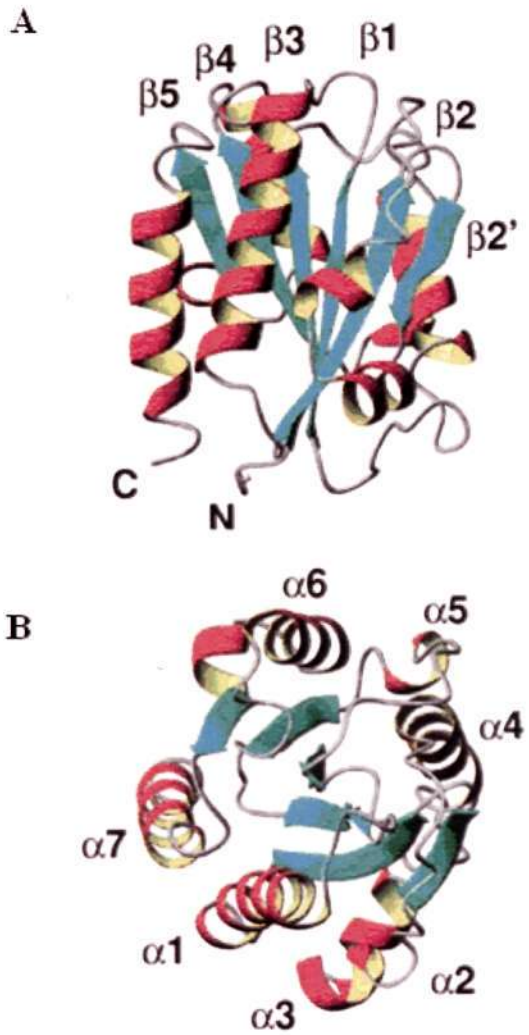

Fig. 1.5 Ribbon diagram of the mean NMR structure of the I-domain of αL subunit showing helices (red/yellow), β-sheets (blue) and loops (gray). The structure is rotated by 90° between views (A) and (B) in order to highlight the (A) β-sheet and the (B) α-helices. The location of the metal ion is not shown, but it would be in the top right of the molecule in A (from Legge et al., 2000).

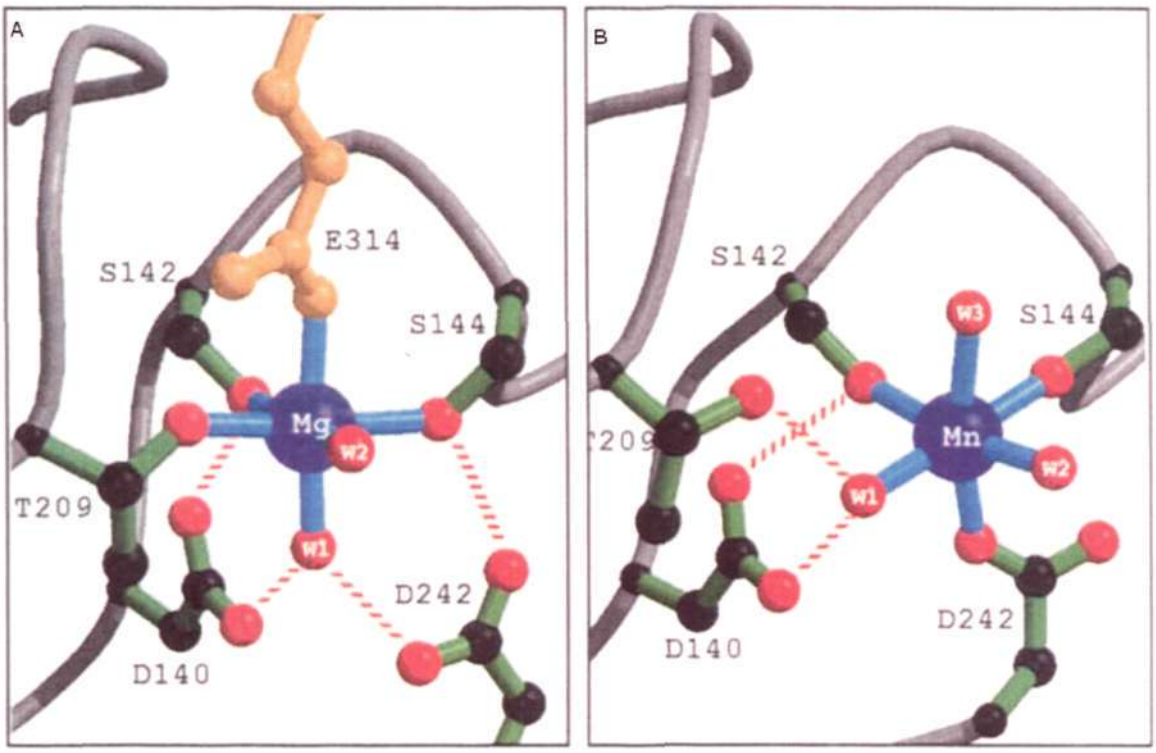

Fig. 1.6 Structural comparisons of the Mg^{2+} and Mn^{2+} bound I-domains. (A) The MIDAS motif in the Mg^{2+} form. (B) The MIDAS motif in the Mn^{2+} form. The color code is oxygen atoms (red), carbon (black), schematic backbone (grey) and the glutamate from a neighbouring molecule (gold). Water molecules are labelled w1-w3. Selected hydrogen bonds are shown as dashed red lines (from Lee et al., 1995a).

C-terminal to the β-propeller, there are three large β-sandwich domains termed the thigh, calf-1 and calf-2. There can be certain degree of movement between the β-propeller and thigh domain interface during integrin activation, and this may be regulated by the Ca^{2+} ions in the propeller (Xiong et al., 2001). Between the thigh and calf-1 is the flexible joint termed the genu, which is capped by a divalent cation. It has been shown that the genu and calf-1 interface is important in maintaining integrin activation, and the extension of the integrin legs may occur by a structural rearrangement at the thigh and calf-1 interface (Xie et al., 2004). The interface between calf-1 and calf-2 domains (~500 $Å^2$) is largely hydrophobic, suggesting that these two domains form a rigid structural entity (Xiong et al., 2001).

1.2.2 The extracellular domains of the integrin β subunit

The integrin β-subunit has eight extracellular domains: the PSI (plexins, semaphorins, and integrins) domain, hybrid domain, I-like domain, four I-EGF (integrin epidermal growth factor) domains, and the βTD (β tail domain) (Fig. 1.3). The integrin β subunit has two domain insertions based on primary amino acid sequence: the I-like domain is inserted into the hybrid domain, which is itself inserted into the PSI domain.

The N-terminal cysteine-rich region of the integrin β-subunit shares sequence homology with the membrane proteins plexins and semaphorins, thus it is termed the PSI (plexins, semaphorins, and integrins) domain (Bork et al., 1999). The PSI domain forms a two-stranded anti-parallel β-sheet flanked by two short helices and it has eight cysteines that are paired by disulfide bonds in a Cys^1-Cys^4, Cys^2-Cys^8, Cys^3-Cys^6, and Cys^5-Cys^7 pattern. Unlike the other Cys, in the primary sequence of the β-subunit, Cys^8 is located in the connecting region between the hybrid domain and I-EGF-1 sequences (Xiong et al., 2004) (Table 1.1).

At the C-terminal of the PSI lies the hybrid domain that is a β-sandwich domain formed from two segments flanking the I-like domain in the primary sequence (Xiong et al., 2004). This was first reported by biochemical analyses using monoclonal antibodies having epitopes that are located in the hybrid domain (Mould et al., 2003b), and subsequently verified by structural studies (Xiao et al., 2004). Functional studies of integrins using conformational sensitive reporter antibodies, HUTS-4 (integrin α5β1) and MEM148 (αLβ2) as examples, suggest movement of the hybrid domain when an integrin is activated (Mould et al., 2003b; Mould et al., 2003c; Tang et al., 2005). Although the hybrid domain does not participate directly in ligand-binding, it is shown to be important in the propagation of activation signal in αLβ2 (Tng et al., 2004). Structural study using liganded-integrin αIIbβ3 also showed large displacement (~62°) of the hybrid domain away from the α subunit, supporting the importance of this domain in integrin ligand-binding (Xiao et al., 2004).

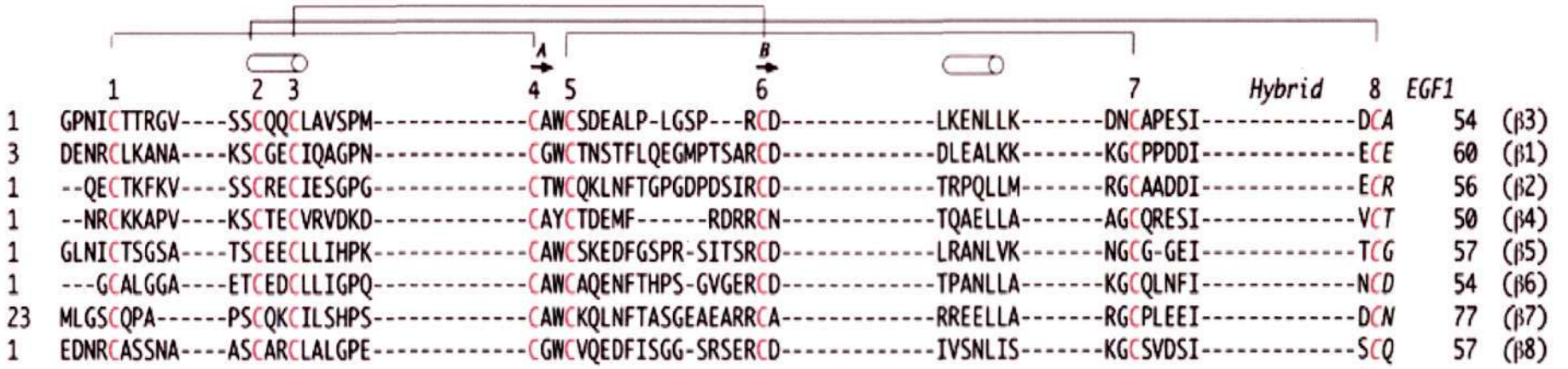

Table 1.1 Sequence alignment and cysteine pairing of the PSI domain from all eight human integrin β subunits (from Xiong et al., 2004).

The I-like domain of the β subunit shares structural similarity with the I-domain in the α subunits. It differs from the I-domain by having two extra loops, one is named SDL (specificity determining loop), which is crucial for integrin dimer formation and ligand binding (Takagi et al., 2002a), and the other interacts with the β-propeller of the α subunit (Arnaout et al., 2005). In addition to the MIDAS, the I-like domain has two other metal ion binding sites termed the ADMIDAS (adjacent to MIDAS) and LIMBS (ligand-induced metal ion binding site). Collective data, from α4β7 (Chen et al., 2003), α5β1 (Mould et al., 2003a) and αLβ2 (Nishida et al., 2006), suggest that the LIMBS and ADMIDAS are the sites for positive and negative regulations by Ca^{2+}, respectively.

In the integrin β-subunit, there are four tandem cysteine-rich repeats known as I-EGF 1-4, which share sequence homology with the epidermal growth factor (EGF) modules. The boundaries of these modules were defined in the β2 subunit (Tan et al., 2001) and the paring of cysteines in these repeats have been characterized in the Cys^1-Cys^5, Cys^2-Cys^4, Cys^3-Cys^6, Cys^7-Cys^8 pattern (Takagi et al., 2001a). Unlike the I-EGF 2, 3, and 4, each of which has eight Cys, the I-EGF 1 has only a total of six Cys engaged in three disulfide bonds with the Cys^2-Cys^4 disulfide pair missing (Shi et al., 2005). Two crystal structures of the I-EGF domains of the β2 subunit have been solved (Shi et al., 2007a; Shi et al., 2005), and the complete I-EGF structures of β3 were also reported recently (Zhu et al., 2008). As in the α subunit genu, the interface between I-EGF 1 and 2 appears to be flexible thereby allowing bending of the β subunit in the bent conformation.

After the I-EGF repeats lies the βTD that consists of a four-strand β sheet (Xiong et al., 2001). Only two weak hydrophobic contacts are found between βTD and I-EGF 4, indicating the interface between them is flexible (Xiong et al., 2001). βTD is not essential for heterodimer formation, but it can restrain β3 integrin in a low affinity state (Butta et

al., 2003). It has been reported that the interaction between the βTD and the I-like domain in the β2 subunit maintains integrin αMβ2 in a resting conformation akin to a "dead-bolt", and the disruption of this interaction is required for αMβ2 activation (Gupta et al., 2007). However, another study demonstrated that the mutation or deletion of the β3 tail domain loops had no effect on the ligand-binding properties of integrins αVβ3 and αIIbβ3 (Zhu et al., 2007).

1.2.3 Integrin transmembrane (TM) domains

The integrin TMs are the transducers of activation signal between the extracellular and intracellular domains. The TM segment has approximately 25-29 amino acids, and it is highly conserved between integrins, and across many species (Ginsberg et al., 2005). It adopts an α-helical conformation, and may be tilted in the membrane (Armulik et al., 1999). In a non-activated integrin, the TMs of the α and β subunits are closely associated with each other. Upon integrin activation, the TMs are separated but the precise nature of the TMs movement remains to be clarified (Arnaout et al., 2005; Wegener and Campbell, 2008) (Fig. 1.7). Homomeric associations (α/α or β/β) of the TMs may contribute towards integrin clustering as shown in integrin αIIbβ3 by mutagenesis, electron microscopy, and immunofluorescence microscopy (Lau et al., 2008; Li et al., 2001; Li et al., 2004; Li et al., 2003b). However, this was not observed in another study, instead only affinity up-regulation of αIIbβ3 was detected by TMs mutations (Luo et al., 2005). Our group also detected activation of the integrin αLβ2 when the packing of the TMs interface was disrupted (Vararattanavech et al., 2009).

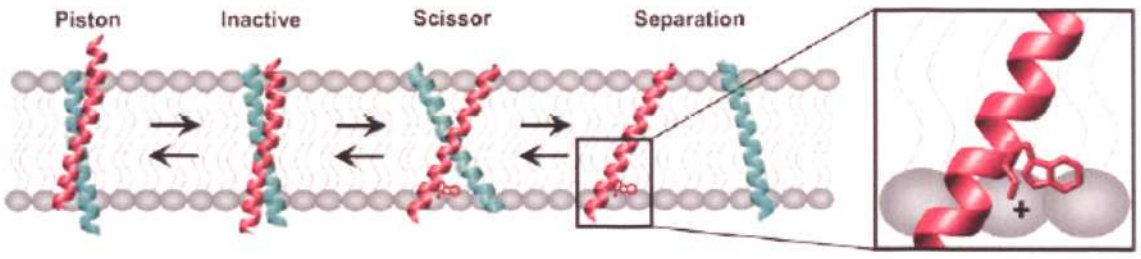

Fig. 1.7 Postulated models of changes in the TM domains during integrin activation in integrin αIIbβ3. The initially interacting TM domains in the inactive state (second from left) shift vertically within the bilayer in the piston model (left). In the scissor model (second from right), the angle between the helices increases following activation. The two TM domains separate completely in the separation model (far right). The αIIb subunit is shown in cyan, and the β3 subunit in red. The inset diagram illustrates 'snorkelling' of residue K716, which allows the positively charged amine in the lysine side-chain to interact with the negatively charged lipid head groups (from Wegener and Campbell, 2008).

1.2.4 Integrin cytoplasmic tail

The cytoplasmic tails of integrin α and β subunits are generally less than 70 residues in length, with the exception of the β4 subunit (Hynes, 2002; Lau et al., 2009; Wegener and Campbell, 2008; Zhu et al., 2009). The β subunit cytoplasmic tails are highly conserved as compared to the α cytoplasmic domains. Despite the weak interaction of the α and β cytoplasmic tails, its disruption will lead to integrin activation (O'Toole et al., 1991; Peterson et al., 1998). In addition to the hydrophobic contacts, an electrostatic contact forming a salt-bridge between the α and β cytoplasmic tails was reported (Hughes et al., 1996). The salt-bridge is formed by an Arg found in the conserved α membrane-proximal sequence GFFKR and an Asp found in the β membrane-proximal sequence LLv-iHDR (highly conserved residues are uppercase, less conserved residues are lowercase, and the dash represents nonconserved residue) (Calderwood, 2004; Williams et al., 1994). Mutation or deletion of these residues or sequences, respectively, induce activation of the integrins (αIIbβ3, αLβ2, and αMβ2), suggesting the importance of this electrostatic contact (Hughes et al., 1996; Hughes et al., 1995; Lu and Springer, 1997; Lu et al., 2001b). The weak nature of the interaction between the α and β cytoplasmic tails together with the use of different segments of the cytoplasmic domains may explain why such interaction was detected only in some studies (Vinogradova et al., 2002). Recently, our group and collaborators showed by NMR studies the interaction of the integrin αL and β2 cytoplasmic tails (Bhunia et al., 2009) (Fig. 1.8). The cytoplasmic tails of the integrin serve as "hubs" for the docking of cytoplasmic proteins, which are important for integrin activation and down-stream signaling (Dunker et al., 2005; Liu et al., 2000). An

expanding list of cytoplasmic proteins that interact with integrin cytoplasmic tails is shown (Table 1.2).

Integrin cytoplasmic tails also contain Ser, Thr, and Tyr phosphorylation sites that are involved in integrin functional-regulation (Czuchra et al., 2006; Fagerholm et al., 2005; Nurmi et al., 2007). Phosphorylation of β2 cytoplasmic peptide on Thr-736 results in the recruitment of 14-3-3 proteins, whereas the unphosphorylated β2 cytoplasmic peptide binds to filamin (Fagerholm et al., 2005; Takala et al., 2008). 14-3-3 proteins are ubiquitously expressed, and they are small dimeric adapter proteins that bind to Ser/Thr phosphorylated sequences in proteins and alter protein localisation or activity (Tzivion and Avruch, 2002). Filamin family comprises of three isoforms, encoding filamin A, B, and C (Stossel et al., 2001). Its binding site in the integrin overlap partially with that of talin (Gahmberg et al., 2009; Kiema et al., 2006), and filamin has been reported to be a negative regulator of integrin ligand binding and of cell migration (Calderwood et al., 2001; Takala et al., 2008). Besides 14-3-3, which competes with filamin for β2 cytoplasmic tail, migfilin has also been reported to inhibit filamin binding to the β2 cytoplasmic tail (Lad et al., 2008). This may provide a finely-regulated mechanism for maintaining signaling specificity mediated by the integrin β cytoplasmic tails (Shi et al., 2007b; Stossel and Hartwig, 2003; Tu et al., 2003).

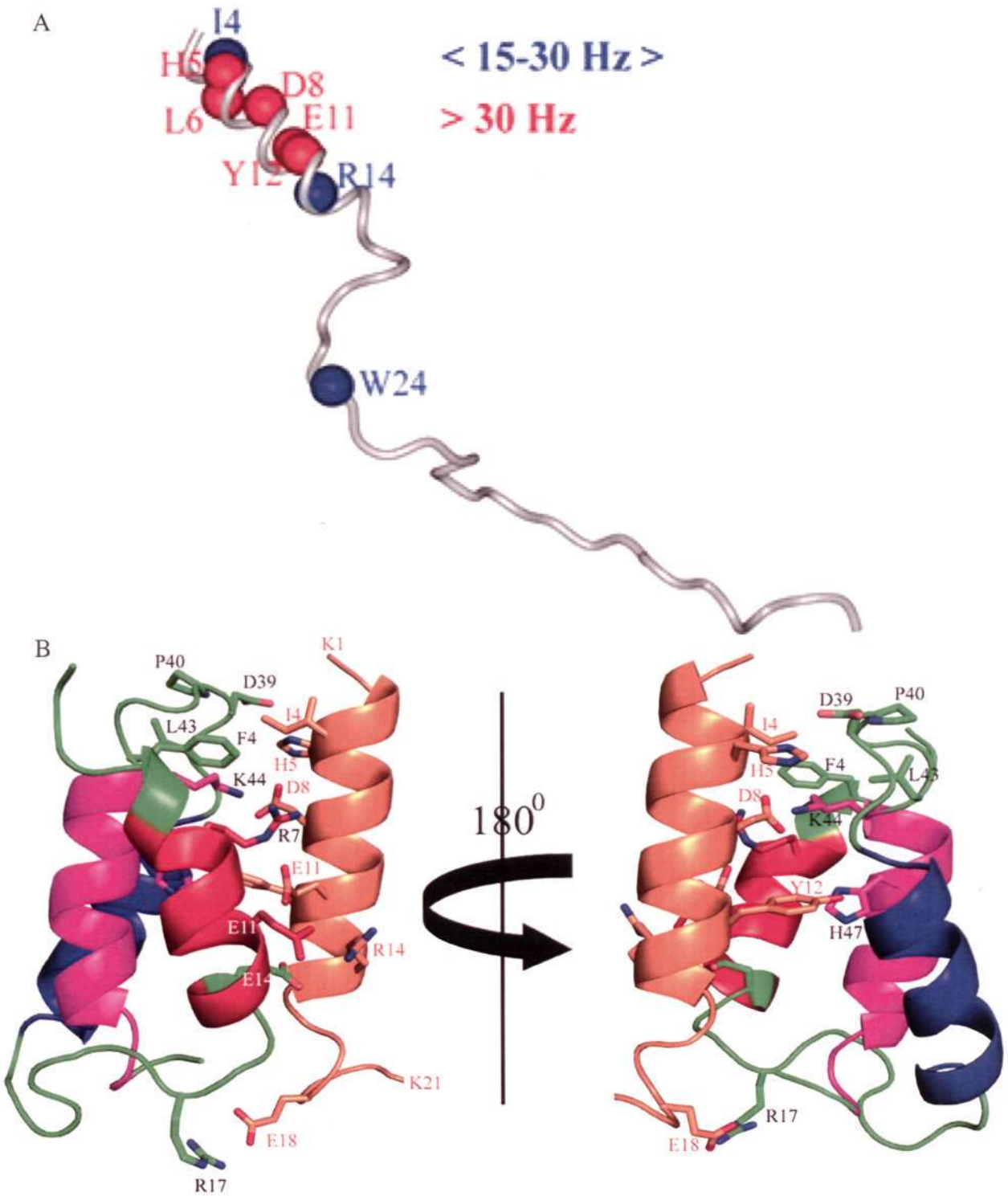

Fig. 1.8 A proposed model of αL and β2 tails complex. (A) Ribbon representation of the conformation of β2 tail showing amino acid residues affected by binding with αL tail. Blue and red represent the combined changes in 1HN and 15N chemical shift of 15–30 Hz and above 30 Hz, respectively. Residues showing ≤10 Hz chemical shift change are not shown. The image was produced with the program PyMOL. (B) Expanded view of the docked interface of the αLβ2 integrin cytoplasmic tail complex showing ionic and hydrophobic interactions between helices, helix 1 (red ribbon) and helix 3 (pink ribbon) of αL and N-terminal helix (orange ribbon) of β2 (from Bhunia et al., 2009).

Adaptor protein	Integrin to which adaptor binds	Reference
Structural adaptors		
α-actinin	β1, β2, β3	(Otey et al., 1993; Pavalko and LaRoche, 1993)
BP180	β4	(Koster et al., 2003; Schaapveld et al., 1998)
Filamin	β1, β2, β3, β7	(Calderwood et al., 2001; Kiema et al., 2006; Loo et al., 1998 Sharma et al., 1995; Travis et al., 2004; Zent et al., 2000)
Myosin	β1, β3, β5	(Jenkins et al., 1998; Sajid et al., 2000; Zhang et al., 2004)
Plectin	β4	(Geerts et al., 1999)
Skelemin	β1, β3	(Reddy et al., 1998)
Talin	β1, β2, β3, β5, β7	(Calderwood et al., 2003; Calderwood et al., 1999; Patil et al., 1999 Sampath et al., 1998; Pfaff et al., 1998)
Tensin	β1, β3, β5, β7	(Calderwood et al., 2003; McCleverty et al., 2007)
Scaffolding adaptors		
14-3-3	β1, β2, β3	(Fagerholm et al., 2005; Han et al., 2001)
β3 endonexin	β3	(Eigenthaler et al., 1997; Shattil et al., 1995)
CD98	β1, β3	(Zent et al., 2000)
Dab1	β1, β2, β3, β5, β7	(Calderwood et al., 2003)
Dab2	β3, β5	(Calderwood et al., 2003)
Dok1	β2, β3, β5, β7	(Calderwood et al., 2003)
Fhl2	β1, β2, β3, β6	(Wixler et al., 2000)
Fhl3	β1	(Samson et al., 2004)
Grb2	β3	(Blystone et al., 1996; Law et al., 1996)
IAP	β3	(Brown et al., 1990)
JAB1	β2	(Bianchi et al., 2000)
Kindlin 2	β1, β3	(Ma et al., 2008; Montanez et al., 2008)
Kindlin 3	β1, β3	(Moser et al., 2008)
Melusin	β1	(Brancaccio et al., 1999)
Numb	β3, β5	(Calderwood et al., 2003)
Paxillin	β1, β3	(Chen et al., 2000; Schaller et al., 1995)
Rack1	β1, β2, β5	(Liliental and Chang, 1998)
Shc	β3, β4	(Dans et al., 2001; Law et al., 1996)
TAP20	β5	(Tang et al., 1999)
WAIT1	β7	(Rietzler et al., 1998)
Catalytic adaptors		
Src	β3	(Arias-Salgado et al., 2003; Arias-Salgado et al., 2005)
Yes	β1, β2, β3	(Arias-Salgado et al., 2005)
Cytohesin 1	β2	(Kolanus et al., 1996)
Eps8	β1, β3, β5	(Calderwood et al., 2003)
ERK2	β6	(Ahmed et al., 2002)
FAK	β1, β2, β3, β5	(Chen et al., 2000; Eliceiri et al., 2002; Schaller et al., 1995)
Fyn	β3	(Arias-Salgado et al., 2005)
ILK	β1, β3	(Hannigan et al., 1996; Pasquet et al., 2002)
Lyn	β1, β2, β3	(Arias-Salgado et al., 2005)
PKD1	β1, β3	(Medeiros et al., 2005; Woods et al., 2004)
PP2A	β1	(Kim et al., 2004)
Shp2	β4	(Bertotti et al., 2006)
Other adaptors		
ICAP1α	β1	(Chang et al., 1997; Zhang and Hemler, 1999)
MIBP	β1	(Li et al., 1999)

Table 1.2 Adaptor proteins that bind to β-integrin cytoplasmic tails (from Legate et al., 2009).

1.3 Integrin affinity or activation states

The simple model of integrin activation describes the conversion of a bent integrin to one that is highly extended in a "switch-blade" motion (Beglova et al., 2002). However, electron microscopy (EM) images and crystal structures of integrins (αIIbβ3, αVβ3, and α5β1) suggest that integrin may adopt at least three quaternary conformations (Takagi et al., 2003; Xiao et al., 2004; Xiong et al., 2001; Xiong et al., 2002). A most convincing report showing three integrin conformers is the EM study of integrins αLβ2 and αXβ2 (Nishida et al., 2006). A bent integrin conformer and two distinct extended conformers were observed. The bent conformer is similar to that seen in the crystal structures of αVβ3 (Xiong et al., 2001; Xiong et al., 2002). The other two extended conformers showed marked differences in the position of their hybrid domains, with one juxtaposed to the α subunit and the other away from the α subunit, which is in line with the activation states previously reported (Xiao et al., 2004) (Fig. 1.9). This difference in the displacment of the hybrid domains will impact the ligand-binding affinity of the integrin. Indeed, a glycan wedge introduced at the interface of the I-like domain and the hybrid domain generated integrins (αIIbβ3, αVβ3, α5β1 and αLβ2) with high affinities (Luo et al., 2003; Tang et al., 2008b). Recently, our group showed that engineered integrin αLβ2 in bent, extended without hybrid domain displacement, and extended with hybrid domain displacement conformers had different ligand-binding affinities (Tang et al., 2008b). The terms (low-, intermediate-, and high-affinity) are commonly used to describe integrin affinity states (Takagi et al., 2003; Xiao et al., 2004; Xiong et al., 2001; Xiong et al., 2002). It is possible that having integrins with different affinity states could allow fine-regulation of integrin-mediated cell adhesion under different micro-environments.

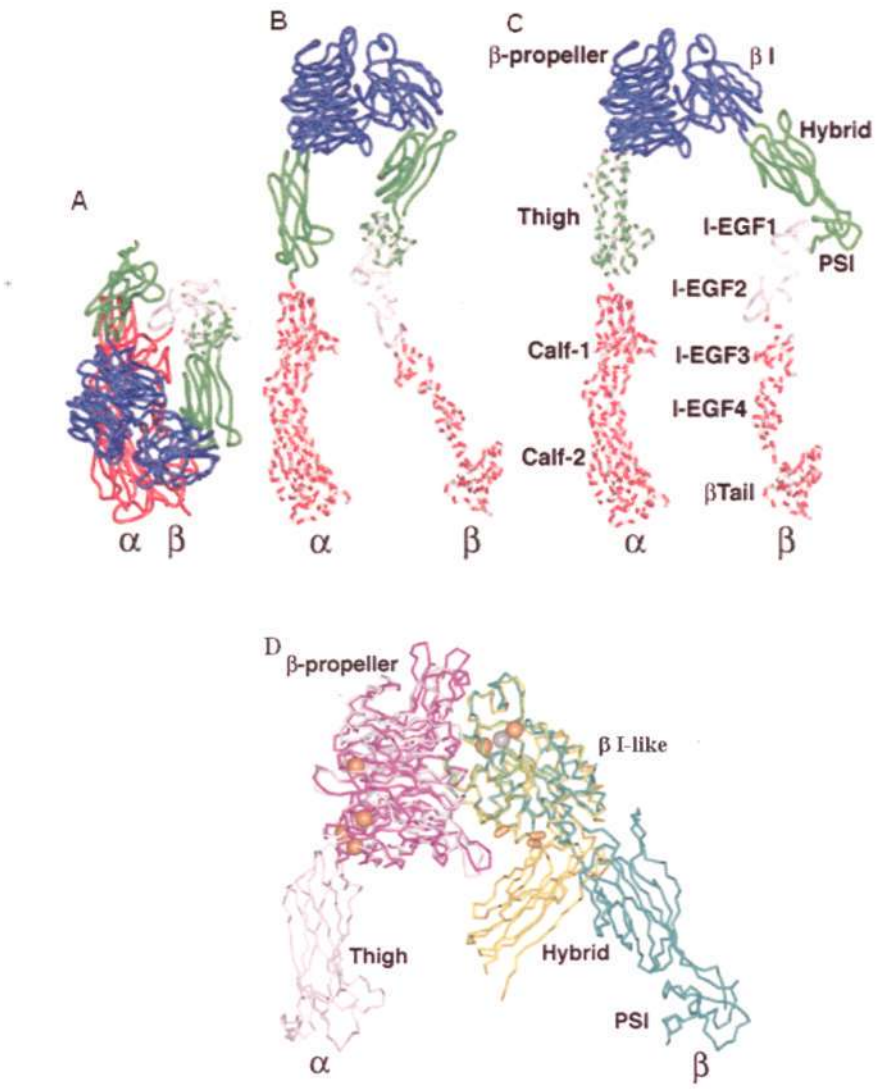

Fig. 1.9 Three conformational states. (A) A bent conformation stands for a low affinity state. (B) An extended form with a 'closed' headpiece conformation represents an intermediate affinity state. (C) An extended conformation with an 'open' headpiece represents a high affinity state. Domains are shown in solid color if known directly from crystal structures, dashed with grey if placed from crystal structures into electron microscopy image averages, and in solid grey for I-EGF 1 and I-EGF 2, which are modelled on I-EGF 3 and I-EGF 4. (D) Hybrid domain displacement. Liganded-open αIIbβ3 and unliganded-closed αVβ3 headpieces are superimposed using the β I-like domain β-sheet. The α and β subunits are colored magenta and cyan in αIIbβ3 and grey and yellow in αVβ3. Calcium and magnesium ions in αIIbβ3 only are gold and silver spheres, respectively (from Xiao et al., 2004).

1.4 Regulation of integrin function

As described earlier, conformational changes in an integrin are coupled with its ligand-binding affinity. The unbending of an integrin in a "switch-blade" motion is a key feature in integrin activation (Ginsberg et al., 2005; Takagi et al., 2002b). The trigger point for an integrin to change from a bent to an extended conformation lies in its cytoplasmic domains. It is becoming clear that the docking of the cytoplasmic protein talin to the integrin β cytoplasmic tail triggers conformational changes that are propagated to the extracellular domains of the integrin (Kim et al., 2003; Liu et al., 2000; Takagi et al., 2001b; Vinogradova et al., 2004). This process of integrin activation is also commonly referred to as "integrin inside-out signaling" (Abram and Lowell, 2009b; Hynes, 1992; O'Toole et al., 1994; O'Toole et al., 1991). Prototypic examples of inside-out signaling include chemokine-triggered activation of αLβ2 on leukocytes (Campbell et al., 1998; Shamri et al., 2005) and agonist activation of αIIbβ3 on platelets (Savage and Ruggeri, 1991; Savage et al., 1992). The integrin inside-out signaling pathway is illustrated (Fig. 1.10).

Talin, which binds to the integrin cytoplasmic tail, is a large (~250 kDa) cytoplasmic protein with two isoforms in vetebrates, referred to as talin 1 and talin 2 (Calderwood et al., 1999; Critchley, 2000; Rees et al., 1990). It contains a large globular head domain (HD) and a long rod domain (Rees et al., 1990). The head domain contains a FERM (four-point-one ezrin radixin moesin) domain with three subdomains (F1, F2, and F3) proceeded by a F0 subdomain. The F3 subdomain has a phosphotyrosine-binding (PTB) motif that binds a conserved membrane proximal NPxY/F (x is other residue) motif in the integrin β cytoplasmic tail (Pearson et al., 2000). The talin rod domain is formed by

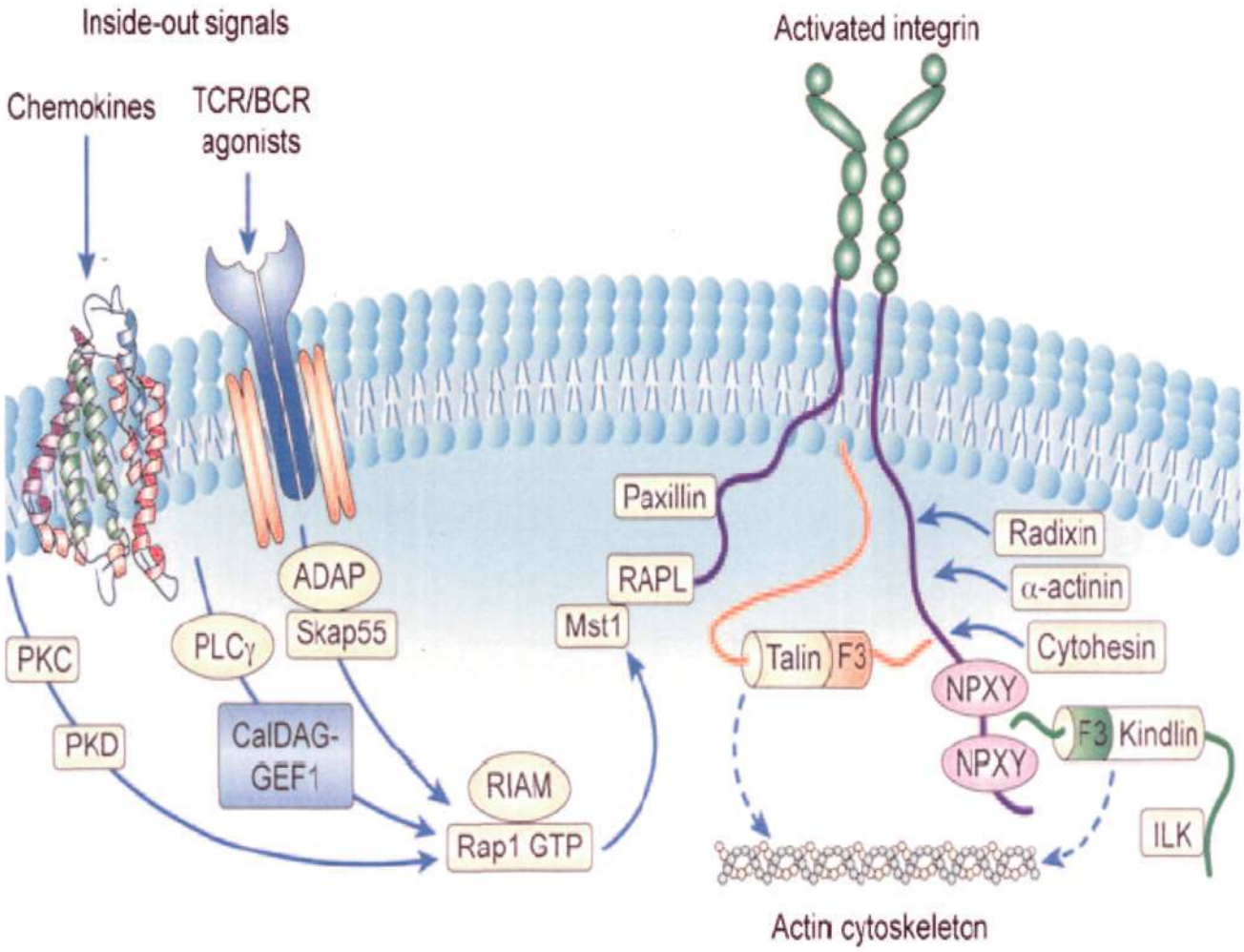

Fig. 1.10 Integrin inside-out signaling. The figure outlines the key signaling pathways that have been implicated in integrin inside-out signaling downstream of chemokine and B- or T-cell receptor stimulation. Initiation of most signaling pathways that lead to integrin activation involve the recruitment of Ras-proximate-1 (Rap1) GTPase. Rap1 activation is controlled by upstream guanine nucleotide exchange factors (GEFs), in particular calcium- and diacylglycerol-regulated guanine nucleotide exchange factor 1 (CalDAG-GEF1), which has been implicated in regulating cell adhesion and migration (Pasvolsky et al., 2007). Following Rap1 activation, its effectors Rap1-GTP-interacting adaptor molecule (RIAM) and Rap1-binding protein (RapL) form a complex with the cytoplasmic tails of integrins. This leads to a critical change in the association of talin with the integrin cytoplasmic tail, and binding of a number of other proteins to the integrin tail, including paxillin, radixin, cytohesin, α-actinin and the kindlins. Altogether, these proteins facilitate separation of the cytoplasmic tails of the integrins, leading to full conformational changes required for high-affinity ligand binding and coupling of the integrin to the actin cytoskeleton. The precise sequence of events from Rap1 activation to integrin tail separation and protein associations is unclear; however, this overall theme is likely common between the β1-, β2- and β3-integrins (from Abram et al., 2009).

α-helical bundles, and it has 11 vinculin cytoplasmic protein-binding sites, two actin-binding sites, another integrin binding site, and a C-terminal dimerization sequence (Critchley and Gingras, 2008) (Fig. 1.11). The function of talin can be regulated either by dimerization, intra-molecular folding and auto-inhibition, or proteolytic cleavage between the head and the rod region by the cytoplasmic protease calpain (Goult et al., 2009; Yan et al., 2001). Pertinent to this thesis, talin HD is well established to be important for integrin activation. Overexpression of talin HD resulted in integrin activation (Calderwood et al., 1999; Eigenthaler et al., 1997), while siRNA-mediated knock-down of talin in cells led to impaired activation of integrin (Li et al., 2007; Smith et al., 2005). Talin 1 knockout in mice is embryonic lethal (Monkley et al., 2000; Priddle et al., 1998). The molecular basis of talin-dependent integrin activation is the separation of the integrin cytoplasmic tails by steric factors when the talin HD binds to the integrin β cytoplasmic domain. Using fluorescence resonance energy transfer (FRET), it was shown that the integrin αLβ2 cytoplasmic tails undergo separation in the presence of talin HD in cells (Kim et al., 2003). Although the F0, F1, and F2 subdomains in talin HD may not participate directly in integrin binding, there are several studies suggesting their importance nonetheless. The F2 subdomain is required for effective integrin activation by the F3 subdomain (Bouaouina et al., 2008; Ulmer et al., 2003), and the F0 subdomain was reported to bind with low affinity to Rap 1-GTP that is an important upstream activator of the integrins (Bouaouina et al., 2008).

Recently, another set of FERM-domain containing proteins known as kindlins were found to be important for integrin functions (Larjava et al., 2008; Ma et al., 2008; Montanez et

al., 2008). Three kindlin isoforms have been reported, and the domain organization of kindlin is shown (Ussar et al., 2006) (Fig. 1.12A). Like talin HD, kindlin has F1, F2 and F3 FERM subdomains, and the F2 subdomain is split by a pleckstrin homology (PH) domain insertion. The kindlin F3 subdomain, which shares similarity with talin F3 domain (Fig. 1.12B), binds to a second NPxY/F motif located at the C-terminal region of the integrin β cytoplasmic tail (Montanez et al., 2008). PH domain is known to interact with Receptor for Activated C Kinases (RACK1) (McCahill et al., 2002), Phosphatidylinositol (4,5)-bisphosphate (PIP2) (Czech, 2000), and many others. Kindlin1 and kindlin2 are ubiquitously expressed, whereas kindlin3 is restricted to the hematopoietic cells (Ussar et al., 2006). Kindlins are important for cell adhesion and spreading (Larjava et al., 2008; Ma et al., 2008; Montanez et al., 2008). Kindlin1 truncated at its C-terminus was shown to lead to abnormal adhesion and migration in keratinocytes (Has et al., 2008; Herz et al., 2006). Kindlin3-deficient mice die shortly after birth owing to severe bleeding from platelet dysfunction and defective inside-out integrin αIIbβ3 signaling (Moser et al., 2008). Loss of kindlin2 in mice results in peri-implantation lethality, and embryonic stem cells from these mice show decreased adhesion on a variety of integrin ligands (Montanez et al., 2008).

Interestingly, kindlin alone does not activate integrins. Instead, kindlin appears to function as co-activators of integrin together with talin. Co-expression of talin and kindlin2 or kindlin3 has a synergistic effect on integrin activation in αIIbβ3 transfected CHO cells and platelets (Montanez et al., 2008; Moser et al., 2008). The kindlins may serve to stabilize talin interaction with the integrin cytoplasmic tail thereby promoting adhesion strengthening via actin cytoskeleton connection (Tu et al., 2003). The precise mechanisms

by which kindlin promotes adhesion strengthening together with talin remain to be clarified.

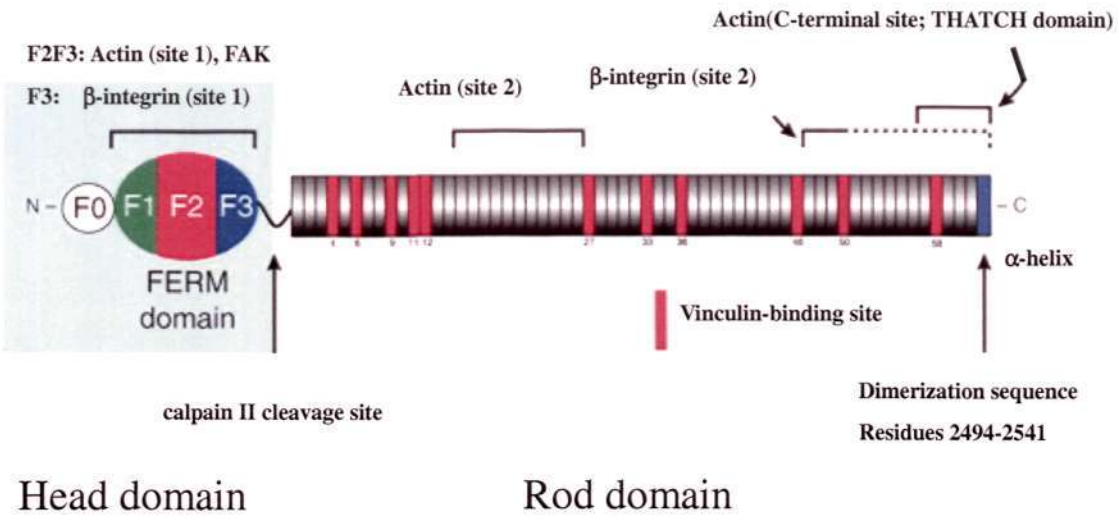

Fig. 1.11 Domain organization and binding partners of talin. A calpain II cleavage site separates the head and rod domains. The three subdomains of the classical FERM domain are represented in green, red and blue. Actin, integrin and vinculin binding sites are indicated. Talin dimerization sequence is indicated in the end of the rod domain (Adapted from Critchley., 2008).

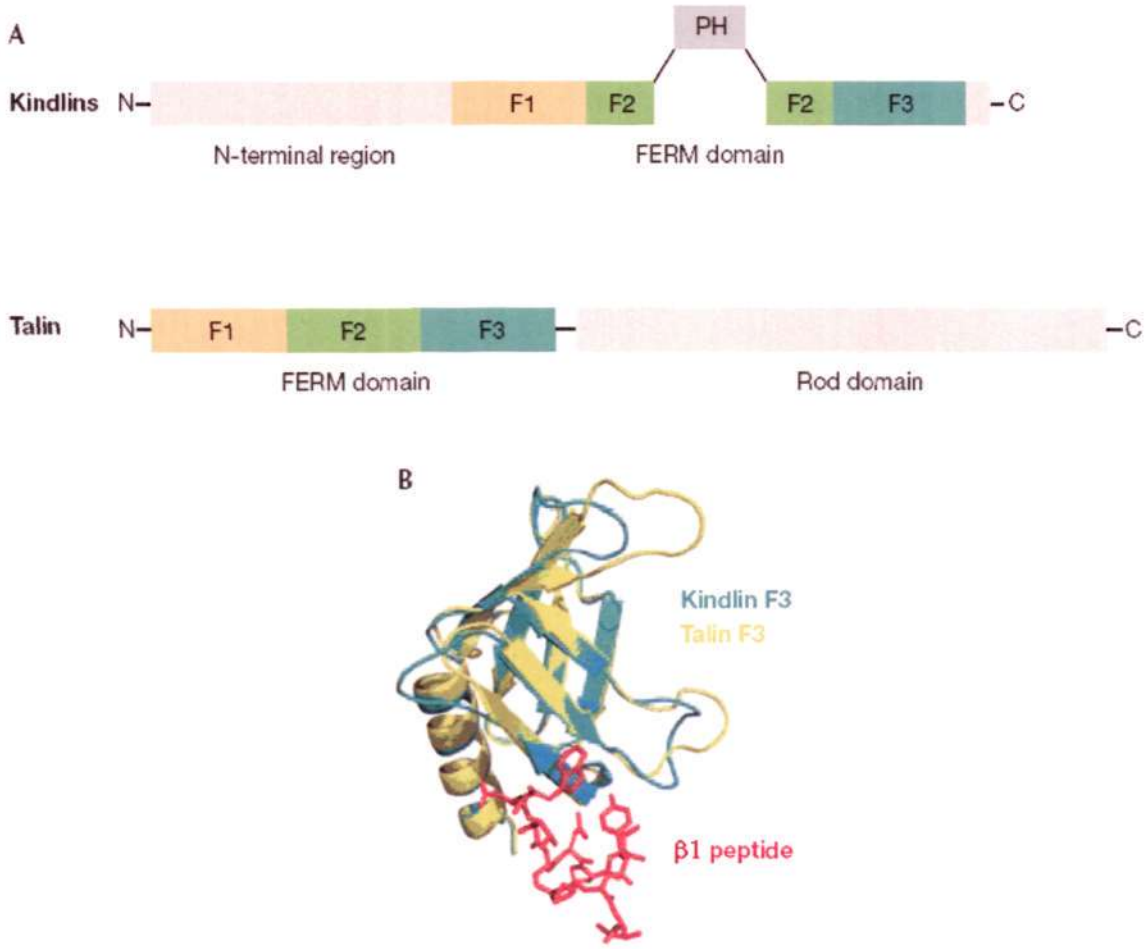

Fig. 1.12 Kindlin domain organization. (A) Domain architecture of kindlins and talin. All members of the kindlin protein family show identical domain architecture (top) showing the three FERM subdomains (F1-F3) characteristically intersected with a pleckstrin homology (PH) domain. (B) Overlay of the kindlin2 F3 subdomain model structure (blue) and the talin F3 subdomain structure (green) in complex with the β1-integrin cytoplasmic tail peptide (red) showing a conserved PTB (phosphotyrosine binding) fold (Adapted from Larjava., 2008).

1.5 The β2 integrins

All four members of the β2 integrins are expressed exclusively on leukocytes: αLβ2 (CD11a/CD18, Leukocyte Function-associated Antigen -1 or LFA-1), αMβ2 (CD11b/CD18, Complement Receptor 3 or Mac-1), αXβ2 (CD11c/CD18, CR4 or p150, 95), and αDβ2 (CD11d/CD18) (Gahmberg et al., 1997) (Table 1.3). These integrins are critical for the transmigration of leukocytes from the circulation to injury or infection sites, activation of neutrophils and monocytes, the phagocytosis of foreign materials and neutrophil apoptosis (Cinamon et al., 2001; Larson et al., 1990; Miles et al., 2008). The importance of the β2 integrins is exemplified in the disease leukocyte adhesion deficiency type (LAD) I in which patients suffered from recurrent bacterial and fungal infections because of poor recruitment of leukocytes into infected tissues.

Table 1.3 β2 integrins on leukocytes (Adapted from Luo et al., 2007)

Integrin	Distribution	Major ligands
αLβ2	Lymphocytes, NK cells, monocytes, macrophages, dendritic cells, neutrophils	ICAM-1, -2, -3, -5
αMβ2	Monocytes, macrophages, neutrophils, NK cells	Factor X, iC3b, heparin, fibrinogen, many others
αXβ2	Monocytes, macrophages, NK cells, dendritic cells	iC3b, fibrinogen, heparin, many others
αDβ2	Monocytes, macrophages, eosinophiles, neutrophils	ICAM-1, VCAM-1

1.5.1 Integrin αLβ2

The main focus in this thesis is the integrin αLβ2 that is expressed on all leukocytes (Barclay et al., 1997). Anti-αLβ2 antibodies have shown that this integrin participates in cytotoxic T cell killing, antigen-induced T cell proliferation and differentiation, NK cell killing, and leukocyte transendothelial extravasation (Davignon et al., 1981; Hildreth et al., 1983; Larson and Springer, 1990). Most leukocytes are normally nonadherent, circulating in the bloodstream as round and non-polarized cells. However, leukocytes also need to interact with other types of cells in various ways. The interaction of the leukocytes with blood vessel endothelium and subsequent recruitment of leukocytes into tissue is a multistep process (Siegelman, 2001). Leukocytes attach loosely to endothelium by the interaction of selectins with carbohydrate ligands on the endothelium. When this interaction occurs, leukocytes can be activated by, for example, immobilized chemokines on the surface of endothelium and will trigger firm adhesion via the integrins (Campbell et al., 1998). This is followed by polarization of the leukocyte with membrane protrusion (lamellipodium) and fingerlike protrusions (filopodia), forming a leading edge guiding the cell body containing the nucleus and an elongated uropod at the rear of the cell (Le Clainche and Carlier, 2008; Long et al., 2004; Sánchez-Madrid and Del Pozo, 1999). The migration process includes A) cell polarization, B) protrusion (pseudopod extension) and adhesion formation, C) release of rear attachment sites and uropod retraction with disassembly of adhesions (Ridley et al., 2003) (Fig. 1.13).

A. Cell Polarization

Regulators of Polarity	
Side/Rear	**Front**
PTEN	Activated Cdc42 & Rac
Myosin II	Cdc42/PARs/aPKC
	PIP_3
	Activated integrin
	MTOC/Golgi
	Microtubules

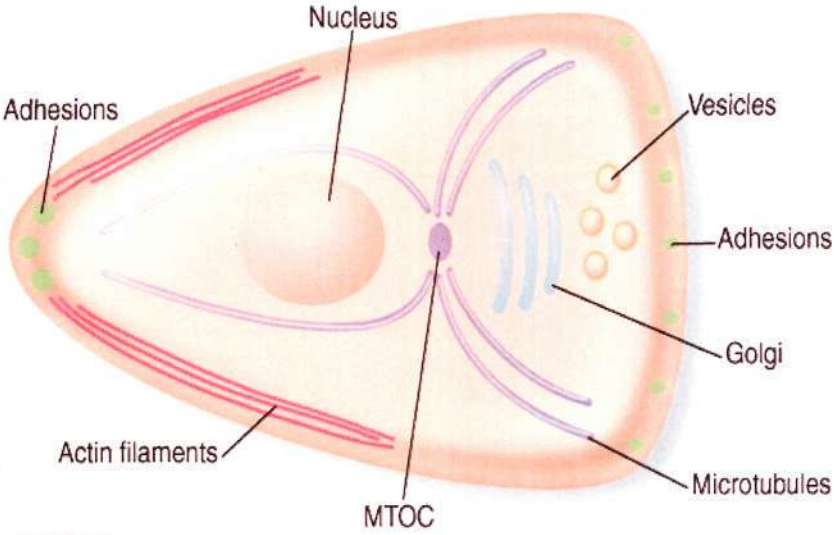

B. Protrusion and Adhesion Formation

Actin Polymerization	
Nucleation	**Polymerization/Organization**
Arp2/3 complex	Profilin
WAVE/WASP	ENA/VASP
Rac/Cdc42	ADP/Cofilin
	Capping proteins
	Cross linkers

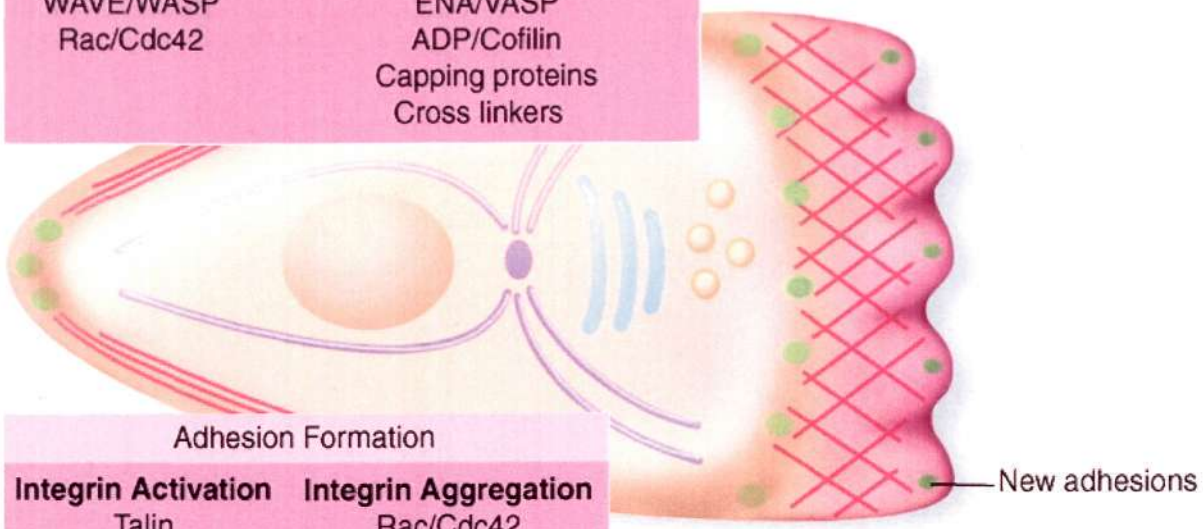

Adhesion Formation	
Integrin Activation	**Integrin Aggregation**
Talin	Rac/Cdc42
PKC	
Rap1	
PI3K	

Translocation

C. Rear Retraction

Rear Retraction
Adhesion Disassembly and Retraction
FAK/Src/ERK
Myosin II
Microtubules
Rho
Ca^{2+}
Calpain
Calcineurin

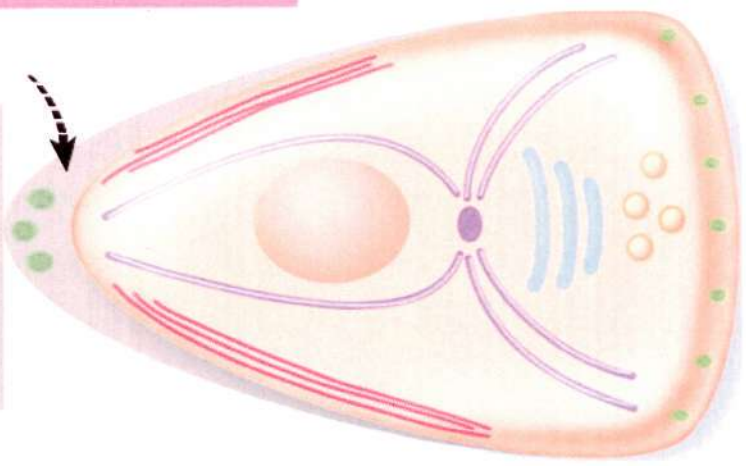

Fig. 1.13 Steps in cell migration. (A) Cell polarization. Cell division control protein 42 homolog (Cdc42), along with Par proteins and atypical protein kinase C (aPKC), are involved in the generation of polarity. Several additional proteins are implicated in polarity, which results in directed vesicle trafficking toward the leading edge, organization of microtubules (in some cells), and the localization of the microtubule-organizing center (MTOC) (in some cells) and Golgi apparatus in front of the nucleus. In the presence of a chemotactic agent, Phosphatidylinositol (3,4,5)-trisphosphate (PIP3) is produced at the leading edge through the localized action of Phosphoinositide 3-kinases (PI3Ks), which resides at the leading edge, and phosphatase and tensin homolog (PTEN), a PIP3 phosphatase that resides at the cell margins and rear. PTEN and myosin II are implicated in restricting protrusions to the cell front. (B) The migration cycle begins with the formation of a protrusion. Wiskott-Aldrich syndrome protein (WASP)/ WASP-family verprolin-homologous protein (WAVE) are targets of Rat sarcoma (ras)-related C3 botulinum toxin substrate (rac), Cdc42, and other signaling pathways. WASP/WAVE proteins regulate the formation of actin branches on existing actin filaments by their action on the Arp2/3 complex (the Actin-Related Proteins). Actin polymerization, in turn, is regulated by proteins that control the availability of activated actin monomers (profilin) and debranching and depolymerizing proteins (actin depolymerizing factors (ADF)/cofilin), as well as capping and severing proteins. Protrusions are stabilized by the formation of adhesions. This process requires integrin activation, clustering, and the recruitment of structural and signaling components to nascent adhesions. Integrins are activated by talin binding and through Protein kinase C (PKC)-, Ras-proximate-1 (Rap1)-, and PI3K-mediated pathways. Integrin clustering results from binding to multivalent ligands and is regulated by Rac. (C) At the cell rear, adhesions disassemble as the rear retracts. This process is mediated by several possibly related signaling pathways that include Sarcoma (Src)/ focal adhesion kinase (FAK)/ extracellular signal-regulated kinases (ERK), Ras homolog gene family (Rho), myosin II, calcium, calcineurin, calpain, and the delivery of components by microtubules. Many of these molecules may also regulate the disassembly of adhesions at the cell front that is behind the leading edge (from Ridley et al., 2003).

The ligands for αLβ2 are the intracellular adhesion molecules (ICAMs) and junctional adhesion molecule (JAM)-1 (Ebnet et al., 2004; Ostermann et al., 2002). ICAMs are single chain type I membrane glycoproteins of the Immunoglobulin-superfamily (IgSF) adhesion molecules. Five ICAMs have been identified and have been given numerical designations based on the chronological order of discovery (Hayflick et al., 1998): ICAM-1 (Marlin and Springer, 1987), ICAM-2 (Staunton et al., 1989), ICAM-3 (de Fougerolles and Springer, 1992), ICAM-4 (Landsteiner-Wiener antigen) (Bailly et al., 1995), and ICAM-5 (telencephalin) (Tian et al., 1997). JAM-1 is specifically localized at the tight junctions of epithelial and endothelial cells and is involved in the regulation of junctional integrity and permeability. JAM-1 can also bind in a heterophilic manner as it serves as a ligand for integrin αLβ2, and plays a key role in the process of leukocyte transmigration (Naik and Eckfeld, 2003). Two major ligands, ICAM-1 and ICAM-3, that are directly relevant to this study will be discussed.

ICAM-1 (CD54) is found to be expressed at low to moderate levels on the surface of endothelial and epithelial cells, leukocytes, dermal fibroblast, melanocytes, and many carcinoma cell types (Anderson and Siahaan, 2003). Its expression, however, can be significantly increased in the presence of cytokines (TNF-α, IL-1, and IFN-γ) (Hersmann et al., 1998) and reactive oxygen species (Hubbard and Rothlein, 2000). ICAM-1 has five immunoglobulin-like domains (D1-D5) and mutational studies have revealed that the crucial residues for αLβ2 binding are found in D1 (Casasnovas et al., 1998). On the cell surface, ICAM-1 exists predominantly in a dimeric form that binds more efficiently to αLβ2 than the transmembrane-lacking monomeric form (Miller et al., 1995). Through interaction with αLβ2, ICAM-1 plays a pivotal role in leukocyte-leukocyte, epithelial-leukocyte, and endothelial-leukocyte contact. Mice deficient in ICAM-1 have

impaired neutrophil emigration, an inability to stimulate T cell proliferation in mixed lymphocyte cultures, resistance to septic shock, and a reduced susceptibility to cerebral ischemia-reperfusion injury (Sligh et al., 1993).

ICAM-3 (CD50) is closely related to ICAM-1 and is also composed of five Ig-like domains, which share 52 % homology with those of ICAM-1 (Barclay et al., 1997). ICAM-3 is expressed on leukocytes and is the only ICAM significantly expressed on epidermal Langerhans cells where presentation of alloantigen or peptide antigen by these cells to $CD4^+$ T cells may require an interaction between ICAM-3 and αLβ2 (Acevedo et al., 1993).

1.5.2 Integrin αMβ2

Integrin αMβ2 heterodimers are mainly expressed on leukocytes of the myeloid monocytic lineage and natural killer lymphocytes (Larson and Springer, 1990). It is a remarkably versatile adhesion and recognition receptor, binding both endogenous as well as an array of microbial ligands (Ehlers, 2000). αMβ2 can cooperate functionally with a variety of other surface receptors, including the urokinase-type plasminogen activator receptor (uPAR) (Tang et al., 2006), Fc gamma receptors (FcγRs) (Fernandez-Calotti et al., 2003), Toll-like receptor 2 (TLR2) (Hajishengallis and Harokopakis, 2007), and CD14 (Ehlers, 2000). The interaction of αMβ2 and uPAR are required for fibrinolysis by myeloid cells (Simon et al., 1993) and it was reported that uPAR changed the conformation of αMβ2 (Tang et al., 2008a). αMβ2 can recognize many pathogens directly and can mediate the phagocytosis of microbes.

The complement proteolysis product iC3b is one of the most important ligands of αMβ2, the efficiency of αMβ2-mediated phagocytosis is enhanced significantly when the foreign

body is opsonized by iC3b (Mayadas and Cullere, 2005). αMβ2 is also involved in modulating the life span of neutrophils (Mayadas and Cullere, 2005).

1.5.3 Integrin αXβ2

Integrin αXβ2 is expressed mainly on myeloid cells and its tissue distribution overlaps with that of αMβ2. It also contributes to leukocyte adhesion to endothelium and phagocytosis (Stacker and Springer, 1991). The ligands of αXβ2 include iC3b (Malhotra et al., 1986; Micklem and Sim, 1985), fibrinogen (Loike et al., 1991; Postigo et al., 1991), ICAM-1 (Blackford et al., 1996), LPG (lipophosphoglycan) (de Fougerolles et al., 1995; Ingalls and Golenbock, 1995), and denatured proteins (Bilsland et al., 1994). αXβ2 is involved in the adhesion of monocytes and neutrophils to endothelium and other cells and substrates (Anderson et al., 1986; Bullard et al., 2007; Keizer et al., 1987a; Keizer et al., 1987b; Stacker and Springer, 1991; te Velde et al., 1987).

1.5.4 Integrin αDβ2

αDβ2 is the last reported member of the β2 integrins (Van der Vieren et al., 1995). It is expressed on myelomonocytic cells, macrophage foam cells and splenic pulp macrophages (Noti, 2002). It can bind to ICAM-3 (Van der Vieren et al., 1995) and VCAM-1 (Van der Vieren et al., 1999). In an experimental model of spinal cord injury, it has been reported that the injection of monoclonal antibodies directed against αDβ2 reduces lesion-induced accumulation of macrophages or neutrophils by approximately 50 % (Mabon et al., 2000).

1.6 Aims of study

The integrin αLβ2 can adopt at least three conformations with different affinity-states,

low, intermediate, and high aforementioned. Although the cytoplasmic protein talin is known to activate αLβ2 by separating its cytoplamic tails, it was not known at the time of this study the affinity state of talin-activated αLβ2. The first part of this study made use of different cell-based approaches to delineate the affinity state of αLβ2 activated by talin.

Apart from talin, there has been a growing list of studies reporting the importance of the cytoplasmic proteins kindlins in integrin activation. Apparently, kindlin alone does not activate integrins. Instead it serves as a co-activator of talin induced integrin affinity up-regulation. At present, the characterization of the hematopoetic cells-restricted kindlin3 regulation of integrin αLβ2 function is lacking. This is investigated in the second part of this study.

Chapter 2 Materials and methods

2.1 Materials

2.1.1 General reagents

Most general chemicals and solvents were of analytical grade, and were obtained from Sigma-Aldrich (St. Louis, MO), BDH Chemicals (West Chester, PA), BD (Franklin Lakes, NJ), Pierce Biotechnology (Rockford, IL), unless otherwise stated. All restriction endonucleases, ligase and other enzymes were obtained from New England Biolabs (Ipswich, MA), Promega (Madison, WI), Fermentas (Canada), Roche (Switzerland), unless otherwise stated and they were used according to the manufacturers' instructions. DNA marker and loading dye were bought from Fermentas (Canada). Protein marker was from New England Biolabs (Ipswich, MA).

2.1.2 Vectors and cDNA

pcDNA3.0 and pcDNA3.1 (+) were bought from Invitrogen (Carlsbad, CA). ICAM-1/Fc and ICAM-3/Fc, both containing the five immunoglobulin-like domains (D1-D5), were kindly provided by Dr. D.L. Simmons (IMM, Oxford). Integrin αL and β2 cDNAs in the expression plasmid pcDNA3.0 were described previously (Tan et al., 2000), and the numbering of integrin amino acids was based on Barclay et al. (Barclay et al., 1997). pEGFP-N1 and pEGFP-C1 were generous gifts from Dr. D.X. Liu and Dr. H.Y. Li, respectively (School of Biological Sciences (SBS), Nanyang Technological University (NTU)).

2.1.3 Cells

Jurkat cells (human T lymphoblast), MOLT-4 cells (human T lymphoblast), SKW 3.0 cells

(human T lymphoblast), HUT-78 cells (human T lymphoblast), 293-T cells (human embryonic kidney cell with SV40 large T antigen), and COS-7 cells (African green monkey kidney cells) were purchased from American Type Culture Collection (ATCC) (Manassas, VA). Peripheral blood T lymphocytes and T lymphoblasts were isolated and provided by collaborators.

2.1.4 Antibodies

MHM24	From Prof. A.J. McMichael (John Radcliffe Hospital, Oxford, UK)
MHM23	From Prof. A.J. McMichael (John Radcliffe Hospital, Oxford, UK)
MEM148	From Prof. V. Horejsi (Prague, Czech Republic)
KIM127	From Prof. M.K. Robinson (CellTech, Slough, UK)
KIM185	From Prof. M.K. Robinson (CellTech, Slough, UK)
1B4	From Prof. S.K.A. Law (SBS, NTU)
m24	From Prof. N. Hogg (London Research Institute, London, UK)
7E4	From Beckman Instruments (Fullerton , CA)

Purified IgGs of MHM24, KIM127, KIM185, and 1B4 were prepared from hybridoma supernatants using Hi-Trap protein G columns (Amersham, New York, NY). Mouse anti-human talin 8d4 was bought from Sigma-Aldrich (St. Louis, MO). Mouse anti-human TCR (T10B9.1A-31), mouse anti-human CD3 (UCHT1), and mouse anti-human actin (Ab-5) were purchased from BD (Franklin Lakes, NJ). Mouse monoclonal antibody against RACK1 (B-3) was bought from Santa Cruz Biotechnology (Santa Cruz, CA). Rabbit anti-hemagglutinin (HA) polyclonal antibody was purchased from Delta Biolabs (Gilroy, CA). Horse radish peroxidase (HRP)-conjugated donkey anti-rabbit IgG and HRP-conjugated sheep anti-mouse IgG were from Amersham (New York, NY).

Rabbit anti-kindlin3 antibody was generated as follows: A kindlin-3-specific peptide (EPEEELYDLSKVVLA) was coupled to Imject Maleimide Activated mcKLH (Pierce Biotechnology, Rockford, IL) and used to immunize rabbits. The antiserum was subsequently affinity purified using a commercial SulfoLink Kit (Pierce Biotechnology, Rockford, IL). The SulfoLink Immobilization Kit for Proteins contains the mild reducing agent 2-mercaptoethylamine (2-MEA), which effectively reduces only certain disulfide bonds in proteins, including those in the region of IgG molecules. After this selective reduction step, excess 2-MEA was removed using a Zeba Desalt Spin Column and the protein was conjugated to SulfoLink Resin through the exposed sulfhydryl groups. Kindin3-specific antibodies were eluted from the column using 100 mM Glycine buffer (pH 2.7) and dialyzed against phosphate-buffered saline (PBS, pH 7.4).

2.1.5 Ligands for cell binding analysis

ICAM-1/Fc and ICAM-3/Fc were prepared by Miss Elianna Bte Mohamed Amin (SBS, NTU). Briefly, 10 large flasks of COS-7 cells were transfected with human ICAM/Fc in expression plasmid πH3M using the DEAE Dextran method of cell transfection. 8-12 days after transfection the tissue culture supernatant was spun and stored at 4 °C. Purified ICAM/Fc was prepared by passing the tissue culture supernatant through protein A sepharose column (GE healthcare, United Kingdom). ICAM/Fc was eluted according to the manufacturer's instructions.

2.1.6 Media

All media were sterilized by autoclaving unless otherwise stated.

LB medium	1 % (w/v) Bacto-tryptone (BD, Franklin Lakes, NJ), 0.5 % (w/v) yeast extract (BD), 1 % (w/v) NaCl
LB agar	LB medium plus 1.5 % (w/v) Bacto-agar (BD)
LA broth	LB medium containing 60 μg/mL ampicillin
LA plate	LB agar plate containing 60 μg/mL ampicillin
LK broth	LB medium containing 30 μg/mL kanamycin
LK plate	LB agar plate containing 30 μg/mL kanamycin
293-T cell culture medium	Dulbecco's modified Eagle's medium (DMEM) (HyClone, Logan, Utah) containing 10 % (v/v) heat-inactivated Fetal Bovine Serum (FBS), 100 IU/mL penicillin, 100 μg/mL streptomycin
HUT-78 cell culture medium	Iscove's modified Dulbecco's medium (IMDM) (HyClone, Logan, Utah) containing 10 % (v/v) heat-inactivated FBS, 100 IU/mL penicillin, 100 μg/mL streptomycin
MOLT-4, COS-7, SKW 3.0, and Jurkat cell culture media	RPMI1640 (HyClone, Logan, Utah) containing 10 % (v/v) heat-inactivated FBS, 100 IU/mL penicillin, 100 μg/mL streptomycin

2.1.7 Solutions

blocking buffer (western)	PBS-T (PBS with 0.1 % (v/v) Tween-20) containing 5 % (w/v) non-fat milk, pH 7.4
blotting buffer (western)	12.5 mM Tris, 96 mM glycine, 10 % (v/v)

	ethanol, pH 8.0
cell freezing media	10 % (v/v) DMSO in heat-inactivated FBS
lysis buffer	50 mM Tris, 150 mM NaCl, 1 % (v/v) NP-40, pH 8.0
10× SDS-PAGE electrophoresis buffer	0.25 M Tris, 1.9 M glycine, 1 % (w/v) SDS
4× resolution gel buffer	0.25 Tris, 0.4 % (w/v) SDS, pH 8.8
4× stacking gel buffer	0.5 M Tris, 0.4 % (w/v) SDS, pH 6.8
sodium bicarbonate buffer	1.36 g sodium carbonate, 7.35 g sodium bicarbonate, pH 9.2
60 mg/mL ampicillin	60 mg/mL in ddH_2O, pH 8.4, filtered (0.22 μm)
30 mg/mL kanamycin	30 mg/mL in ddH_2O, pH 8.4, filtered (0.22 μm)

2.2 Methods

2.2.1 General methods for DNA manipulation

2.2.1.1 Miniprep, midiprep and maxiprep of plasmid DNA

For small-scale purification of plasmid DNA, 5 mL LB with appropriate antibiotics was inoculated with a single colony of *Escherichia coli* that contains recombinant plasmid from an agar plate and incubated at 37 °C with constant shaking overnight. A QIAprep Spin Miniprep Kit (QIAGEN, Valencia, CA) was used to extract DNA according to the manufacturer's instructions. For midiprep and maxiprep plasmid, the bacteria clone was cultured in 3-5 mL LB in 15 mL tube for 8-12 h before being transferred to a flask

containing 100 mL LB with antibiotics and incubated with shaking overnight. Plasmid Midi Kit (Axygen, Union City, CA) and Plasmid Maxi Kit (QIAGEN, Valencia, CA) were used according to the manufacturers' instructions.

2.2.1.2 Quantitation of DNA

The concentration of DNA was determined using DU 530 Life Science UV/Visible Spectrophotometers (Beckman Coulter, Fullerton, CA) by its absorbance at wavelength 260 nm based on the calculation: 50 μg/mL double-stranded DNA gives an OD_{260} of 1. The OD_{280} was also read and the ratio of OD_{260}/OD_{280} was calculated to estimate the purity of the DNA solutions. An OD_{260}/OD_{280} ratio between 1.6 and 2.0 was considered satisfactory.

2.2.1.3 Restriction endonuclease digestion

Restriction endonuclease digestions were usually carried out in a 20-80 μl reaction volume: 2-5 U of enzyme used frequently for up to 500 ng DNA together with Bovine Serum Albumin (BSA) and appropriate buffer at 37 °C for 2-3 h for restriction digestions. Digestions with more than one enzyme were carried out simultaneously in a suitable buffer as recommended by the manufacturer. When the buffer requirements were incompatible, restriction digestions were performed sequentially with individual buffer for each enzyme.

2.2.1.4 DNA electrophoresis

A 40 mL 1 % (w/v) agarose gel (agarose was melted in 1×TAE (Tris-acetate-EDTA, pH 8.0)) was regularly used for analysis of 0.1-8 kb DNA fragments. Ethidium bromide was added to a final concentration of 1 μg/mL followed by casting in a mini-gel apparatus. Electrophoresis was carried out in a horizontal gel apparatus with the gel submerged in 1x TAE. DNA samples were loaded with loading dye. DNA fragments were visualized by

fluorescence over a UV light (302 nm, UV transilluminator TM-20, UVP), under which DNA/EB complexes fluoresce and the image was recorded with a Gel Doc 1000 imaging system (Bio-RAD, Italy).

2.2.1.5 Purification of DNA fragments from agarose gel

When a particular fragment of DNA in a mixture of fragments was required, e.g. in ligations or as a PCR template, it was routinely separated from other fragments by agarose gel electrophoresis. Gel slice containing the DNA fragments to be purified was cut from the gel using a razor blade, carefully avoiding their exposure to the UV light. DNA was extracted using a QIAquick Gel Extraction Kit (QIAGEN, Valencia, CA).

2.2.1.6 DNA ligation

DNA vectors with complementary ends to be used for ligation were prepared by restriction enzyme digestion and where necessary treated with alkaline phosphatase and purified using agarose gel electrophoresis. Vector DNA (~ 10 ng) and insert DNA (20-40 ng) were ligated by incubation at RT for 2-3 h, using 1U of T4 DNA ligase with ligase buffer provided together with the enzyme in a 20 µl reaction volume. A reaction with uncut vector, a reaction without insert DNA, and a reaction without both insert DNA and T4 DNA ligase were included in the experiments as controls.

2.2.1.7 Preparation of *Escherichia coli* competent cells

The *Escherichia coli* strain DH5α was used to prepare competent cells in advance which were stored at -70 °C. A fresh plate of cells was prepared by streaking out cells from frozen stocks and growing at 37 °C for overnight. On the second day, an individual colony was picked and grown in 10 mL LB broth culture overnight. On the third day, 5 mL of overnight culture was transferred into each of two flasks containing 500 mL LB broth followed by incubation at 37 °C with aeration until the culture reaches OD_{550} of 0.5.

This should take approximately 2 h. The cells were transferred to centrifuge bottles and spun at 4 °C for 8 min at 8000 rpm. Pellets were gently resuspended in 250 mL ice cold 0.1 M $CaCl_2$ and combined into a single bottle. Cells were resuspended again in 250 mL ice cold 0.1 M $CaCl_2$ and centrifuged at 8000 rpm at 4 °C for 8 min. Finally the pellet was resuspended in 43 mL ice cold 0.1 M $CaCl_2$ in ddH_2O with 7 mL sterile glycerol. Competent cells were distributed into convenient aliquots (0.2 mL) in cold microcentrifuge tubes. Cells were stored at -70 °C. An aliquot of the cells was used to assay for viability, purity and competence.

2.2.1.8 Transformation of plasmid DNA

Competent cells (50-100 μl) are necessary for one reaction. Competent cells were thawed on ice. Plasmid DNA (1 μg) or ligation product (10 μl of the ligation product aforementioned) was added to cells followed by incubation on ice for 30 min. This was followed by a heat shock in a 42 °C water bath for 2 min and on ice for another 2 min. LB broth (500 μl) was added to the tube. The tube was incubated at 37 °C with constant shaking at 150-200 rpm for 30 min to 1h. 50-500 μl of the mixture was spread out onto LB agar plates containing the appropriate antibiotics.

2.2.1.9 Standard PCR protocol

PCR was routinely performed in a 50 μl reaction volume containing 1 μg template DNA, 1 μM of each oligonucleotide primer, 200 μM of each dNTP, and 1 U DNA polymerase. Taq polymerase (Fermentas, Canada) was used for PCR colony screening. Pfu DNA polymerase (Promega, Madison, WI), which possesses a 3'-5' proof-reading activity resulting in a twelve-fold increase in fidelity of DNA synthesis over Taq DNA polymerase, was used for high fidelity DNA synthesis. Each polymerase has its own reaction buffer, normally supplied by the manufacturer. The reaction mixtures were subjected to a varying

number of cycles of amplification using the DNA Thermal Cycler as required for different PCR reactions (MJ research, Waltham, MA).

2.2.1.10 Selection of colonies that contain recombinant genes of interest

After transformation of competent cells, colonies of interest were identified using either PCR screening or restriction digestion, depending on the availability of suitable PCR primers for screening and the degree of background indicated by the control plates. Each colony to be tested was used to inoculate 15 µl LB. 1 µl of this inoculated LB broth was added to a 25 µl PCR reaction containing 0.5 U Taq polymerase. A negative control and, where possible, a positive control were included in the experiment. Colonies containing the recombinant plasmid of interest were identified by the size of their PCR products using agarose gel electrophoresis. Positives from PCR screening were confirmed using restriction digestion. Where necessary, DNA sequencing of the plasmids was performed (Research Biolabs, Singapore).

2.2.1.11 Site-directed mutagenesis

Point mutations were made using a QuikChange Site-Directed Mutagenesis (SDM) Kit (Strategene, Santa Clara, CA), following the manufacturer's protocols. Overlapping primers with the desired mutations were used in the long PCR cycle. The restriction enzyme Dpn I was used to digest the original template. The Dpn I treated PCR product was transformed in competent *Escherichia coli* and plated onto LB agar plates with appropriate antibiotics. All constructs were verified by sequencing (Research Biolabs, Singapore).

2.2.1.12 mRNA extraction and reverse transcription PCR

mRNA Isolation Kit (Roche, Switzerland) was used for mRNA extraction according to the manufacturer's instructions. Briefly, cells were washed twice with ice cold PBS and

lysed by adding lysis buffer. Biotin-labeled oligo (dT)20 probe was added to the cell lysate and mixed. Magnetic particles were separated from storage buffer by magnetic separation and washed once with lysis buffer. Thereafter, cell lysate with oligo (dT)20 probe was combined with the magnetic particles and incubated at 37 °C for 5 min. The magnetic particles were separated from the fluid by magnetic separation and washed three times with washing buffer. Finally, redistilled water was added to the magnetic particles and incubated at 65 °C for 2 min. mRNA was separated from magnetic particles and transferred to a fresh RNase-free tube.

QIAGEN One Step RT-PCR Kit (QIAGEN, Valencia, CA) was subsequently used for reverse transcription PCR of mRNA. The reverse transcription of mRNA to cDNA was carried out by Omniscript™ Reverse Transcriptase/ Sensiscript™ Reverse Transcriptase at 50 °C for 30 min. Standard PCR procedures were followed to obtain the cDNA of interest.

2.2.2 General methods for cell culture

All cells were maintained in 5 % CO_2 at 37 °C in a humidified incubator using Nunc tissue culture flasks or dishes (Nunc, Rosklide, Denmark).

2.2.2.1 Cell storage in liquid nitrogen

Cells were sedimented at 400 g for 5 min, resuspended in cell freezing medium at a concentration of 5 x 10^6 cells/ml and dispensed into Cryo Vials (Greiner, Monroe, NC). Cells were frozen in a NALGEN™ Cryo 1 °C freezing Container (Thermo Fisher Scientific, Waltham, MA) at -70 °C for 24 h to achieve a -1 °C/min cooling rate. Thereafter the vials were transferred into liquid nitrogen for long term storage.

2.2.2.2 Cell recovery from liquid nitrogen

Cells were removed from the liquid nitrogen storage and quickly thawed at 37 °C in a water bath. Cells were left resting in 10 ml warmed medium for 5 min and centrifuged (400 g, 5 min) to remove DMSO. The cell pellet was resuspended in complete media and cultured in 5 % CO_2 at 37 °C in a humidified incubator.

2.2.2.3 Culture of 293-T and COS-7 cells

293-T cells were maintained in DMEM medium containing 10 % (v/v) heat-inactivated FBS, 100 IU/ml penicillin, and 100 μg/ml streptomycin at 37 °C in a humidified 5 % CO_2 incubator. Cells were passaged every two days when they reach subconfluency. Cells were washed twice in PBS, incubated in 0.25 % (w/v) trypsin (Invitrogen, Carlsbad, CA) at 37 °C for 1 min, followed by tapping of each flask to dislodge the adherent cells. Trypsin was subsequently inactivated by adding complete medium and cells were directly seeded into fresh culture medium in new flasks or dishes at desired density. COS-7 cells were cultured similarly, except that RPMI1640 was used.

2.2.2.4 Culture of MOLT-4, Jurkat, SKW 3.0 and HUT-78 cells

MOLT-4, Jurkat, and SKW 3.0 cells were maintained in complete RPMI1640 medium. HUT-78 cells were maintained in complete IMDM medium. Both media were supplemented with 10 % (v/v) heat-inactivated FBS, 100 IU/ml penicillin, and 100 μg/ml streptomycin. Cells were passaged by diluting cells with fresh media after reaching the density of 10^6 cells/ml.

2.2.2.5 Generation and maintainance of peripheral blood T lymphocytes

Peripheral blood T lymphocytes (PBTLs) were isolated by the method of negative selection (NS) or positive selection (PS) from human peripheral blood mononuclear cells. Briefly, using the method of PS, peripheral blood mononuclear cells were stained with fluorescein isothiocyanate-conjugated anti-αβ TCR (T10B9.1A-31) followed by

anti-fluorescein isothiocyanate mAb conjugated to MicroBead (Miltenyi Biotec, Auburn, CA) on ice for 30 min. Labeled cells were washed once, loaded on an LS MACS column, and $\alpha\beta^+$ T cells were eluted according to the manufacturer's instructions. Using the method of NS, peripheral blood mononuclear cells were processed and loaded onto a T Cell Enrichment Column (R&D Systems, Minneapolis, MN) according to manufacturer's instructions. In both cases, purified cells were allowed to recover in complete RPMI1640 culture medium overnight. Ex vivo expansion of PBTLs to obtain T lymphoblasts was performed by maintaining cells in RPMI1640 supplemented with 10 % heat-inactivated FBS, 2 μg/ml PHA, and 1 nM recombinant interleukin-2 (Chiron, Emeryville, CA).

2.2.3 Transfection of cells

2.2.3.1 Tranfection and harvesting of 293-T and COS-7 cells

Cells were split into 6 cm dishes the night before to give around 70-90 % confluence at the day of transfection. On the next day, 40 μl Poly-fect reagent (QIAGEN, Valencia, CA) was added to 150 μl serum-free medium containing 4 μg expression plasmids. After 5-10 min incubation, 1 ml full media was added to the Poly-fect and DNA mixture and applied to cells slowly as recommended by the manufacturer.

24-48 h after transfection, the cells in each dish were washed in PBS and detached in 2 ml of 0.5 mM EDTA in PBS by incubation at RT for 5 min with gentle rocking. Cells were collected and mixed with 5 ml full media and transferred to centrifuge tubes. Cells were spun down (400 g, 5 min, 4 ^{o}C) for subsequent analysis.

2.2.3.2 Transfection of MOLT-4 and HUT-78 cells

The EGFP-tagged talin HD expression plasmid (2 μg) was transfected into MOLT-4 cells (2 x 10^6 cells per reaction) using the Amaxa Nucleofector device and Cell Line Nucleofector Kit L as per the manufacturer's instructions (Amaxa Gmbh, Germany).

HUT-78 cells (0.5 x 10^6 cells per reaction) were transfected with 5 μg of talin siRNA or its control siRNA (Ambion, Austin, TX) using Cell Line Nucleofector Kit R (Amaxa Gmbh, Germany). The cell pellet was resuspended in room temperature (RT) in desired solution plus plasmids or siRNA. The nucleofection sample was transferred into an Amaxa certified cuvette and air bubbles were avoided. The Nucleofector programs (C-005 for MOLT-4 cells and V-001 for HUT-78 cells) were selected to electroporate the samples. The successfully electroporated samples were added to the prewarmed 12-well plates containing 1 ml medium and cultured for 24-48 h before analysis.

2.2.3.3 Transfection of SKW 3.0 cells

The expression plasmid (10 μg each) (EGFP, EGFP-kindlin3, EGFP-kindlin3 W600A, EGFP-kindlin3 F3 deleted, or EGFP-kindlin3 PH deleted) was transfected into SKW 3.0 cells (2 x 10^6 cells per reaction) using Microporator MP-100 (a pipette type electroporator) and reagents as per the manufacturer's instructions (NanoEnTek, Korea). The same number of cells per reaction was transfected with 5 μg of talin siRNA or its control siRNA (Ambion, Austin, TX). The cell pellet was resuspended in R buffer with desired plasmids or siRNA. The samples were added into gold tips (100 μl) which were connected to the provided pipette and air bubbles were avoided. The optimized microporation program (pulse voltage, width, and number: 1350 V, 20 ms, 2) was used to electroporate the samples. Electroporated cells were added to the prewarmed 6-well plates containing 2 ml medium and cultured for 24-48 h before analysis.

2.2.3.4 Flow cytometry analysis for integrin expression

Flow cytometry analysis of integrin cell surface expression was performed as described previously (Tan et al., 2000). Briefly, cells were incubated with 20 µg/ml primary mAb in RPMI wash buffer (RPMI1640 medium containing 5 % (v/v) heat-inactivated FBS and 10

mM HEPES (pH 7.4)) at 4 °C for 1 h. Thereafter, cells were washed and incubated with FITC-conjugated sheep anti-mouse F $(ab)_2$ secondary Ab (1:400 dilution) (Sigma-Aldrich, St. Louis, MO) at 4 °C for 45 min. Stained cells were washed once and fixed in 1 % (v/v) formaldehyde in PBS. Cells were analyzed on a FACSCalibur and data were processed using CellQuest Pro software (BD, Franklin Lakes, NJ). Expression index was calculated by (% cells gated positive) x (geomean fluorescence intensity).

2.2.3.5 Flow cytometry using αLβ2 activation reporter mAbs

Peripheral blood T lymphocytes and T lymphoblasts were incubated with 20 μg/ml mAb MHM24, CD3, MEM148, KIM127 or m24 in RPMI wash buffer (RPMI1640 medium containing 5 % (v/v) heat-inactivated FBS and 10 mM HEPES (pH 7.4)) at 37 °C for 0.5 h. Cells were washed once followed by incubation with FITC-conjugated secondary antibody at 4 °C for 45 min. Samples were fixed in 1 % (v/v) formaldehyde in PBS and analyzed by flow cytometry analysis aforementioned.

2.2.3.6 Flow cytometry for EGFP-kindlin3 and DsRed-talin HD expression

The expression of 293-T tranfectants bearing EGFP-kindlin3 and DsRed-talin HD was verified by flow cytometry. Cells were washed once and were resuspended in 1 % (v/v) formaldehyde in PBS and analyzed by flow cytometry analysis aforementioned with relevant fluorescence compensation. The percentage of cells in each quadrant is stated.

2.2.3.7 Flow cytometry sorting of transfected SKW 3.0 cells

Transfected SKW 3.0 cells (EGFP, EGFP-kindlin3, EGFP-kindlin3 W600A, EGFP-kindlin3 F3 deleted, or EGFP-kindlin3 PH deleted) were sorted with a Flow Cytometry Aria system (BD, Franklin Lakes, NJ) based on the same gate showing the same level of EGFP fluorescence emission signal. Sorted cells were collected into complete RPMI1640 medium.

2.2.3.8 Cell surface labeling and preparation of whole cell lysate

Harvested MOLT-4 and HUT-78 cells were washed twice in PBS followed by incubation in freshly prepared sulfo-NHS-biotin (Pierce Biotechnology, Rockford, IL) at 0.5 mg/ml in PBS on ice for 30 min. The reaction was quenched by washing surface-labeled cells once in PBS containing 10 mM Tris-HCl (pH 8.0) and 0.1 % BSA (w/v). Thereafter, cells were incubated with 3 μg mAbs (irrelevant mAb, MHM23, or MEM148) with or without Mg^{2+}/EGTA (5 mM $MgCl_2$ and 1.5 mM EGTA) in RPMI wash buffer (RPMI1640 medium containing 5 % (v/v) heat-inactivated FBS and 10 mM HEPES (pH 7.4)) at 37 °C for 30 min. Each sample was washed twice with PBS and lysed in 350 μl lysis buffer (10 mM Tris-HCl (pH 8.0), 150 mM NaCl, 1 % (v/v) Nonidet P-40) with protease inhibitors (Complete Protease Inhibitor Cocktail Tablets, Roche, Switzerland) on ice for 30 min. Cell debris were removed by centrifugation at 12000 g at 4 °C for 10 min. The cell lysates in the supernatant were transferred into fresh microfuge tubes.

2.2.3.9 Preparation of protein A sepharose with rabbit anti-mouse IgG conjugation

1 g of protein A sepharose (PAS) (Amersham, New York, NY) was swollen in PBS and rotated at 4 °C overnight. Thereafter, the PAS beads, which occupied a bed volume of approximately 4 ml, were sedimented by centrifugation (3000 g, 5 min, 4 °C), washed twice and resuspended to a 25 % (v/v) suspension in PBS. 4 g of rabbit anti-mouse IgG (RaM) (Sigma-Aldrich, St. Louis, MO) was added and the mixture was rotated at 4 °C for 1 h. The PAS-RaM beads were washed twice in PBS and resuspended to a 25 % (v/v) suspension in PBS and stored at 4 °C. PAS-RAM beads were used for immunoprecipitation assays hereafter.

2.2.3.10 Immunoprecipitation and immunoblotting of biotinylated cell lysates

PAS-RAM (100 μl bead suspension) was added to the 350 μl cell lysates of biotinylated samples and the mixture was rotated at 4 °C for 1.5 h. The PAS-RaM was sedimented by centrifugation (3000 g, 2 min, 4 °C) and the supernatant was discarded. The PAS-RaM was washed in 1 ml lysis buffer for three times. Finally, 40 μl protein solubilisation buffer containing 40 mM dithiothreitol (DTT) was added to the PAS-RaM which was subsequently vortexed and heated at 100 °C for 10 min. The immunoprecipitated proteins were stored at -20 °C or resolved by SDS-PAGE (details below). Biotinylated proteins that were transferred onto PVDF membranes by Western blotting (details below) were probed with a streptavidin-HRP (Horse radish peroxidase) conjugate (1:1000 dilution) (Amersham, New York, NY) and were then detected by Enhanced Chemiluminescence (ECL).

2.2.3.11 Immunoblotting of whole cell lysates

HA-tagged talin HD was probed using rabbit anti-HA antibody followed by HRP-conjugated donkey anti-rabbit IgG and detected by ECL. For talin knock-down by siRNA, the endogenous talin and actin of HUT-78 and SKW 3.0 cells were probed with anti-talin mAb 8d4 and anti-actin mAb, respectively, followed by HRP-conjugated sheep anti-mouse IgG and ECL detection. The expression of EGFP-kindlin3, EGFP-kindlin3 W600A, EGFP-kindlin3 F3 deleted, and EGFP-kindlin3 PH deleted mutants were probed with purified rabbit anti-kindlin3 mAb followed by HRP-conjugated donkey anti-rabbit IgG and ECL detection, while the αL co-expression was detected with anti-αL mAb followed by HRP-conjugated sheep anti-mouse IgG and ECL detection.

2.2.3.12 Sodium dodecyl sulphate polyacrylamide gel electrophoresis (SDS-PAGE)

SDS-PAGE was performed as described by Laemmli (1970) with slight modifications. Protein sample (15 μl for minigel system) was mixed with an equal volume of sample

loading buffer (2×) in the presence of 40 mM DTT under reducing conditions. Electrophoresis was carried out at 200 V in a Mini Electrophoresis Set (Bio-RAD, Italy) in SDS-PAGE electrophoresis buffer.

2.2.3.13 Western blotting

Proteins separated by SDS-PAGE were transferred onto a PVDF membrane (Immobilon-P, Millipore) by western blotting. The PVDF membrane was prepared according to the manufacturer's instructions. Briefly, the membrane was equilibrated by washing in ethanol for 10 sec, then water for 10 min until miscible, and then in blotting buffer (12 mM Tris-HCl, 95 mM glycine, 10 % (v/v) ethanol) for 5-10 min. The SDS-PAGE gel was equilibrated by washing in blotting buffer once. Proteins were electrotransferred onto the PVDF membrane in a semi-dry western blot apparatus (Bio-RAD, Italy). After protein transfer, the PVDF membrane was transferred to blocking buffer and rotated at RT for an hour or at 4 °C overnight.

2.2.3.14 Coating microtitre plates with ICAMs for cell adhesion assay

Goat anti-human IgG (Fc specific) (100 µl, 5 µg/mL in sodium bicarbonate buffer (pH 9.2), Sigma-Aldrich, St. Louis, MO) was dispensed into each well of a Polysorb microtitre plate (Nunc, Rosklide, Denmark) followed by incubation at 4 °C overnight. Thereafter, the solution was discarded and 150 µl of 0.5 % (w/v) BSA in PBS (blocking solution) was added to each well and incubated at 37 °C for 30 min. The blocking solution was discarded and 50 µl of ICAM-1/Fc or ICAM-3/Fc (1 µl /mL in PBS containing 0.1 % BSA (w/v)) was added into each well. After incubation at RT for 2-3 h, the wells were washed twice in RPMI wash buffer before use.

2.2.3.15 Immobilized ligand cell adhesion assay

Adhesion assays of 293-T cells, COS-7 cells, MOLT-4 cells, HUT-78 cells, SKW 3.0

cells, peripheral blood T lymphocytes, and T lymphoblasts to ICAM-1 or -3 coated Polysorb microtiter wells (Thermo Fisher Scientific, Waltham, MA) were performed as reported previously (Tan et al., 2000). Briefly, each microtiter well was coated with ICAM/Fc aforementioned. Cells were labeled with 3.0 mM 2,7-bis-(2-carboxyethyl)-5-(and-6) carboxyfluorescein fluorescent dye (Molecular Probes, Eugene, OR) at 37 °C for 20 min followed by washing in RPMI wash buffer to remove the excess dye. Thereafter, cells (2×10^4 cells/well) were incubated in RPMI wash buffer at 37 °C for 30 min with or without Mg^{2+}/EGTA (5 mM $MgCl_2$ and 1.5 mM EGTA) and/or KIM185 (10 μg/ml), for activating purposes. αL-specific function-blocking mAb MHM24 (10 μg/ml) was included to demonstrate binding specificity. Cell fluorescence, which indicates the number of cells adhering to ligand-coated wells, is measured using FL600 fluorescent plate reader (Bio-Tek Instruments, Winooski, VT). Data were analysed and presented as % of cells bound to the ligand ICAM-1 or -3.

2.2.3.16 Soluble ligand binding assay

Soluble ICAM (sICAM) binding assay was performed as previously described (Tang et al., 2005). For activating studies, Mg^{2+}/EGTA (5 mM $MgCl_2$ and 1.5 mM EGTA) and/or activating mAb KIM185 (10 μg/ml) were used. The function-blocking mAb MHM24 (10 μg/ml) was used in all blocking conditions to demonstrate αLβ2-mediated ligand binding specificity. For the TCR/CD3 cross-linking experiment, 5 μg/ml anti-αβ TCR (T10B9.1A-31) and 5 μg/ml anti-CD3 (UCHT1) were used. sICAM-bound cells were detected by flow cytometry analysis and presented as histogram plots. For HUT-78 cells electroporated with talin siRNA or control siRNA, the number of cells gated positive was determined and normalized to the highest number of cells gated positive in that experiment, and presented as % cells gated positive.

2.2.3.17 Live cell imaging

Cells were allowed to adhere to ICAM-1 or -3 (with or without 750 ng/ml Stromal cell-derived factor 1α (SDF-1α), Calbiochem, Germany) -coated detachable Polysorb microtiter wells (Nunc, Rosklide, Denmark) or glass-bottomed 35 mm dish (Iwaki, Japan or MatTek, Ashland, MA). Samples treated with or without Mg^{2+}/EGTA (5 mM $MgCl_2$ and 1.5 mM EGTA) and/or KIM185 (10 μg/ml) were added to the ICAM-1 or -3 coated wells and incubated at 37 °C for 15 mins. Non-adherent cells were removed by gentle washing. The microwell containing cells was mounted with an adaptor onto the stage of a Zeiss Axiovert 200M inverted microscope (Zeiss, Germany) housed in a closed humidified system with temperature (37 °C) and CO_2 control. Images of live cells were taken using 20× or 20×1.6 objectives. Images captured at indicated time intervals with a Coolsnap HQ CCD camera (Photometrics, Tucson, AZ) were analyzed using the software MetaMorph (Molecular Devices Corporation, Downington, PA).

2.2.3.18 Confocal imaging of SKW 3.0 cells

Glass bottomed 35 mm dish was coated with Protein A (Calbiochem, Germany) in 20 % of bicarbonate buffer in PBS at 4 °C overnight followed by coating with ICAM-1 (10 μg/ml) and SDF-1α (750 ng/ml) at 4 °C for 2-3 h. SKW 3.0 cells transfected with EGFP were seeded onto the 35 mm glass bottom dish in RPMI wash buffer at 37 °C for 30 min in a humidified 5 % CO_2 incubator. The bound cells were fixed with 3.7 % (w/v) paraformaldehyde in PBS for 10 min and washed once in PBS before sealing with a cover slip (VFM, UK) for EGFP localization studies.

To check the co-localization of kindlin3 with αLβ2, talin, or RACK1, poly-L-lysine slides (Thermo Fisher Scientific, Waltham, MA) were used to coat with ICAM-1 (1 μg/ml) and SDF-1α (750 ng/ml) following the same method as coating microtitre plates with ICAMs

for cell adhesion assay aforementioned. EGFP-kindlin3 transfected SKW 3.0 cells (0.5 x 10^6 cells per sample) were allowed to bind the ICAM-1 and SDF-1α at 37 °C for 30 min, followed by fixation with 3.7 % (w/v) paraformaldehyde in PBS for 10 min. To allow staining of irrelevant antibody, αLβ2, talin or RACK1, cells were permeabilized with 0.3 % (v/v) Triton X-100 in CSK buffer (10 mM Pipes-KOH (pH 7), 100 mM NaCl, 300 mM sucrose, 3 mM $MgCl_2$ and 1mM EGTA (pH 6.8)) for 5 min and washed 3 times with PBS, followed by incubation with 100 µl of primary irrelevant mAb control, mAb 7E4 (1:500 dilution), mAb 8d4 (1:500 dilution), or anti-RACK1 mAb (1:100 dilution) in PBS at RT for 1 h. Cells were washed in PBS before adding in 100 µl goat-anti-mouse Alexa594 secondary antibody in PBS (1:1000 dilution) (Molecular Probes, Eugene, OR). The slides were washed 3 times before sealing with cover slip (VFM, UK).

Confocal z-sectioned images were collected on a Zeiss Axiovert LSM-510-META-inverted microscope and data were analysed by a Zeiss LSM Image Examiner (Zeiss, Germany).

2.3 Plasmid construction details

All constructs were verified by sequencing (Research Biolabs, Singapore).

2.3.1 Integrin plasmids information

The β2 cDNA in J8.1E (Douglass et al., 1998) was used as a template for the construction of the β2 in mammalian expression vector pcDNA3.0 (Invitrogen, Carlsbad, CA) (Fig. 2.1). KpnI and SpeI were used to digest β2 cDNA from J8.1E and the fragment was ligated into pcDNA3.0 vector which was digested with KpnI and XbaI (SpeI and XbaI digested DNA fragments have compatible ends). αL cDNA plasmids were in pcDNA 3.0 vector with the restriction cutting sites KpnI and XbaI. Point mutations were made by

using QuickChange Site-Directed Mutagenesis Kit (Strategene, Santa Clara, CA). Specific forward (F) and reverse (R) primers to make the salt bridge disrupting substitution D709R in the β2 subunit are shown and mutated bases are underlined:

β2 D709R:

F 5' CTGATCCACCTGAGCCGCCTCCGGGAGTACAGG 3'

R 5' CCTGTACTCCCGGAGGCGGCTCAGGTGGATCAG 3'

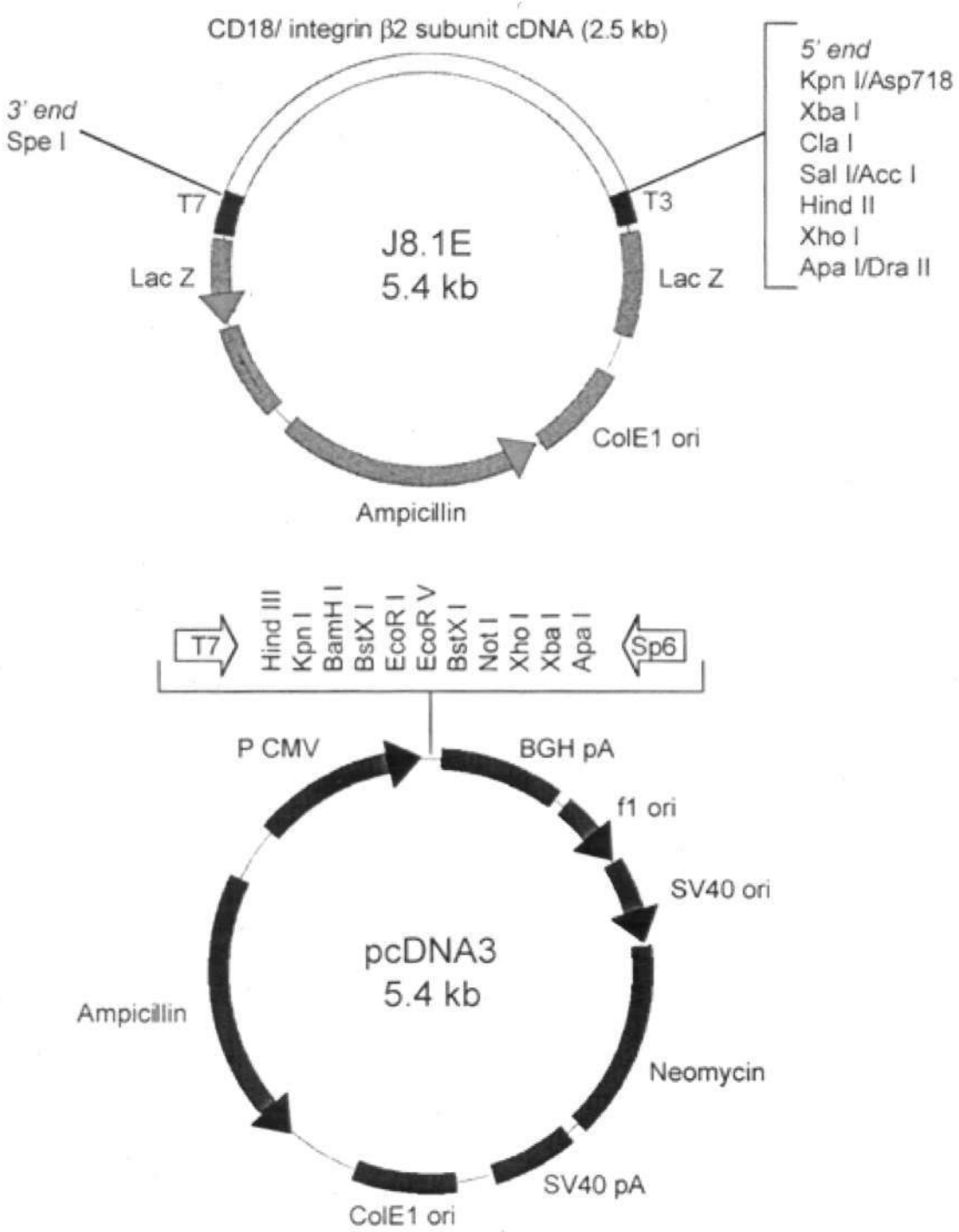

Fig. 2.1 Schematic illustration of plasmid J8.1E and pcDNA3.0. The β2 cDNA in J8.1E (Dougless et al., 1998) was used as a template for the construct of the β2 in mammalian expression vector pcDNA3.0. KpnI/SpeI was used to digest β2 cDNA from J8.1E and the fragment was ligated into pcDNA3.0 vector which was digested with KpnI and XbaI (SpeI and XbaI digested DNA fragment have compatible ends). αL plasmid was in pcDNA3.0 vector with the restriction cutting sites KpnI and XbaI.

2.3.2 Integrin interacting protein constructs

2.3.2.1 Talin constructs

Human talin 1 HD (Met^{1}-Gln^{435}) cDNA was generated by reverse transcription-PCR of mRNA isolated from THP-1 (ATCC, Manassas, VA) using relevant forward and reverse primers containing the XhoI and KpnI restriction sites, respectively. The reverse transcription-PCR product was cloned into the mammalian expression plasmid pXJ40-HA (Manser et al., 1997; Xiao et al., 1991) digested with restriction enzymes XhoI and KpnI, thereby generating an N-terminal HA tag in fusion with talin HD (pXJ40-HA-talin-HD). A similar N-terminal HA-tagged mouse talin HD (residues 1-435) construct has been reported and found to activate integrin αLβ2 in K562 transfectant (Kim et al., 2003). Specific forward (F) and reverse (R) primers are shown:

F 5' CCGCTCGAGATGGTTGCACTTTCACTG 3'

R 5' CGGGGTACCTTATTGCTGCTGCAGGACTG 3'

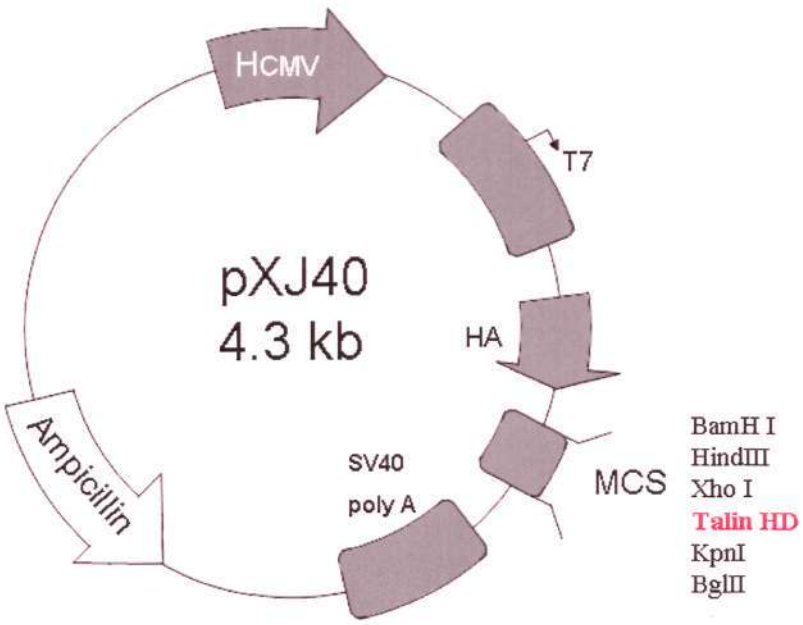

Fig. 2.2 Schematic illustration of expression plasmid talin HD in pXJ40. The RT-PCR products digested with restriction enzyme sites of XhoI and KpnI were ligated into pXJ40 plasmid that was also digested using the same cutting sites. Talin HD was cloned into pXJ40 plasmid with an N-terminal HA tag.

Talin HD-EGFP construct was generated from PCR cloning of talin HD from pXJ40-HA-talin-HD using forward primer containing an XhoI site and reverse primer containing a KpnI site. The reverse primer in this case also contained two extra bases to allow fusion of talin HD in frame with the C-terminal EGFP in the expression plasmid pEGFP-N1. Specific forward (F) and reverse (R) primers are shown:

F 5' CCGCTCGAGATGGTTGCACTTTCACTG 3'

R 5' CGGGGTACCCCTTGCTGCTGCAGGACTG 3'

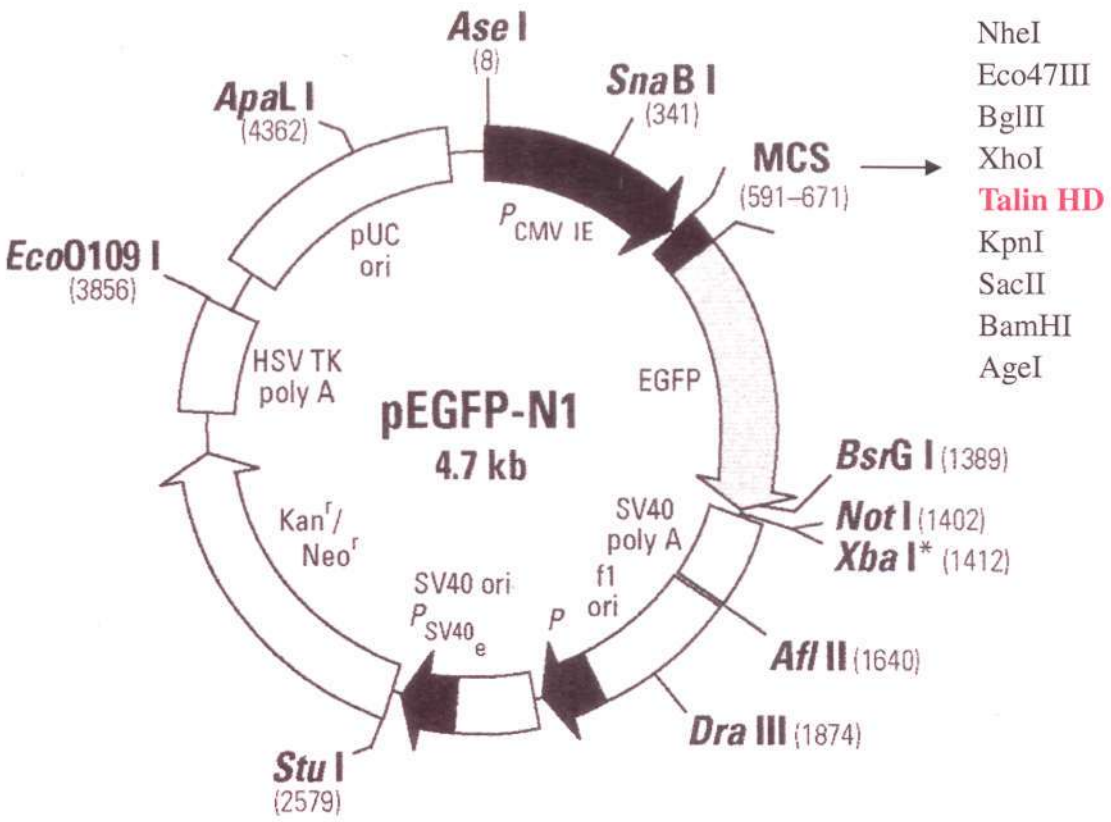

Fig. 2.3 Schematic illustration of plasmid talin HD in pEGFP-N1.
Talin HD was amplified from pXJ40-HA-talin HD. The PCR products digested with restriction enzyme sites of XhoI and KpnI were ligated into pEGFP-N1 plasmid that was also digested using the same cutting sites. Talin HD was cloned into pEGFP-N1 plasmid with a C-terminal EGFP tag.

DsRed was PCR amplified from pIRES2-DsRed plasmid with forward and reverse primers containing HindIII and EcoRI restriction sites respectively. The amplified product was digested with HindIII and EcoRI, and inserted into pcDNA 3.1 (+) plasmid using the same enzyme sites. Specific forward (F) and reverse (R) primers are shown:

F 5' CCCAAGCTTATGGCCTCCTCCGAGGAC 3'

R 5' CCGGAATTCCAGGAACAGGTGGTGG 3'

DsRed-Talin HD construct was generated by PCR cloning of talin HD from pXJ40-HA-talin-HD using forward primer containing an XhoI site and reverse primer containing an XbaI site. Specific forward (F) and reverse (R) primers are shown:

F 5' CCGCTCGAGATGGTTGCACTTTCACTG 3'

R 5' GCTCTAGATTATTGCTGCTGCAGGACTG 3'

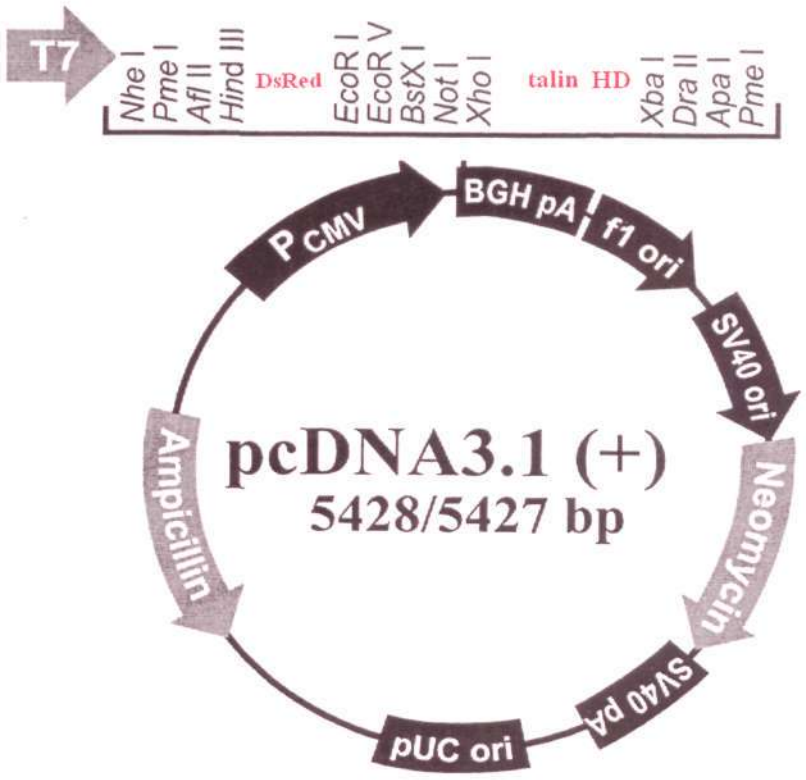

Fig. 2.4 Schematic illustration of expression plasmid DsRed-talin HD in pcDNA 3.1 (+). The first step was generating DsRed-pcDNA 3.1 (+). Talin HD was amplified from pXJ40-HA-talin HD using forward primer containing an XhoI site and reverse primer containing an XbaI site. The digested products were subsequently ligated into DsRed-pcDNA 3.1 (+) using T4 ligase following manufacturer's protocols. Talin HD was generated into pcDNA 3.1 (+) plasmid with an N-terminal DsRed tag.

2.3.2.2 Kindlin3 constructs

Human kindlin3 cDNA was generated by reverse transcription-PCR of mRNA isolated from Jurkat cell (ATCC, Manassas, VA) using relevant forward and reverse primers containing the EcoRI (containing an extra base pair to allow fusion of kindlin3 in frame with the N-terminal EGFP in the expression plasmid pEGFP-C1) and KpnI restriction sites, respectively. Specific forward (F) and reverse (R) primers are shown:

F 5' CCGGAATTCCATGGCGGGGATGAAGAC 3'

R 5' CGGGGTACCTCAGAAGGCCTCATGGCC 3'

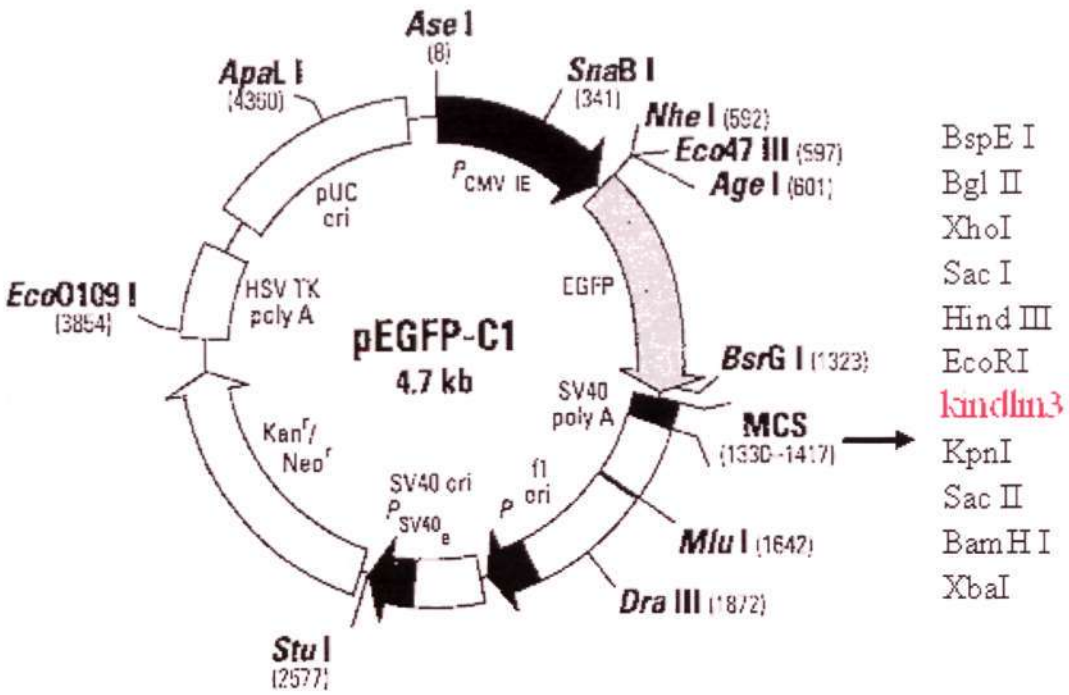

Fig. 2.5 Schematic illustration of expression plasmid kindlin3 in pEGFP-C1.
The PT-PCR products digested with restriction enzyme sites of EcoRI and KpnI were ligated into pEGFP-C1 plasmid that was also digested using the same cutting sites. Kindlin3 was cloned into pEGFP-C1 plasmid with cutting sites of EcoRI and KpnI with an N-terminal EGFP tag.

Point mutations of kindlin3 in pEGFP-kindlin3 were made based on kindlin3 in pEGFP-C1 by using QuikChange Site-Directed Mutagenesis Kit, thereby generating an N-terminal EGFP tag in fusion with kindlin3 W600A mutation. F3 subdomain was deleted by introducing a stop codon at Phe^{551}, thereby generating F3-deleted EGFP-kindlin3 (Met^{1}-Leu^{550}). PH-deleted EGFP-kindlin3 was generated in two steps: The first PCR reaction used EGFP-kindlin3 as a template in separate reactions containing P1 and P2, or P3 and P4 primers, generating two fragments (Met^{1}-Pro^{350} and Ala^{462}-Phe^{667}); the second PCR used these two fragments as templates with P1 and P4 primers, thereby generating EGFP-kindlin3 with PH domain deleted. Specific primers are listed below with mutated bases underlined:

1. EGFP-kindlin 3 W600A:

F 5' CAGCAACATGCGCCAGGCGAATGTCAACTGGGAC 3'

R 5' GTCCCAGTTGACATTCGCCTGGCGCATGTTGCTG 3'

2. EGFP-kindlin 3 F3 deleted:

F 5' GGCCTGGCAGTCCCTGTGAGACTTCGGCATCTCCTA 3'

R 5'TAGGAGATGCCGAAGTCTCACAGGGACTGCCAGGCC 3'

3. EGFP-kindlin 3 PH deleted:

P1 5' CCGGAATTCCATGGCGGGGATGAAGACAG 3'

P2 5' CTGGTGTAGCTGCTGTCGGCCCCCCCCCC

TGGGATGGTGGTGAGGCTGTCCA 3'

P3 5' TGGACAGCCTCACCACCATCCCAGGGGG

GGGGGCCGACAGCAGCTACACCAG 3'

P4 5' CGGGGTACCTCAGAAGGCCTCATGGCC 3'

Chapter 3 The cytosolic protein talin induces an intermediate affinity integrin αLβ2

3.1 Introduction

The integrin ectodomain can be segregated into two collective regions referred to as the headpiece and tailpiece (Luo et al., 2007) (Fig. 3.1). The headpiece participates in ligand-binding. Structural studies of αIIbβ3, αVβ3, and α5β1 suggest at least three integrin ligand-binding affinity states having different conformations (Luo et al., 2007; Takagi et al., 2002b; Takagi et al., 2003; Xiao et al., 2004b; Xiong et al., 2001). The low affinity integrin is represented by an acutely bent structure with a closed headpiece. By contrast, a high affinity integrin adopts an extended conformation with open headpiece derived from hybrid domain displacement. The intermediate affinity integrin conformation is proposed to be a collection of bent structures with open headpieces or extended structures with closed headpieces (Xiao et al., 2004). Electron microscopy study of soluble recombinant β2 integrins reveals three major conformers (Nishida et al., 2006), the bent conformer and two extended conformers with open and closed headpieces.

Previously, we reported the requirement of integrin αLβ2 (leukocyte function-associated antigen-1 or CD11a/CD18) having different affinity states for the adhesion to its ligands intercellular adhesion molecule-1 (ICAM-1) (CD54) and -3 (CD50) (Tang et al., 2005). Whereas an intermediate affinity αLβ2 bound ICAM-1, a high affinity αLβ2 was required for ICAM-3 binding. The Inserted (I)-domain (also known as the αA domain)

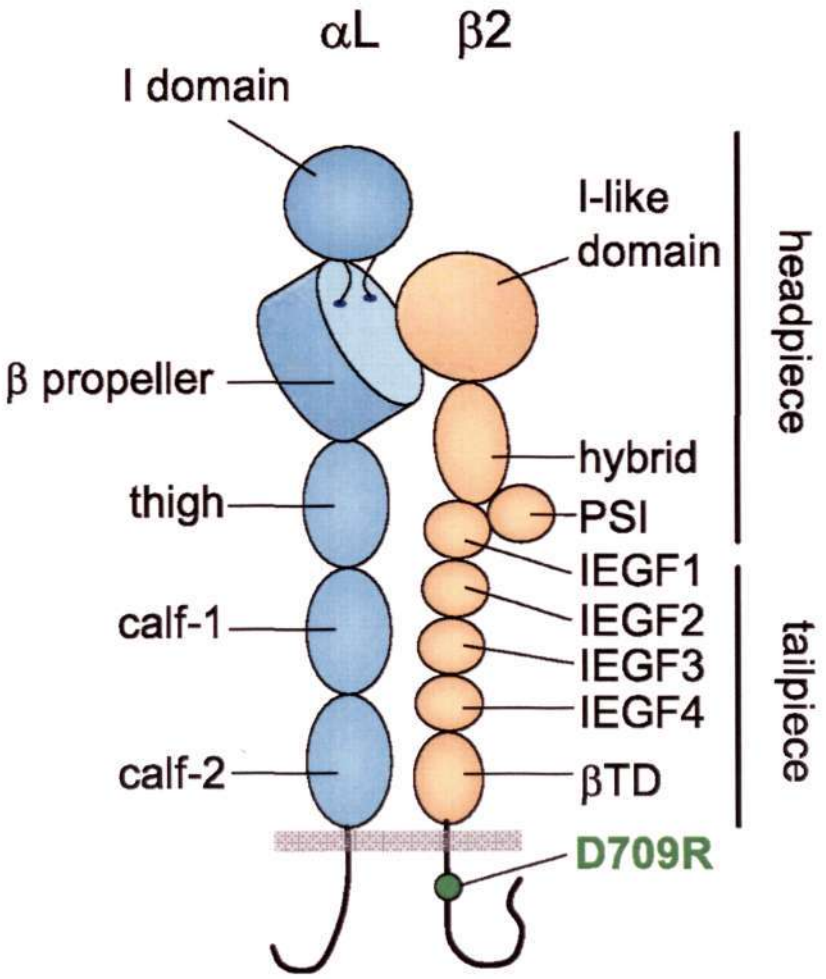

Fig. 3.1 Illustration of the integrin αLβ2 domain organization. The designations of headpiece and tailpiece are based on Luo et al. (Luo et al., 2007). I domain, inserted domain; PSI, plexin-semaphorin-integrin domain; IEGF, integrin-epidermal growth factor fold; βTD, β tail domain. The salt bridge disrupting substitution D709R in the β2 subunit is shown.

(Arnaout et al., 2005) is the primary ligand-binding domain of αLβ2. The order of binding affinities to different ICAMs using engineered isolated αL I domain is ICAM-1 > ICAM-2 > ICAM-3 (Shimaoka et al., 2001). Further, it was reported that an extended intermediate affinity αLβ2, stabilized by the small molecule allosteric antagonist XVA143, promoted rolling adhesion of leukocytes in shear flow (Salas et al., 2004). Thus, the transition of αLβ2 across different affinity states may be required to fine-tune leukocyte adhesiveness during distinct stages of leukocyte homeostasis.

The talin HD is shown to activate αLβ2 by forced separation of its cytoplasmic tails as determined by fluorescence resonance energy transfer analyses (Kim et al., 2003). However, whether talin promotes an intermediate affinity or high affinity αLβ2 has not been fully characterized. Herein, we report that talin HD promotes an intermediate affinity αLβ2 in surrogate transfectants and in T cells as determined by ICAM adhesion and binding assays, activation reporter mAbs analyses, and migration studies.

3.2 Results

3.2.1 Talin HD induced an intermediate affinity αLβ2 that constitutively adhered to ICAM-1 but not ICAM-3

The described role of talin in integrin activation prompted us to compare its contribution toward αLβ2-mediated adhesion to ICAM-1 and ICAM-3. COS-7 cells were transfected with αLβ2 or αLβ2 and HA-tagged talin HD, which contains the major integrin interaction site (Calderwood et al., 1999). The expressions of αLβ2 and talin HD were determined by flow cytometry analyses and anti-HA immunoblotting, respectively (Fig. 3.2A). The levels of αLβ2 expression in both transfectants were comparable. The talin

HD transfectant showed a high level of talin HD expression as determined by anti-HA immunoblotting. Interestingly, the adhesion profiles to ICAMs were different between the two transfectants. Although αLβ2 transfectants adhered to ICAM-1 only in the presence of the activating agent Mg^{2+}/EGTA (ME in all figures) or the β2-specific activating mAb KIM185 (Andrew et al., 1993), transfectants bearing αLβ2 and talin HD showed constitutive ICAM-1 adhesion, albeit at a lower level than that in the presence of an activating agent (Fig. 3.2B). Transfectants expressing αLβ2 adhered to ICAM-3 only when both Mg^{2+}/EGTA and KIM185 were included, which was consistent with that reported previously (Tang et al., 2005). Transfectants bearing αLβ2 and talin HD adhered to ICAM-3 when Mg^{2+}/EGTA or KIM185 was included. In all cases, MHM24 (an αL-specific function-blocking mAb) abrogated adhesion, demonstrating αLβ2-mediated adhesion specificity. In addition, we examined the capacity of these transfectants to bind sICAMs (Tang et al., 2005) (Fig. 3.2C). Consistent with the adhesion profiles to the ICAMs, transfectants bearing αLβ2 and talin HD showed detectable levels of sICAM-1 binding (shaded histogram) even in the absence of the activating agents as compared with transfectants bearing only αLβ2.

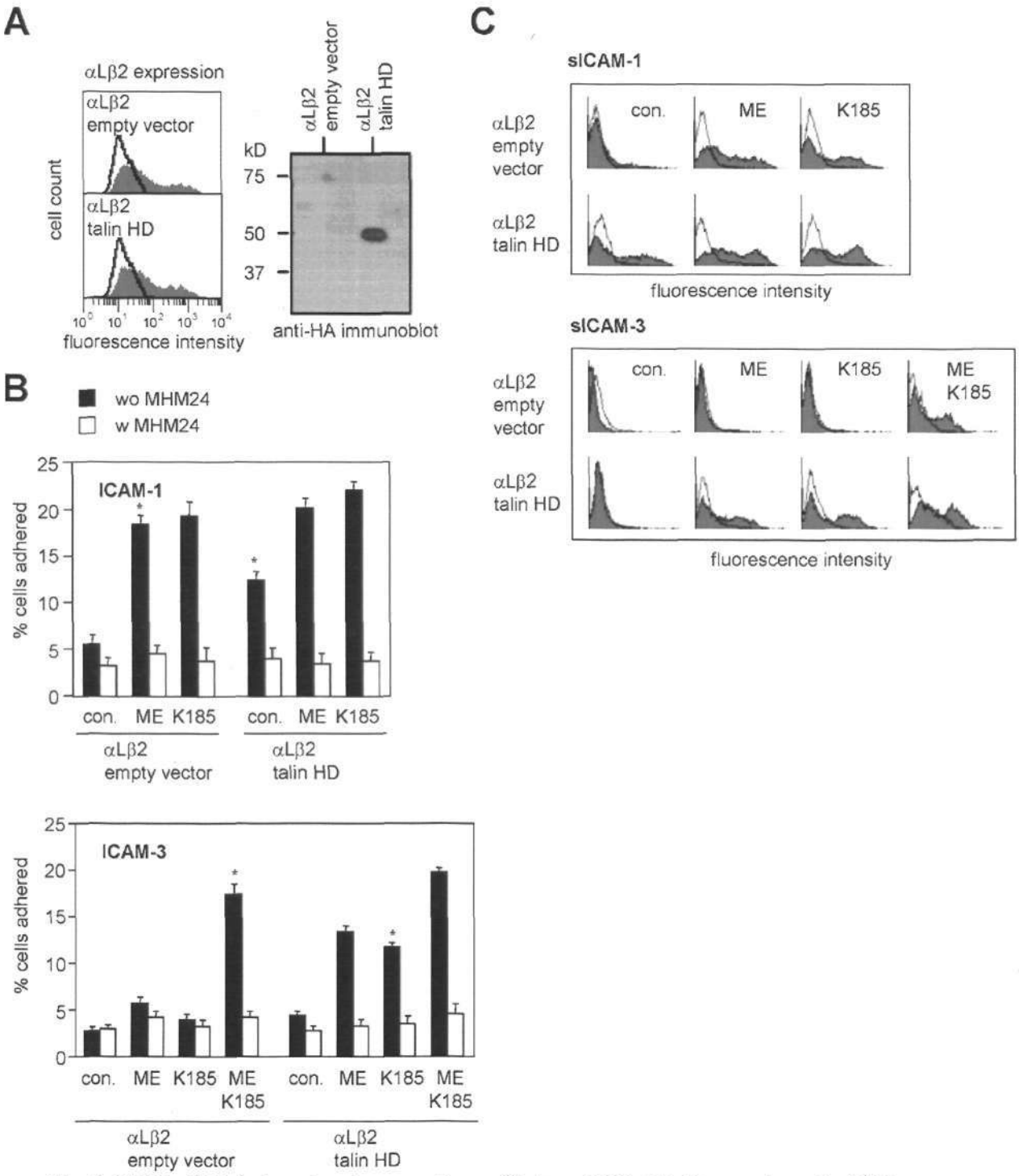

Fig. 3.2 Talin HD induced an intermediate affinity αLβ2. (A) Expression of αLβ2 on transfectants was detected by staining with heterodimer αLβ2-specific mAb MHM23 (shaded histogram) followed by flow cytometry. Open histogram, irrelevant mAb. Transfected HA-talin HD was detected by immunoblotting cell lysates with anti-HA antibody. Empty vector, pXJ40-HA. (B) Adhesion of transfectants bearing αLβ2 with or without talin HD co-expression on ICAM-1 and ICAM-3. Adhesion specificity was demonstrated using the function-blocking mAb MHM24. con.: control condition without any additives. ME: 5 mM $MgCl_2$ and 1.5 mM EGTA. K185:10 μg/ml KIM185. *, $p<0.05$, (Student's t test), with respect to con. of the experiment. (C) sICAM binding of transfectants as determined by flow cytometry (open histogram:in the presence of MHM24).

Transfectants bearing αLβ2 and talin HD showed detectable levels of sICAM-3 binding in the presence of only one activating condition Mg^{2+}/EGTA or KIM185, whereas transfectants bearing only αLβ2 required the presence of Mg^{2+}/EGTA and KIM185. Binding specificity was verified by mAb MHM24 (open histogram). We previously proposed that, in the presence of one activating agent such as Mg^{2+}/EGTA or KIM185, an intermediate affinity αLβ2 is induced that allows effective adhesion to ICAM-1 but not ICAM-3 (Tang et al., 2005). In the presence of both Mg^{2+}/EGTA and KIM185, a high affinity αLβ2 is generated that mediates not only ICAM-1 but also ICAM-3 adhesion. Thus, the constitutive binding of talin HD/αLβ2 transfectant to ICAM-1, but not ICAM-3, and its capacity to bind ICAM-3 when only one activating agent was included suggest that talin HD induces an intermediate affinity αLβ2.

3.2.2 Salt bridge disruption in αLβ2 cytoplasmic tails generated an intermediate affinity αLβ2

The effect of talin HD on αLβ2 ligand binding recapitulates integrin activation via inside-out signaling. Talin HD was reported to induce the separation of the αLβ2 cytoplasmic tails (Kim et al., 2003). Similarly, the disruption of a membrane proximal salt bridge linking the two cytoplasmic tails of αIIbβ3 was shown to promote its activation (Hughes et al., 1996). However, whether the separation of cytoplasmic tails by salt bridge disruption induces an intermediate or high affinity αLβ2 requires clarification. A salt bridge-disrupted αLβ2 variant (αLβ2 D709R) (Fig. 3.1) was generated to examine its ICAM-binding properties with or without talin HD overexpression. The expression level of αLβ2 D709R was analyzed by flow cytometry, and talin HD was detected by anti-HA immunoblot (Fig. 3.3A). The αLβ2 D709R transfectant showed constitutive adhesion to

ICAM-1, and the co-expression of talin HD did not significantly alter the adhesion profile (Fig. 3.3B). The αLβ2 D709R transfectant only adhered to ICAM-3 when activated by at least Mg^{2+}/EGTA or KIM185. A similar adhesion profile was seen in the presence of talin HD co-expression. The study was reinforced with sICAM binding assays that showed similar sICAM binding profiles (Fig. 3.3C). Hence, it is apparent that salt bridge disruption promotes an intermediate affinity but not a high affinity αLβ2. We reasoned that talin HD overexpression had minimal effect on αLβ2 D709R-mediated binding to ICAMs, because the αLβ2 cytoplasmic tails should have already undergone forced separation as a result of the D709R substitution.

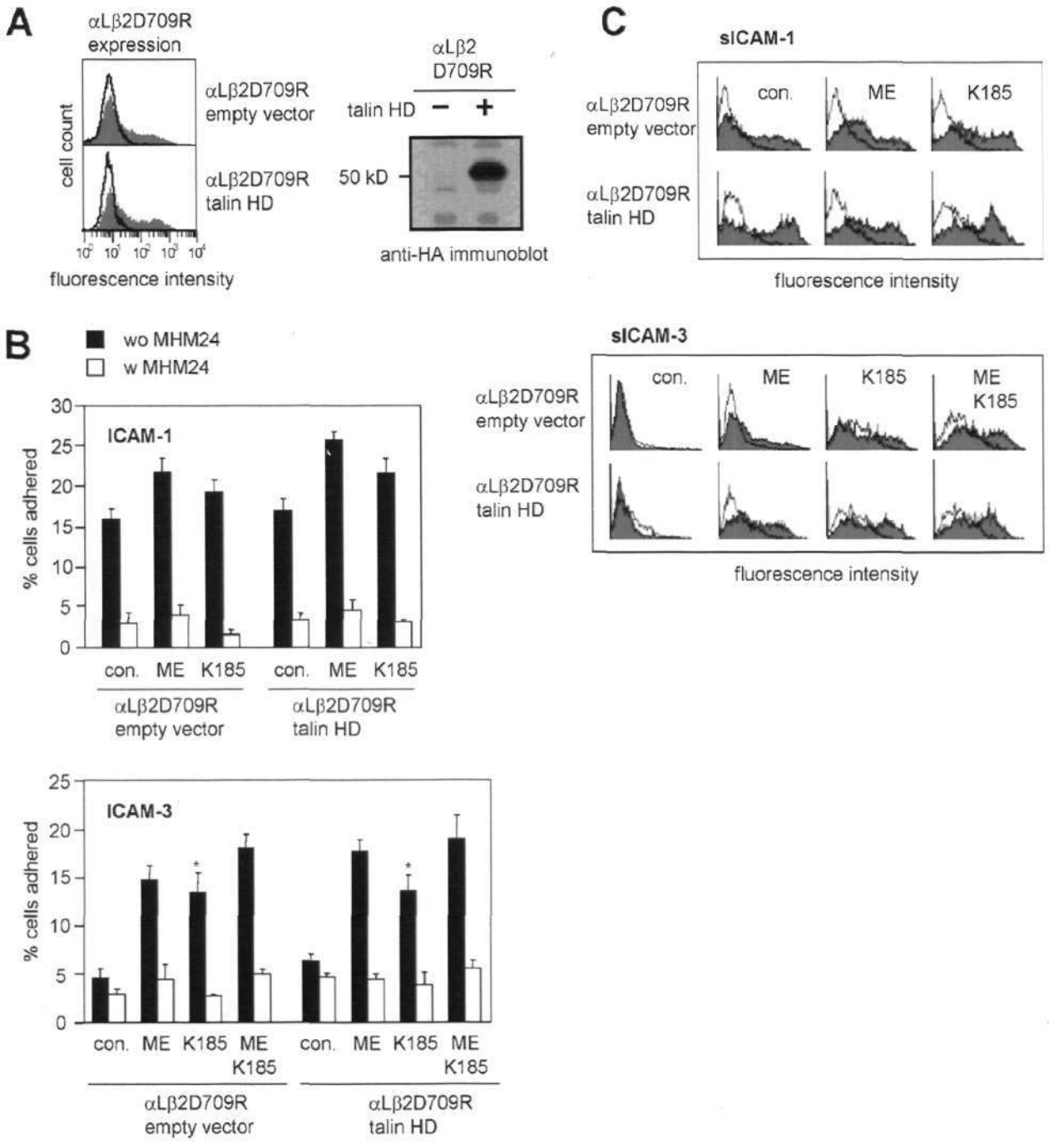

Fig. 3.3 Cytoplasmic tails salt bridge disruption induced an intermediate affinity αLβ2. (A) Detection of αLβ2 D709R and talin HD was performed as described in Fig. 3.2A. (B) Adhesion of transfectants bearing αLβ2 D709R with or without talin HD co-expression on ICAM-1 and ICAM-3. Adhesion specificity was demonstrated using the function-blocking mAb MHM24. con.: control condition without any additives. ME: 5 mM $MgCl_2$ and 1.5 mM EGTA. K185:10 μg/ml KIM185. *, $p<0.05$, (Student's t test), with respect to con. of the experiment. (C) sICAM binding of transfectants as determined by flow cytometry (open histogram: in the presence of MHM24).

3.2.3 Talin induced expression of an intermediate affinity αLβ2 on T-cell line HUT-78

Next, we asked whether talin promotes a population of intermediate affinity αLβ2 on T cells. We made use of two T cell lines HUT-78 and MOLT-4 in this study. Differences in the activity of αLβ2 on these cells were detected (Fig. 3.4A). Unlike MOLT-4 that required Mg^{2+}/EGTA for adhesion to ICAM-1 (Tang et al., 2005), HUT-78 showed constitutive ICAM-1 adhesion. Whereas MOLT-4 required a combination of Mg^{2+}/EGTA and KIM185 to adhere to ICAM-3, only Mg^{2+}/EGTA was required for HUT-78 adhesion to ICAM-3. Thus, these data suggest the presence of a population of intermediate affinity αLβ2 on HUT-78.

The αLβ2 activation reporter mAb MEM148 reacts with a β2 hybrid domain epitope that is masked in non-activated αLβ2 (Tang et al., 2005). Interestingly, MEM148 precipitated surface biotin-labeled αLβ2 from HUT-78 but not MOLT-4 in the absence of exogenous αLβ2-activating agent (Fig. 3.4B). αLβ2 was precipitated by MEM148 from MOLT-4 when Mg^{2+}/EGTA was included. The mAb MHM23 (β2 integrin heterodimer-specific) was included as a control. These data support the presence of a population of active αLβ2 on HUT-78.

Talin promoted the expression of intermediate affinity αLβ2 in transfectants, thus we examined whether the population of active αLβ2 on HUT-78 was induced by talin. To this end, endogenous talin expression in HUT-78 was reduced using siRNA (Fig. 3.5A).

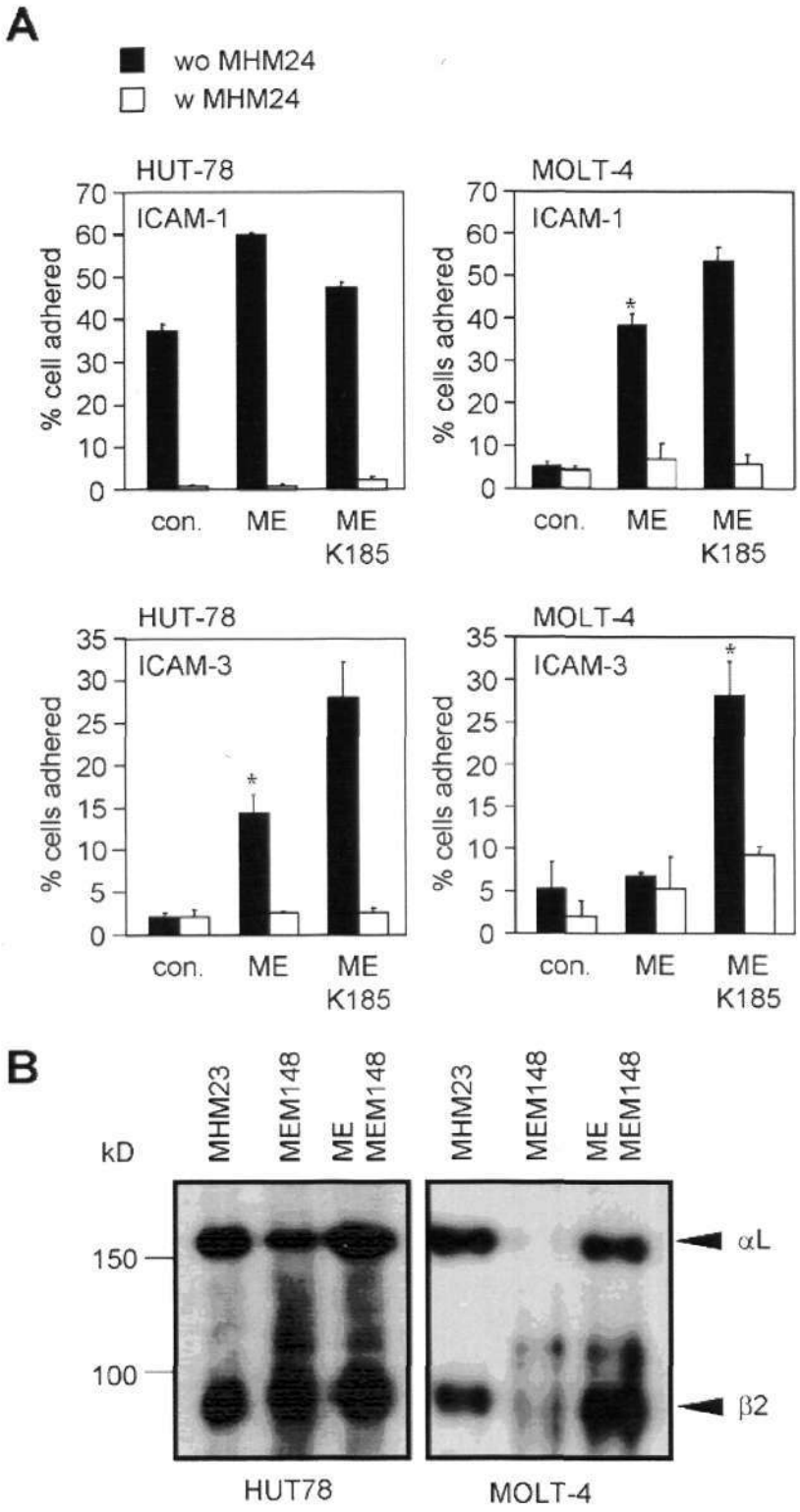

Fig. 3.4 A population of an intermediate affinity αLβ2 on HUT-78. (A) αLβ2-mediated adhesion of HUT-78 and MOLT-4 to ICAM-1 and ICAM-3. Adhesion specificity was demonstrated using the function-blocking mAb MHM24. con.: control condition without any additives. ME: 5 mM $MgCl_2$ and 1.5 mM EGTA. K185:10 μg/ml KIM185. *, $p<0.05$, (Student's t test), with respect to con. of the experiment. (B) Cell surface αLβ2 on HUT-78 and MOLT-4 were labeled with biotin followed by immunoprecipitation with the αLβ2 activation reporter mAb MEM148 in the absence or presence of ME. The mAb MHM23 was included as a control.

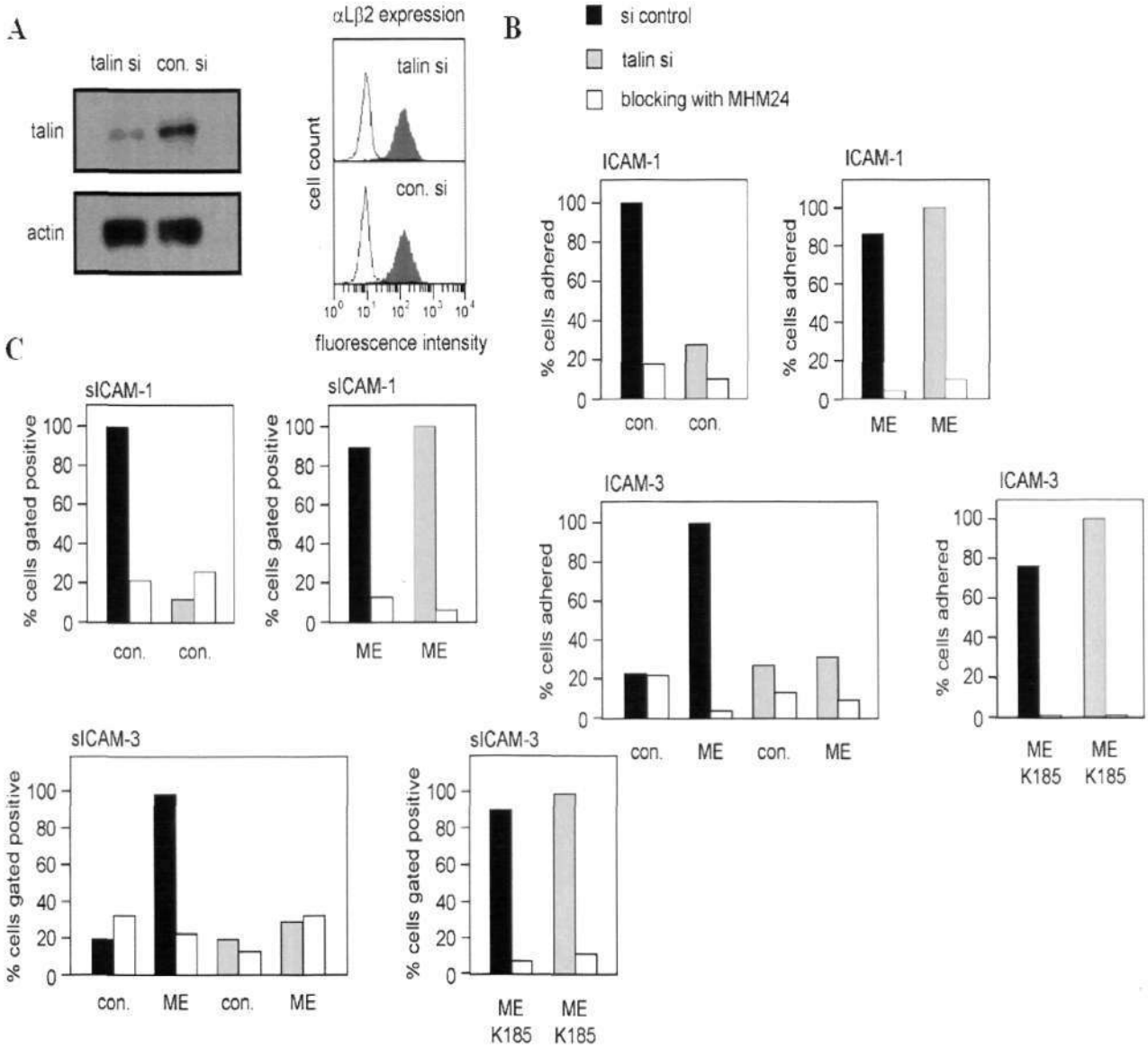

Fig. 3.5 The intermediate affinity αLβ2 was promoted by talin on HUT-78. (A) Knockdown of endogenous talin expression in HUT-78 using siRNA. The level of talin knockdown was shown by immunoblotting for talin (mAb 8d4) in cell lysates of HUT-78 transfected with talin siRNA or a control siRNA. Actin was immunoblotted as a control for total protein loaded. The expression of αLβ2 on HUT-78 was not affected by the transfection of siRNA as determined by flow cytometry using the mAb MHM23 (shaded histogram). Irrelevant mAb (open histogram). (B) Adhesion of talin knockdown HUT-78 to ICAM-1 and ICAM-3. Representative data are shown. The number of cells adhered to the ICAMs was counted and normalized to the highest number of adherent cells in that experiment, and presented as % cells adhered. (C) sICAM binding of talin knockdown HUT-78 as determined by flow cytometry. The number of cells gated positive for sICAM bound was determined and normalized to the highest number of cells gated positive for that experiment and presented as % cells gated positive. Representative data of two independent experiments are shown.

The expression of αLβ2 on HUT-78 transfected with talin siRNA was similar to that transfected with control siRNA as determined by flow cytometry. HUT-78 transfected with talin siRNA showed reduced adhesion to ICAM-1, which was in contrast to that of the control siRNA. Representative data are shown (Fig. 3.5B). Adhesion to ICAM-1 could be restored in talin knockdown cells when treated with Mg^{2+}/EGTA, suggesting that αLβ2 on these cells was functional. Talin knockdown also abrogated HUT-78 adhesion to ICAM-3 in the presence of Mg^{2+}/EGTA, but adhesion was restored in the presence of Mg^{2+}/EGTA and KIM185. sICAM binding assays were also performed, and similar binding profiles were observed (Fig. 3.5C). Taken together, talin contributes toward the generation of a population of an intermediate affinity αLβ2 on HUT-78.

HUT-78 adhered to and migrated on immobilized ICAM-1 (data not shown). We also examined whether talin promoted MOLT-4 adhesion and migration on the ICAMs. MOLT-4 is non-adherent to the ICAMs unless the αLβ2 is activated (Tang et al., 2005). MOLT-4 was transfected with talin HD-EGFP. Transfected cells, which were monitored by EGFP emission signal with a fluorescence microscope of a live-cell imaging system, constitutively adhered to and migrated on ICAM-1 (Fig. 3.6A). Transfected cells also migrated on ICAM-3 but required Mg^{2+}/EGTA or KIM185, consistent with the requirement of two αLβ2 activation steps for effective binding to ICAM-3. The motility of these cells was calculated and presented as a box plot (Fig. 3.6B). Therefore, these data suggest that talin promotes a population of an intermediate affinity αLβ2 that could mediate effective migration on ICAMs.

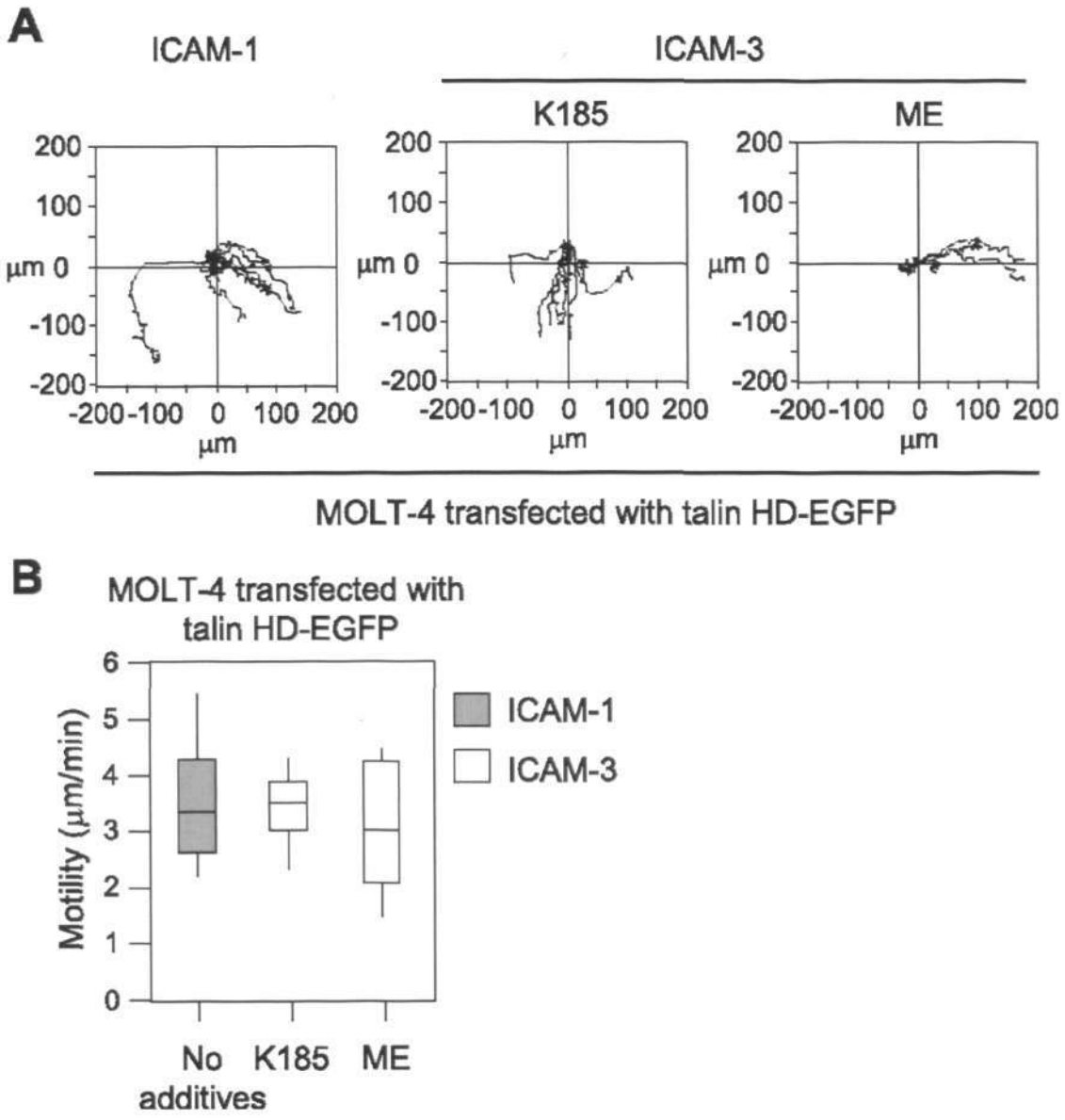

Fig. 3.6 Migration of MOLT-4 on ICAMs when transfected with talin HD. (A) MOLT-4 was transfected with talin HD fused with EGFP and allowed to migrate on ICAM-1 or ICAM-3. In line with the adhesion assays, MOLT-4 transfected with talin HD adhered to and migrated on ICAM-1. An additional activating agent Mg^{2+}/EGTA (ME) or KIM185 (K185) was required to promote talin HD-transfected MOLT-4 to adhere and migrate on ICAM-3. Migrating cells were visualized and recorded using a fluorescence microscope live-cell imaging system under 37 °C for 2 h. The migratory tracks of 15 talin HD-transfected (based on EGFP emission signal) cells in the recorded field were generated using Metamorph®, and the trajectories were presented on an X-Y (microns) plot with the origin of each recorded cell positioned at X = 0 μm, Y = 0 μm. (B) Box plot presentation of cell motility (microns/min).

3.2.4 T lymphoblasts express a population of intermediate affinity αLβ2

We extended the investigation to examine the affinity state of αLβ2 on primary T cells. Human PBTLs were isolated by two procedures. Whereas PS T lymphocytes showed higher purity as compared with NS ones, as determined by flow cytometry using anti-αβ TCR mAb (Fig. 3.7A), PS may trigger T-cell response and transient αLβ2 activation as opposed to the untouched T cells obtained via the method of NS. Hence, we allowed the purified cells to recover overnight in culture and tested both isolated T cells in ICAM adhesion assays, which gave similar adhesion profiles (Fig. 3.7B). Adhesion to ICAM-1 required activation of αLβ2 with Mg^{2+}/EGTA or KIM185, and adhesion to ICAM-3 required both activating agents. Adhesion specificity was demonstrated by MHM24. Thus, only PS PBTL was shown for subsequent assays. The binding profiles of PS PBTL to the sICAMs were also consistent with the adhesion profiles (Fig. 3.7C).

The migration of PHA/interleukin-2-expanded T cells (henceforth referred to as T lymphoblasts) on ICAM-1 has been reported (Dustin et al., 1997; Smith et al., 2005). We asked whether T lymphoblasts express intermediate or high affinity αLβ2. T lymphoblasts and PS PBTLs were stained with the αLβ2 activation reporter mAbs MEM148 (Tang et al., 2005) and m24 (Dransfield and Hogg, 1989) at different temperatures, because epitope expression of these mAbs is temperature-dependent. Afore-mentioned, MEM148 epitope resides in the β2 hybrid domain and is masked in the inactive αLβ2 conformer (Tang et al., 2005). The m24 epitope is located in the β2

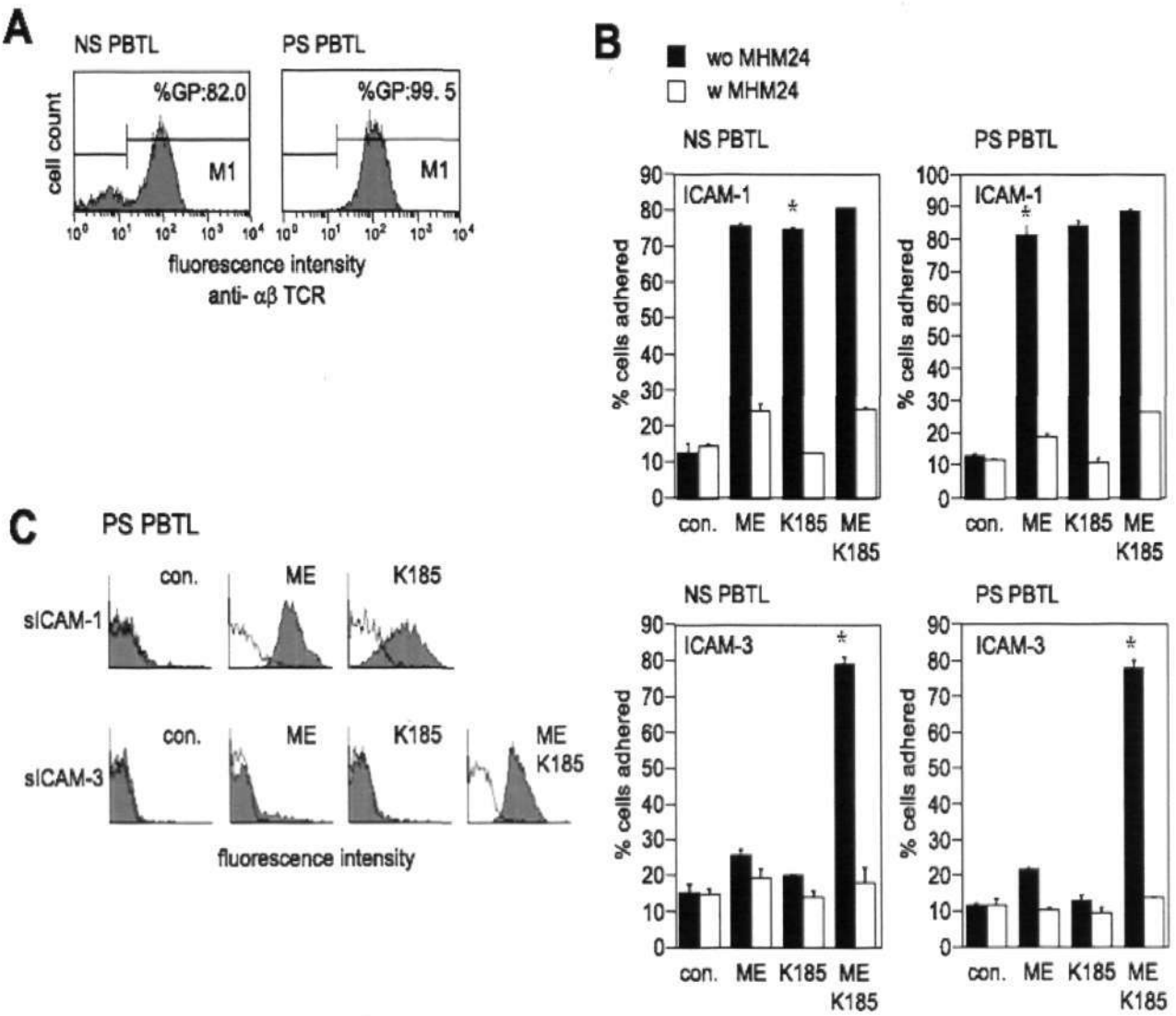

Fig. 3.7 A resting affinity αLβ2 is expressed on human PBTLs. (A) The purity of PBTLs isolated based on NS and PS procedure was assessed by flow cytometry. T cells were stained with an anti-αβ TCR mAb. The region M1 was gated to exclude background staining with an irrelevant mAb. %GP: % gated positive. (B) αLβ2-mediated adhesion of NS and PS PBTLs on ICAMs. Adhesion specificity was demonstrated using MHM24. con.: control condition without any additives. ME: 5 mM $MgCl_2$ and 1.5 mM EGTA. K185:10 μg/ml KIM185. *, $p<0.05$, (Student's t test), with respect to con. of the experiment. (C) sICAM binding of PS PBTLs under different conditions. Open histogram, in the presence of MHM24.

I-like domain (Salas et al., 2004). Significant positive stainings of T lymphoblasts but not PS PBTLs by these mAbs were detected at 37 °C (Fig. 3.8A). Staining of T lymphoblasts was reduced at 4 °C. MHM24 and anti-CD3 were included as controls. Hence, the T lymphoblasts express an activated population of αLβ2. As determined from adhesion assays, T lymphoblasts expressed a population of intermediate affinity αLβ2 that mediated constitutive adhesion to ICAM-1 and required only one activating agent to promote their adhesion to ICAM-3 (Fig. 3.8B). This was further demonstrated by sICAM binding assays (Fig. 3.8C).

Because Mg^{2+}/EGTA and KIM185 are exogenous αLβ2-activating agents, we further addressed the affinity state of αLβ2 on PBTLs when activated by physiological stimulus. PS PBTLs that were allowed to recover in culture overnight were subjected to sICAM binding assays. Cross-linking of TCR/CD3 with relevant antibodies triggered activation of αLβ2 with concomitant binding to sICAM-1 (Fig. 3.8D). However, the activation was not sufficient to promote sICAM-3 binding, which required the addition of Mg^{2+}/EGTA or KIM185. These data suggest that TCR/CD3 cross-linking induces formation of a population of intermediate affinity αLβ2 on PBTL.

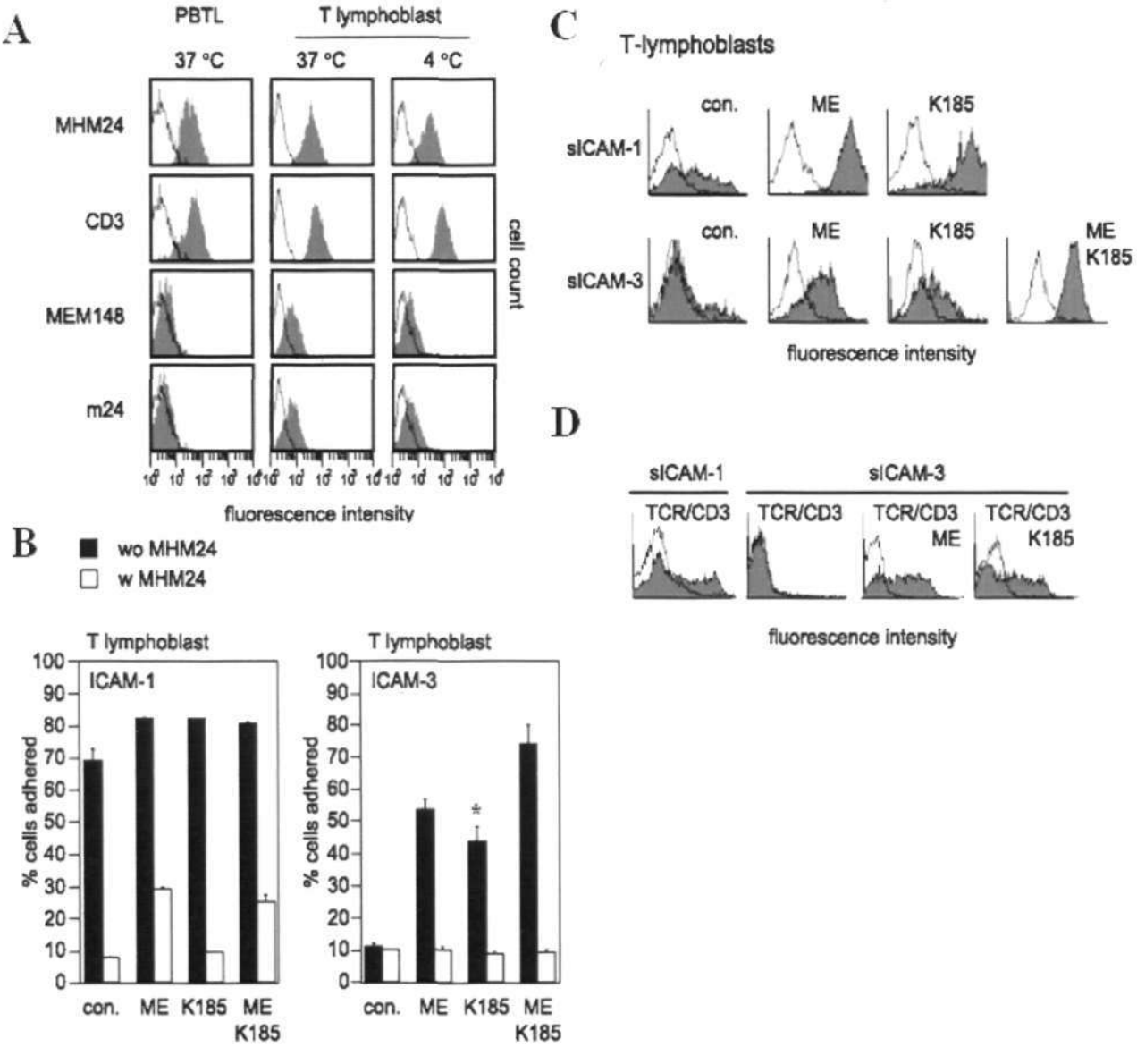

Fig. 3.8 A population of an intermediate affinity αLβ2 on human T lymphoblasts. (A) Flow cytometry analyses of PS PBTLs and T lymphoblasts using different αLβ2 activation reporter mAbs, MEM148 and m24, at different temperatures, 37 °C or 4 °C. MHM24 and anti-CD3 mAbs were used as controls. Open histogram, irrelevant mAb. (B) αLβ2-mediated adhesion of T lymphoblasts to ICAMs under different conditions. con.: control condition without any additives. ME: 5 mM $MgCl_2$ and 1.5 mM EGTA. K185:10 μg/ml KIM185. *, $p<0.05$, (Student's t test), with respect to con. of the experiment. (C) sICAM binding of T-lymphoblasts under different conditions. (D) sICAM-binding of PS PBTL activated by TCR/CD3 cross-linking.

Finally, we examined whether the population of an intermediate affinity αLβ2, induced by an exogenous activating agent on PBTLs and expressed constitutively on T lymphoblasts, can support random migration of these cells on ICAM-1. PS PBTLs adhered to and migrated on ICAM-1 only in the presence of either Mg^{2+}/EGTA or KIM185 activation (Fig. 3.9). In line with the presence of a population of intermediate affinity αLβ2 on T lymphoblasts, these cells adhered to and migrated on ICAM-1 without any activating agent. Representative images of PS PBTL and T lymphoblasts migrating on ICAM-1 with time are shown. Cell motility is calculated and presented as a box plot.

3.3 Discussion

The avidity of integrin-mediated adhesion can be regulated by integrin valency (van Kooyk and Figdor, 2000) and affinity changes (Kim et al., 2004; Luo et al., 2007). Accumulating evidence demonstrates that the integrin undergoes conformational changes when activated via the process of inside-out signaling. These changes modulate integrin ligand-binding affinity. The integrin αLβ2 may adopt different conformations having a low, intermediate, or high affinity state. It was reported that association of talin with the β3 cytoplasmic tail is the final step in integrin αVβ3 and αIIbβ3 activation (Tadokoro et al., 2003). This mode of activation may be extrapolated to αLβ2 inside-out activation when talin expression in transfectants led to the separation of αLβ2 cytoplasmic tails with concomitant activation of αLβ2 to bind ICAM-1 (Kim et al., 2003). However, it remains to be determined as to whether talin induces αLβ2 into an intermediate or high affinity state.

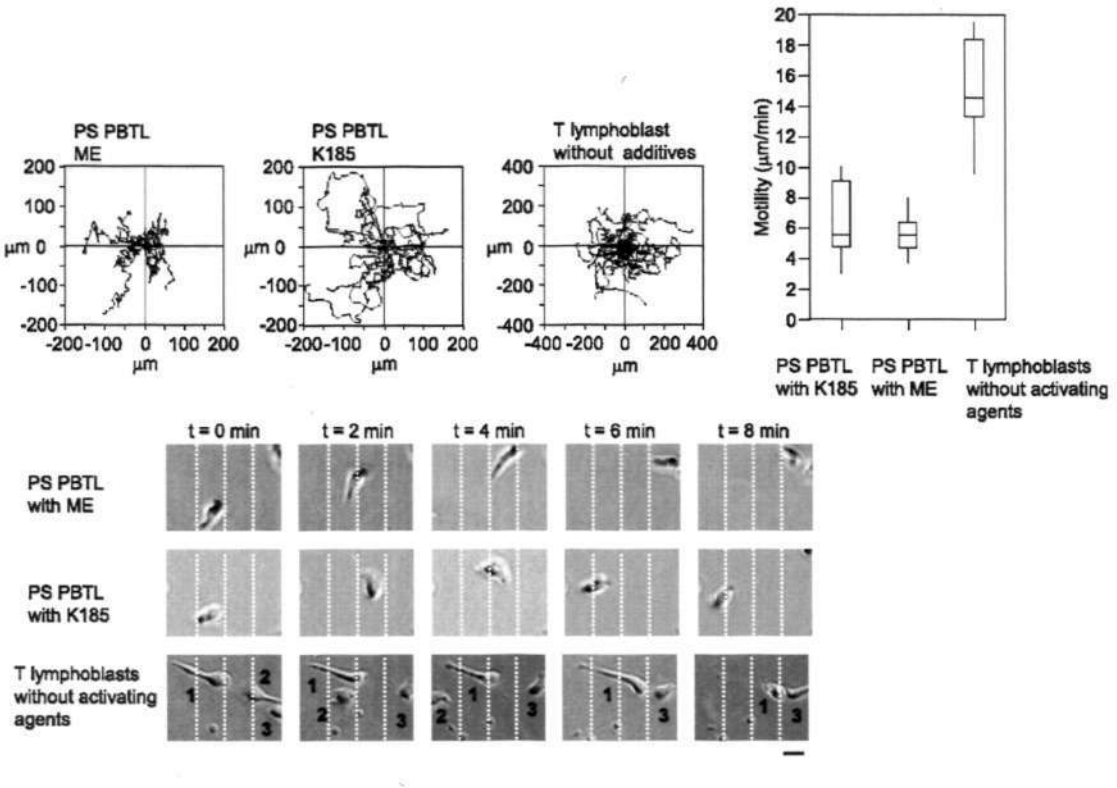

Fig. 3.9 Motility of PS PBTLs and T lymphoblasts on ICAM-1. Migratory tracks of 15 cells from one representative experiment were plotted as described in Fig. 3.6. Box plot presentation of cell motility (microns/min). Phase-contrast microscopy images of PS PBTLs and T lymphoblasts migrating on ICAM-1 with time (only an interval of 8 min is shown). Bar: 10 μm.

Previously, our group refined the assignment of the αLβ2 affinity state based on its capacity to bind different ICAMs (Tang et al., 2005). An intermediate affinity αLβ2 was assigned when it bound to ICAM-1 but not ICAM-3, and a high affinity αLβ2 was conferred when it bound to ICAM-1 and ICAM-3. The present data suggest that talin induces an intermediate affinity αLβ2. Overexpression of talin HD in transfectants co-expressing αLβ2 promoted constitutive cell adhesion to ICAM-1 but not ICAM-3. Adhesion to ICAM-3 could, however, be induced when transfectants were treated with an additional exogenous αLβ2-activating agent such as Mg^{2+}/EGTA or KIM185, which is in accord with the double activation regiment required for αLβ2 to bind ICAM-3 (Tang et al., 2005). Similar binding profiles to sICAMs were also detected.

Interestingly, we detected a population of intermediate affinity αLβ2 expressed constitutively on the T cell line HUT-78. The HUT-78 adhesion profiles to ICAMs were similar with that of transfectants bearing αLβ2 and talin HD. The reduction in constitutive HUT-78 adhesion to ICAM-1 when talin expression was diminished by the method of siRNA also supports the contribution of talin in the generation of an intermediate affinity αLβ2 on these cells.

T lymphoblasts derived from PHA/interleukin-2-expanded PBTLs showed similar adhesion and binding profiles to ICAMs when compared with that of HUT-78. These data also suggest the presence of a population of an intermediate affinity αLβ2 on these cells. It has been difficult for us to investigate talin knockdown in T lymphoblasts. Nonetheless, we could expect the involvement of talin in the induction of intermediate affinity αLβ2 in view of successful talin knockdown reported by others. T lymphoblast αLβ2–ICAM-1 adhesion was diminished in talin-knockdown cells (Simonson et al., 2006), and talin

knockdown was also found to impair αLβ2-mediated migration of T lymphoblasts on ICAM-1 (Smith et al., 2005).

The intermediate affinity αLβ2 on HUT-78 and T-lymphoblasts reacted with the activation reporter mAb MEM148, which reports hybrid domain displacement (Tang et al., 2005). It was proposed that different integrin conformers could exist in dynamic equilibrium on the cell surface (Luo et al., 2007). One population of integrin conformers can predominate over the other(s) depending on the cellular status and the microenvironment. Thus, we cannot, at present, exclude the possibility of other αLβ2 conformers on HUT-78 or T lymphoblasts that may also function as intermediate affinity receptors.

It may be asked whether talin-induced binding to ICAM-3 in the presence of Mg^{2+}/EGTA or KIM185 is a result of more αLβ2 being activated into intermediate affinity conformers or it is a consequence of the conversion of existing talin-induced intermediate affinity αLβ2 to a high affinity state. We reasoned that the binding to ICAM-3 in this case could not simply be attributed to an increase in number of intermediate affinity αLβ2, but a shift from intermediate affinity to high affinity αLβ2 is required for effective binding. There are compelling findings supporting a major requirement of a high affinity αLβ2 conformer to bind ICAM-3. Biophysical studies have shown that the binding affinity of the αLβ2 I domain to ICAM-1 is at least 20-fold higher than to ICAM-3 (Shimaoka et al., 2001). Subsequently, an engineered high affinity αL I domain was employed for structural determination of αL I domain in complex with ICAM-3 (Song et al., 2005). In this study, transfectants bearing αLβ2 D709R, which has a cytoplasmic tail salt bridge disrupting mutation, adhered constitutively to ICAM-1 but not ICAM-3. Adhesion to

ICAM-3 was promoted when either Mg^{2+}/EGTA or KIM185 was included. It is unlikely that Mg^{2+}/EGTA or KIM185 promoted the formation of more intermediate affinity αLβ2, because all αLβ2 expressed on the transfectant carry the D709R mutation, which intrinsically activates αLβ2. Rather Mg^{2+}/EGTA or KIM185 converts αLβ2 D709R to a high affinity conformer that binds ICAM-3 effectively. Furthermore, we also found that a leukocyte adhesion deficiency type I mutation N329S in the β2 I-like domain induced a constitutively active αLβ2 that bound not only ICAM-1 (Tng et al., 2004) but also ICAM-3 effectively (Cheng et al., 2007). These observations support the requirement of a high affinity αLβ2 conformer to bind ICAM-3. From this study, talin-activated αLβ2 bound to ICAM-1 but not ICAM-3. Thus, it is reasonable to draw the conclusion that talin promotes an intermediate affinity αLβ2.

In an elegant study on talin-dependent T-cell migration, a population of clustered high affinity αLβ2 was detected and maintained by talin at the mid-cell zone of migrating T lymphoblast on ICAM-1 by using the activation reporter mAb m24 (Smith et al., 2005). Indeed, we could also detect m24 staining of αLβ2 on T lymphoblasts by flow cytometry in the absence of activating agent at physiological temperatures. However, we could only observe T lymphoblasts adhering to ICAM-3 when an additional activating agent Mg^{2+}/EGTA or KIM185 was included in the assay, which suggests a predominant population of an intermediate affinity αLβ2 on these cells. Aforementioned, it is possible that there may exist a small population of high affinity αLβ2 on T lymphoblasts. However, an intermediate affinity αLβ2 induced by allosteric antagonists XVA143 also reacted with m24 (Salas et al., 2004). The structural data of isolated αL I domain in complex with ICAM-1 reveals that the binding of ICAM-1 to the I domain favors additional conformational change from an intermediate to the open conformation

(Shimaoka et al., 2003). Coupled with the displacement of hybrid domain observed from EM images of fibronectin-bound αVβ1 headpiece (Takagi et al., 2003), and the crystal structure of fibrinogen-mimetic-bound αIIbβ3 headpiece (Xiao et al., 2004), the binding of ICAM-1 to an intermediate affinity αLβ2 may induce a liganded high affinity αLβ2 conformation. It is therefore interesting in subsequent studies to examine whether the ICAM-1-bound αLβ2 at the mid-cell zone of migrating T lymphoblasts adopts a high affinity conformation using other reporter mAbs such as 327C and 327A, which report extended αLβ2 with full I domain activation but are currently not available to us (Beals et al., 2001; Shamri et al., 2005).

In conclusion, the present study utilizing differential adhesion and binding assays to ICAMs and reporter mAbs suggests that talin promotes an intermediate affinity αLβ2. Recently, it was reported that talin is required for αLβ2-mediated immune synapse formation between T cell and antigen presenting cell and the requirement of talin-mediated αLβ2 clustering predominates over talin-induced αLβ2 affinity up-regulation (Simonson et al., 2006). However, it is also well documented that disrupting αLβ2 affinity up-regulation by leukocyte adhesion deficiency type I I-like domain mutations blunted αLβ2-mediated adhesion to ICAMs (Cheng et al., 2007; Mathew et al., 2000). Further, talin-induced conformational and affinity changes of αLβ2 have been reported (Kim et al., 2003). Additionally, the F3 subdomain of talin interacts with the membrane proximal α-helical region of the integrin cytoplasmic domain (Rodius et al., 2008; Wegener et al., 2007), and is likely to affect the activation state of integrins by disrupting the association between the α and β integrin subunits (Bhunia et al., 2009). Taken together, it is apparent that the overall adhesiveness or avidity of an αLβ2-mediated cell-cell contact or cell-substrate adhesion is dependent on both affinity

change and clustering. Other than talin, cytosolic proteins that were reported to interact with αLβ2 cytoplasmic tails include RAPL (Katagiri et al., 2003), cytohesin-1 (Geiger et al., 2000), and JAB-1 (Perez et al., 2003). These observations raise the interesting possibility of a network of molecules that may regulate the transition of αLβ2 from one affinity state to another. In addition, cytosolic proteins such as the adaptor protein SLAP-130 (Peterson et al., 2001), and the Rac-1 guanine nucleotide exchange factor Vav-1 (Krawczyk et al., 2002) are reported to control αLβ2 clustering. Together, these molecules may work in concert to allow the fine-tuning of αLβ2-mediated T cell adhesion in different microenvironments.

Chapter 4 The cytosolic proteins kindlin3 and talin HD co-activate integrin αLβ2

4.1 Introduction

In the previous chapter, we reported that the cytosolic protein talin induced an intermediate affinity αLβ2 to sufficiently bind ICAM-1. Recently another family of FERM domain-containing proteins, kindlins, was shown to interact with integrin β cytoplasmic tails (Harburger et al., 2009; Ma et al., 2008; Montanez et al., 2008). An extension of our study, we cloned kindlin2 and kindlin3 by RT-PCR from the T cell line Jurkat (Fig. 4.1). Based on EST assembly, two RNA splice variants of kindlin3 were deposited in the GenBank: Kindlin3 long form (NM_178443) that expresses a 667 amino acids protein, and kindlin3 short form (NM_031471) that expresses a 663 amino acids protein. We cloned both splice variants of kindlin3. Interestingly, we were able to clone two RNA splice forms of kindlin2: the kindlin2 short form (680 amino acids) and kindlin2 long form (687 amino acids). Kindlin2 short form (NM_006832) was reported previously, whereas kindlin2 long form has not been reported. This was deposited into the GenBank with accession number EU 979385.

Because we are interested in the regulation of leukocyte-restricted integrin αLβ2, we focused on kindlin3 with expression restricted to the hematopoetic cells (Ussar et al., 2006). Kindlin3 interacts directly with β1 and β3 integrins and co-activates β1 and β3 integrins with talin (Moser et al., 2008). While the mechanism(s) of kindlin3 regulation of integrin αLβ2 is being investigated in our lab, two recent reports on kindlin3 provided strong evidence that kindlin3 is important for β2 integrins-mediated

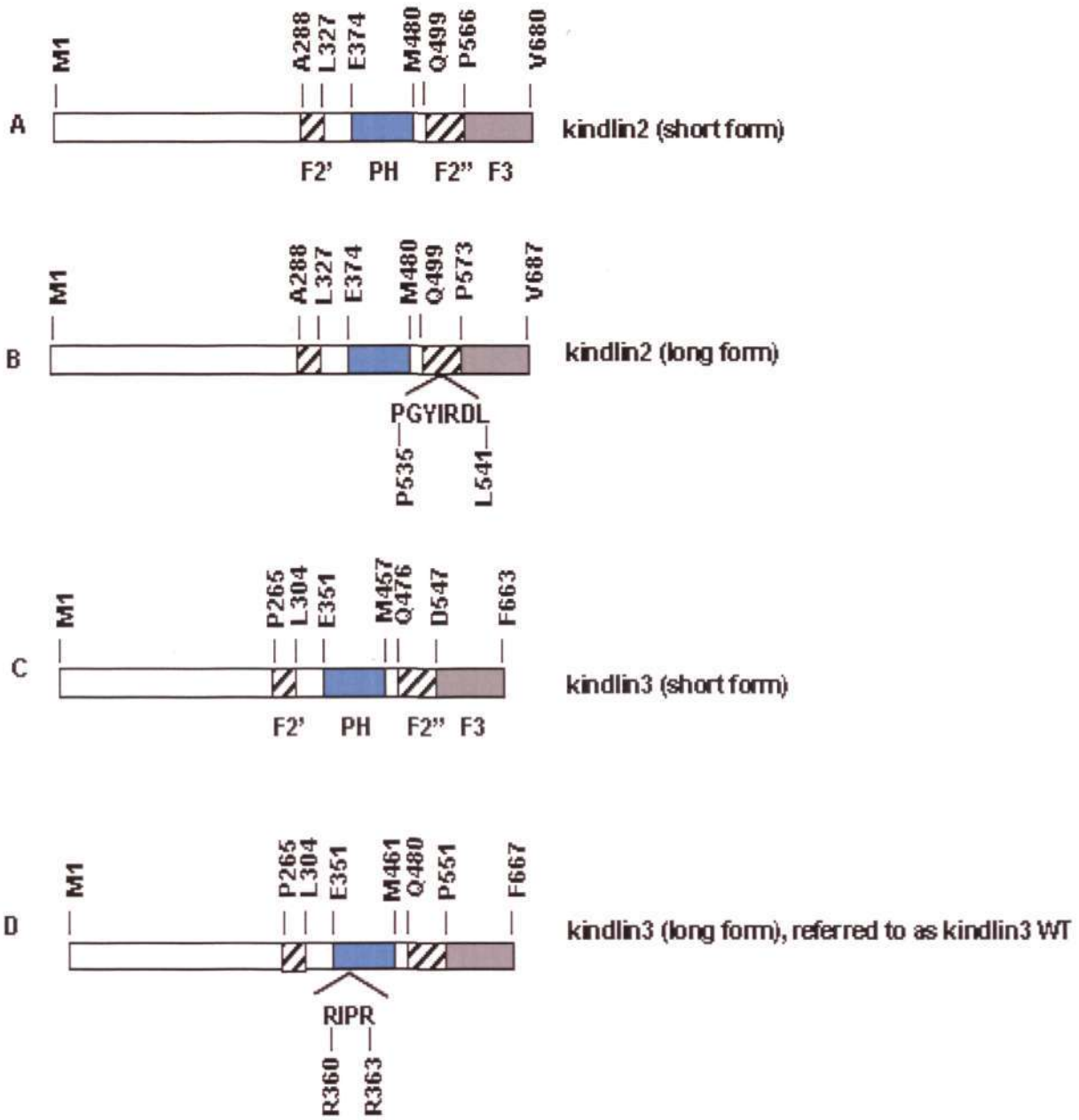

Fig. 4.1 Schematic diagram of the kindlin2 and kindlin3. (A) Domain organization of kindlin2 short form. (B) Domain organization of kindlin2 long form, which was deposited into the GenBank with accession number EU 979385. (C) Domain organization of kindlin3 short form. (D) Domain organization of kindlin3 long form that is investigated in this chapter.

adhesion and migration (Malinin et al., 2009; Moser et al., 2009a). One of these articles described leukocyte adhesion deficiency type (LAD) III of patients having kindlin3 mutations (Malinin et al., 2009). In this case, lymphocytes from LAD III individuals showed impaired integrin activation. The other article describes defective β2 integrin-dependent attachment and spreading of polymorphonuclear (PMN) cells on endothelial cells from kindlin3 null-mice (Moser et al., 2009a). The identification of kindlins as co-activators together with talin of integrins adds another level of complexity in terms of integrin function regulation. It is apparent that the model of talin as the primary molecule that contributes toward the final step of integrin activation requires refinement. There is still much to be learned in terms of the role of kindlins in integrin regulation (Moser et al., 2009b). For example, kindlin1 and kindlin2 appear to exert integrin-specific activation effects because overexpression of kindlin1 or kindlin2 in CHO cells in the absence of talin overexpression had an inhibitory effect on endogenous integrin α5β1 and stably expressed integrin αIIbβ3 in these cells (Harburger et al., 2009). This inhibitory effect, which is contrary to the widely reported role of kindlins as co-activators of integrins, appears to involve mechanism that is independent of the kindlin-binding site of the integrin cytoplasmic tail. Notably, kindlin2 was also reported to have a suppressive function in the metastasis of mesenchymal cells (Shi and Wu, 2008).

Of particular interest to us are the contributions of different regions of kindlin3 towards integrin αLβ2 regulation in leukocytes, which have not been described. Two major impediments to the understanding kindlin3 regulatory function are the lack of structural data and poor knowledge of molecule(s) other than the β integrins that may interact with it. Below describes the studies we have performed to investigate these aspects of kindlin3.

4.2 Results

4.2.1 Kindlin3 and talin HD synergistically increased binding affinity of αLβ2 to ICAM-1 which required both PH domain and F3 subdomain

The described co-activation effect of kindlin3 (long form) on β1 and β3 integrins along with talin prompted us to compare its contribution toward αLβ2-mediated adhesion to ICAM-1, more importantly, the contribution of the different regions or domains of kindlin3 in this setting. Kindlin3 long form (henceforth referred to as kindlin3) was cloned into pEGFP-C1 expresion vector to generate an EGFP-kindlin3 fusion plasmid. Two mutants were generated using this plasmid. A PH domain deleted kindlin3 referred to as EGFP-kindlin3 PHΔ and a F3 subdomain deleted kindlin3 referred to as EGFP-kindlin3 F3Δ (Fig. 4.2.1A). The talin head domain (HD) was also cloned into pcDNA3.1 (+) in fusion with a DsRed (fluorescent red protein) tag. The cloing strategies of these constructs are described in the materials and methods section.

To assess the contribution of kindlin3 domains to the regulation of integrin αLβ2, 293-T cells were transiently transfected with these combinations of expression plasmids: (i) αLβ2, (ii) αLβ2 and EGFP-kindlin3, (iii) αLβ2 and DsRed-talin HD, (iv) αLβ2, EGFP-kindlin3, and DsRed-talin HD, (v) αLβ2, EFGP-kindlin3 F3Δ, and DsRed-talin HD, (vi) αLβ2, EFGP-kindlin3 PHΔ, and DsRed-talin HD. The expression levels of EGFP-kindlin3 and DsRed talin HD were determined by flow cytometry using the FL1 and FL2 channels, respectively, with appropriate compensation (Fig. 4.2.1B). The % gated positive cells were indicated for each gated quadrant. To further verify the expression of EGFP-kindlin3 PHΔ and EGFP-kindlin3 F3Δ, cell lysates of 293-T transfected with these kindlin3 plasmids were immunoblotted with polyclonal

anti-kindlin3 antibody (generated in Dr. Tan S.-M. lab) (Fig. 4.2.2C). The migration profiles of the protein bands corresponding to EGFP-kindlin3 PHΔ and EGFP-kindlin3 F3Δ were consistent with their corresponding domain deletions in these constructs. The construct EGFP-kindlin3 W600A will be discussed in the next section. The expression levels of αLβ2 in all transfectants were also assessed by imunoblotting with an anti-αL-specific antibody, and they were comparable amongst the samples (Fig. 4.2.2D). The activity of the αLβ2 in these transfectants was assayed by allowing cells to adhere to immobilized ICAM-1 as described in the previous chapter (Fig. 4.2.2E). The specificity of αLβ2-mediated adhesion of cells to ICAM-1 was verified using the function-blocking αLβ2-specific antibody MHM24. We observed that cells transfected with αLβ2 and EGFP-kindlin3 adhered poorly to ICAM-1, which was comparable to that of cells transfected with αLβ2 only. Cells transfected with αLβ2 and DsRed talin HD showed enhanced ICAM-1 adhesion. Cells transfected with αLβ2, DsRed talin HD, and EGFP-kindlin3 showed further increase in ICAM-1 adhesion. These data are in line with the reported properties of talin as an activator of integrins and kindlin as a co-activator of integrins. The synergistic property of kindlin3 and talin on αLβ2 activation was reduced when either the F3 subdomain or the PH domain of kindlin3 was deleted albeit different levels of reduction.

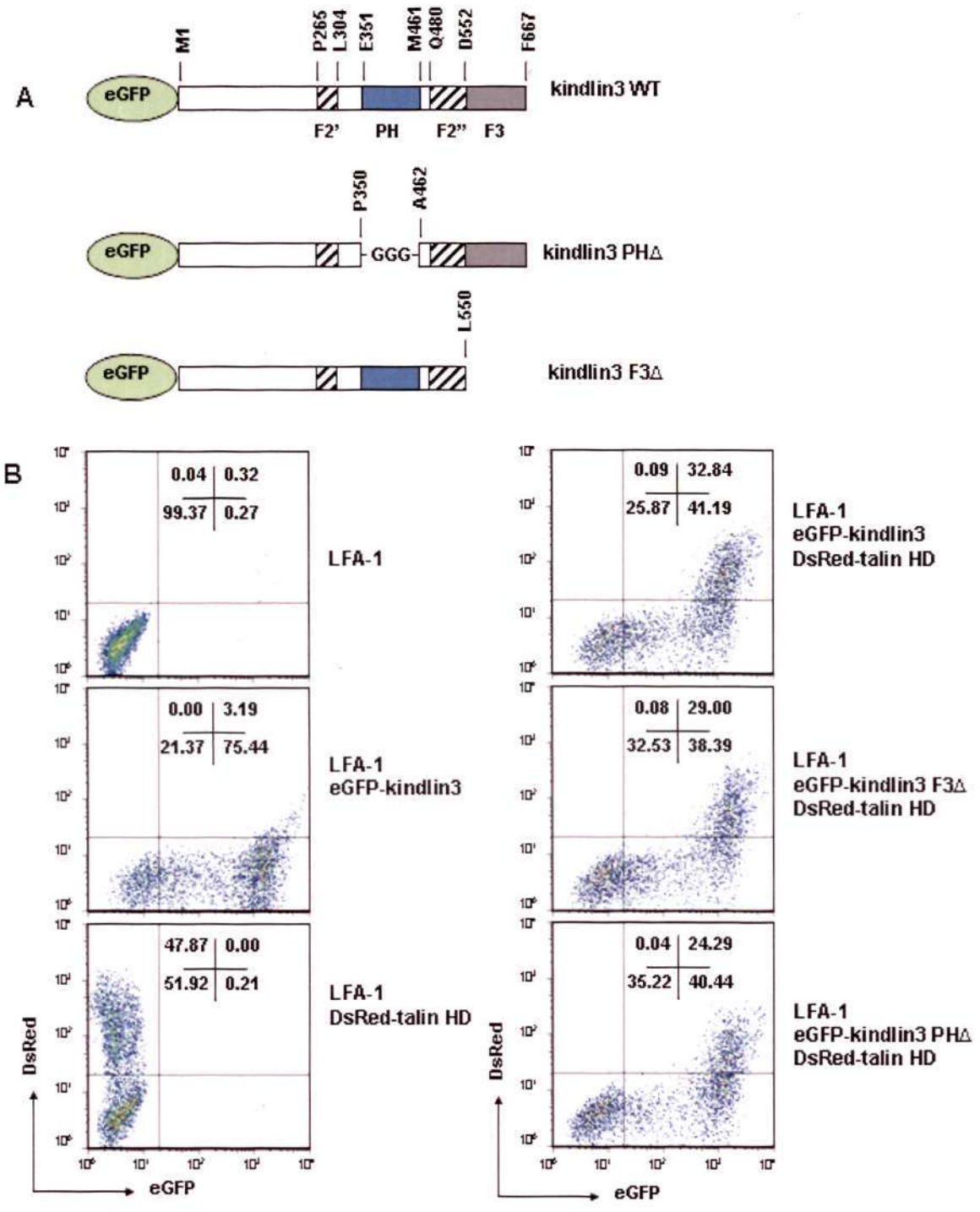

Fig. 4.2.1 Kindlin3 and talin HD synergistically increased binding affinity of αLβ2 which required both PH domain and F3 subdomain. (A) Schematic domain organizations for EGFP-kindlin3, EGFP-kindlin3 PHΔ, and EGFP-kindlin3 F3Δ. (B) Expression of EGFP-kindlin3 and DsRed-talin HD was detected by flow cytometry.

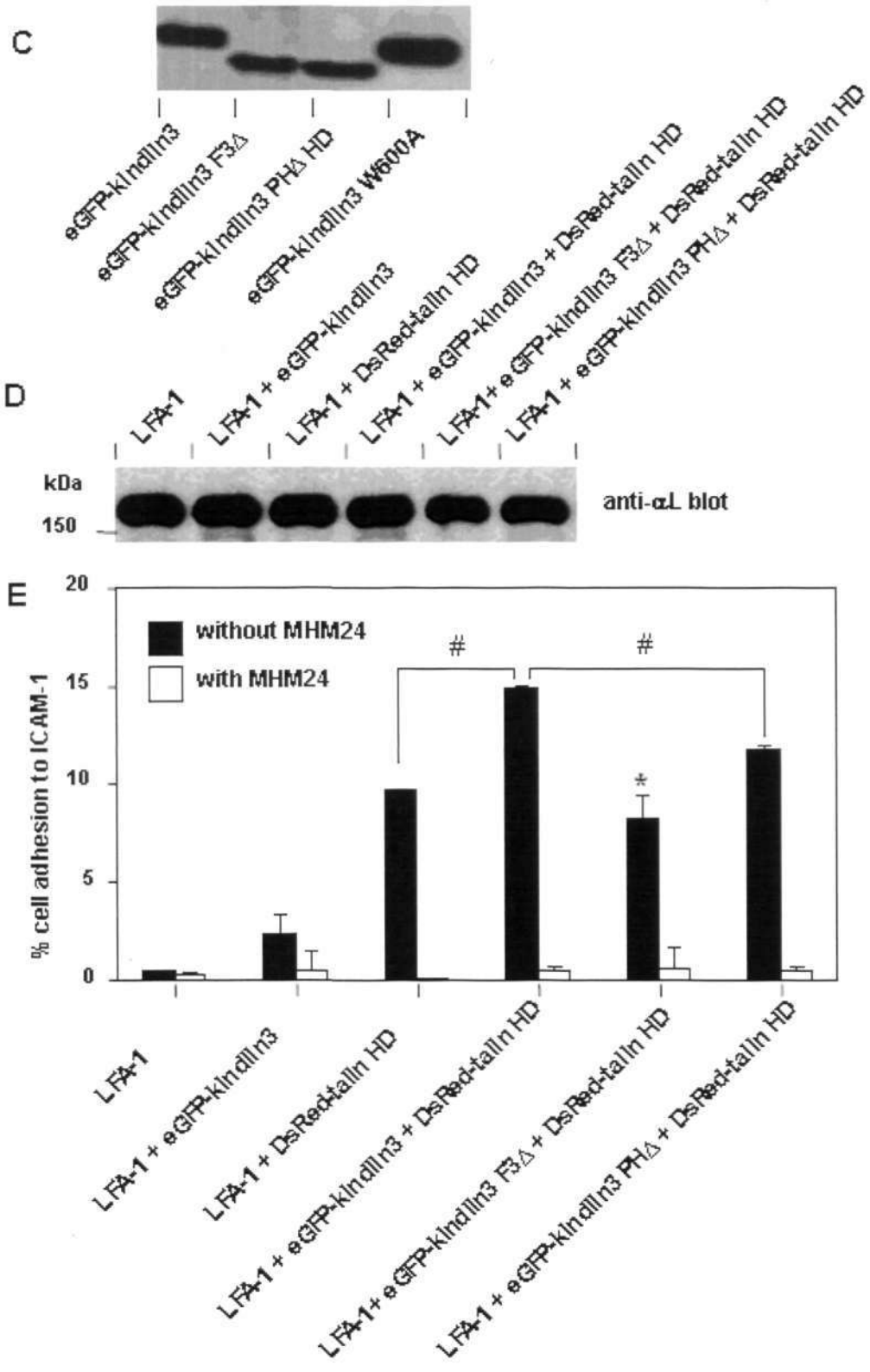

Fig. 4.2.2 Kindlin3 and talin HD synergistically increased binding affinity of αLβ2 which required both PH domain and F3 subdomain. (C) Transfected EGFP-kindlin3 and mutants were detected by immunoblotting cell lysates with anti-kindlin3 antibody. (D) Transfected αL was detected by anti-αL antibody. (E) Adhesion of respective transfectants on ICAM-1. Adhesion specificity was demonstrated using the function-blocking mAb MHM24. *, $p<0.05$, with respect to LFA-1; #, $p<0.05$. All statistical analyses were performed using Student's t test.

It was reported that mutations W612A in kindlin1 and W615A in kindlin2 abrogated their interactions with the integrin β1A cytoplasmic tail (Harburger et al., 2009). Both W612 and W615 are located in the F3 subdomains of the kindlin1 and kindlin2, respectively. Thus, we made the corresponding mutation in kindlin3 that is W600A to assess the effect of this mutation on the synergistic activation property of kindlin3 on αLβ2. We adopted the same strategy as before by generating EGFP-kindlin3 W600A, and testing its effect in 293-T transfectants co-expressing αLβ2 with DsRed talin HD. The expression levels of EGFP-kindlin3, EGFP-kindlin3 W600A and DsRed talin HD were determined by two-color flow cytometry (Fig. 4.3A). The levels of αLβ2 expression in all transfectants were comparable as determined by anti-αL immunoblot (Fig. 4.3B). Kindlin3 functions as a co-activator of αLβ2 with talin HD. However, kindlin3 W600A and talin HD co-expression failed to maintain the synergistic effect on αLβ2 (Fig. 4.3C). αLβ2 with talin HD and kindlin3 W600A showed significantly lower adhesion to ICAM-1 than that of αLβ2 with talin HD and kindlin3. The conserved tryptophan W600 in the F3 subdomain of kindlin3 is required for its co-activating effect.

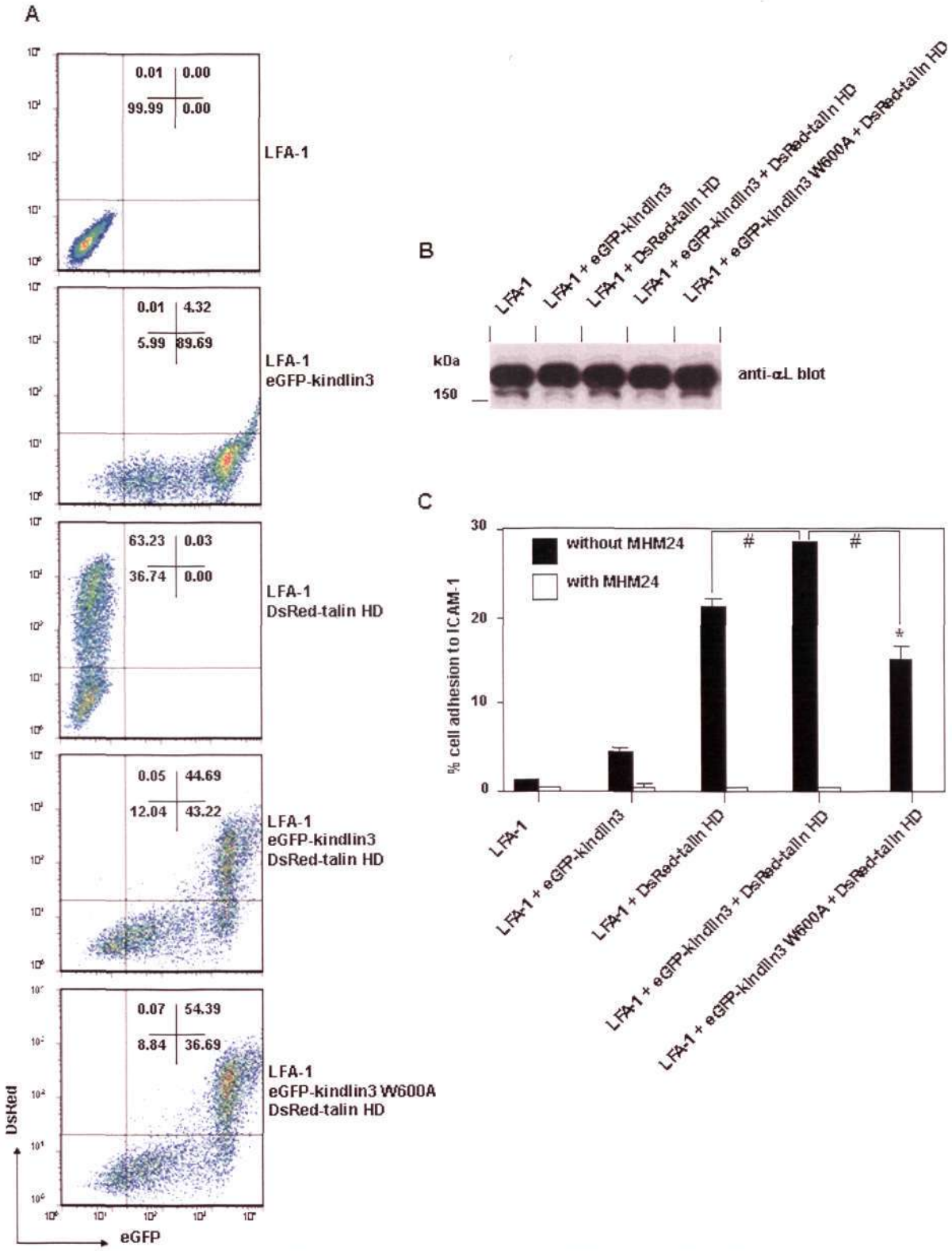

Fig. 4.3 The synergistic effect of kindlin3 and talin HD on αLβ2 affinity upregulation is dependent on Trp^{600} in F3 subdomain. (A) Expression of EGFP-kindlin3 and DsRed-talin HD was detected by flow cytometry. (B) Transfected αL was detected by immunoblotting cell lysates with anti-αL antibody. (C) Adhesion of respective transfectants on ICAM-1. Adhesion specificity was demonstrated using the function-blocking mAb MHM24. *, $p<0.05$, with respect to LFA-1; #, $p<0.05$. All statistical analyses were performed using Student's t test.

4.2.2 The T cell line SKW 3.0 expresses constitutively activated αLβ2 induced by talin

We aim to examine the contribution of kindlin3 in αLβ2-mediated migration. To achieve this, we made use of a T cell line SKW 3.0 that is amenable to plasmids transfection. Unlike the T cell line Jurkat that does not adhere to immobilized ICAM-1 without integrin activation and does not polarize well in the presence of chemokine stimulus, SKW 3.0 showed constitutive αLβ2-mediated ICAM-1 adhesion as determined by cell adhesion assay (Fig. 4.4A). In this case, Jurkat cells required the αLβ2 activating agent Mg^{2+}/EGTA to adhere to ICAM-1, whereas significant SKW 3.0 adhesion to ICAM-1 even without Mg^{2+}/EGTA supplement was observed. In all cases, adhesion was specifically mediated by αLβ2 because addition of the function-blocking anti-αLβ2 specific mAb MHM24 abrogated all adhesion. The constitutively activated αLβ2 on SKW 3.0 was induced by talin because siRNA-mediated reduction of endogenous talin expression in SKW 3.0 effectively diminished its constitutive ICAM-1 adhesion property as compared to cells treated with control siRNA (Fig. 4.4B & C). Adhesion to ICAM-1 could be restored in talin knockdown cells when treated with Mg^{2+}/EGTA, suggesting that αLβ2 on these cells was functional (Fig. 4.4C). The expression of αLβ2 on SKW 3.0 transfected with talin siRNA was similar to that transfected with control siRNA as determined by flow cytometry, which excludes the possibity of poor binding due to reduction of αLβ2 expression in these cells as a result of the siRNA treatment (Fig. 4.4D).

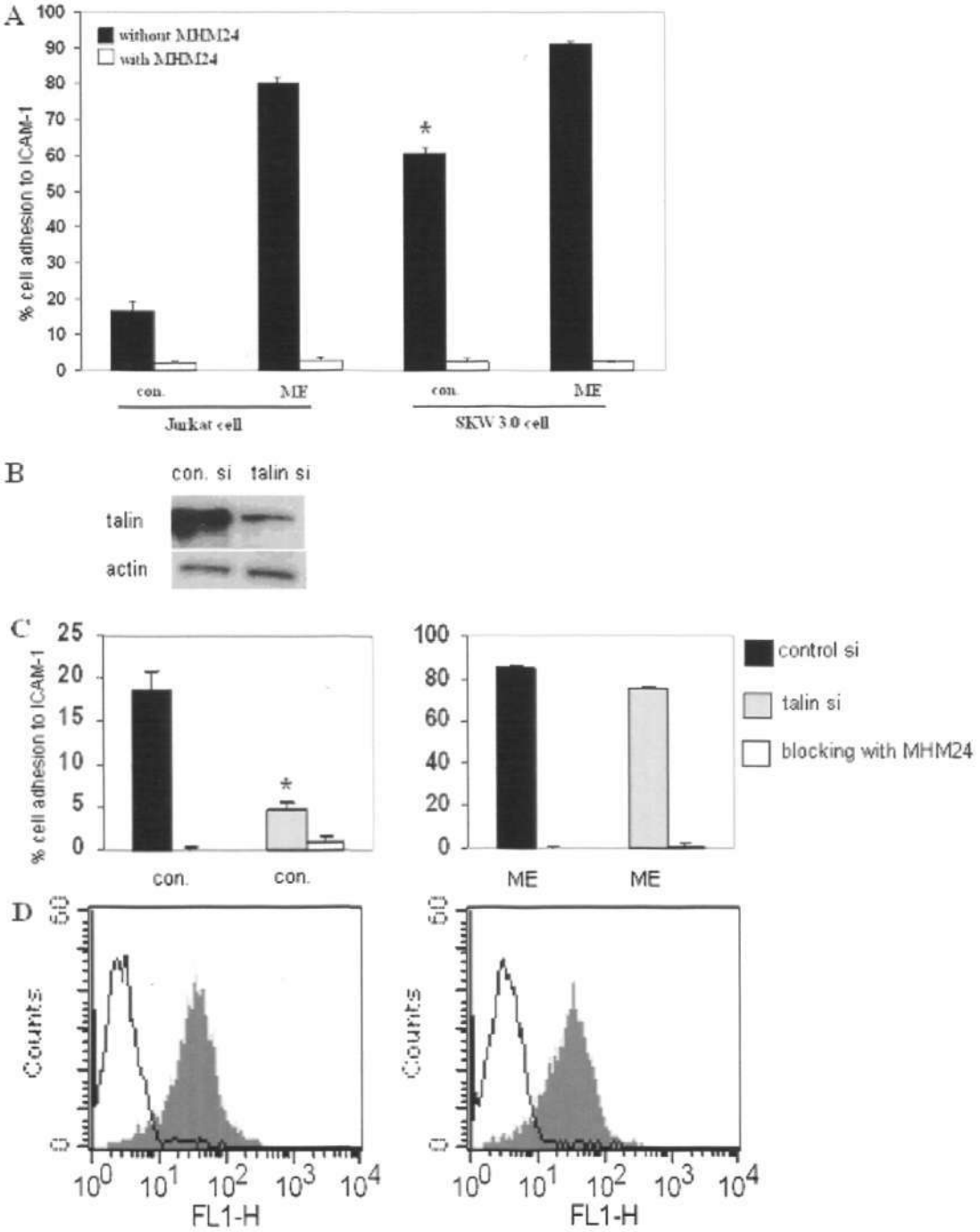

Fig. 4.4 Talin induced expression of activated αLβ2 on T-cell line SKW 3.0.
(A) αLβ2-mediated adhesion of Jurkat and SKW 3.0 cells to ICAM-1. con.: control condition without any additives. ME: 5 mM $MgCl_2$ and 1.5 mM EGTA. *, $p<0.05$, (Student's t test), with respect to con. of Jurkat cell. (B) Knockdown of endogenous talin expression in SKW 3.0 using siRNA. The level of talin knockdown was shown by immunoblotting for talin (mAb 8d4) in cell lysates of SKW 3.0 transfected with talin siRNA or a control siRNA. Actin was immunoblotted as a control for total protein loaded. (C) Adhesion of talin knockdown SKW 3.0 to ICAM-1 in the presence or absence of ME. *, $p<0.05$, (Student's t test), with respect to con. of cells treated with control siRNA. (D) The expression of αLβ2 on SKW 3.0 was determined by flow cytometry using the mAb MHM24 (shaded histogram). Irrelevant mAb (open histogram).

We next examined the migratory property of SKW 3.0 cells that were transfected with EGFP-kindlin3 and mutants. Cells were transfected with the relevant EGFP-kindlin3 plasmids by electroporation and sorted on a flow cytometry cell sorter so as to collect cells expressing equivalent level of EGFP-kindlin3 and mutants (quadrant P1 in Fig. 4.5A). These sorted cells were allowed to adhere and migrate on glass-bottom dishes coated with ICAM-1 and the chemokine SDF-1α. Similar coating of ICAM-1 and SDF-1α was reported by others (Morin et al., 2008). The migrating cells were visualized on a live-cell imaging system at 37 ºC for 20 min. Thereafter, the migratory tracks and motility (μm/min) of the cells were analyzed and plotted. We first compared cells transfected with EGFP empty vector on ICAM-1 with or without SDF-1α, and observed that SDF-1α treatment significantly increased the motility of these cells (Fig. 4.5B). Interestingly, cells transfected with EGFP-kindlin3 showed reduced motility as compared to cells transfected with EGFP empty vector even in the presence of SDF-1α. Cells transfected with EFGP-kindlin3 PHΔ, EGFP-kindlin3 F3Δ, and EGFP-kindlin3 W600A showed similar migratory profiles when compared to cells transfected with empty EGFP vector. The migration speed of these cells was also calculated and plotted (Fig. 4.5C). Whilst analyzing the migratory properties of SKW 3.0 transfected with EGFP-kindlin3 and mutants, we were also able to observe the distribution of EGFP-kindlin3 and mutants in these cells (Fig. 4.6). Whereas a homogenous distribution of EGFP in polarized SKW 3.0 was observed, EGFP-kindlin3 localized primarily at the leading edge of the migrating cells. Subtle difference was also observed between EFGP-kindlin3 and mutants. Although EGFP-kindlin3 W600A, EGFP-kindlin3 PHΔ, and EGFP-kindlin3 F3Δ were detected at

the leading edge of the migrating cells, they could also be detected at the uropod region of the cells as compared to EGFP-kindlin3. Collectively, these data suggest that both the integrin-binding site (absent in EGFP-kindlin3 W600A and EGFP-kindlin3 F3Δ) and the PH domain (absent in EGFP-kindlin3 PHΔ) are important for the localization of kindlin3 to the leading edge of αLβ2-mediated migrating T cells.

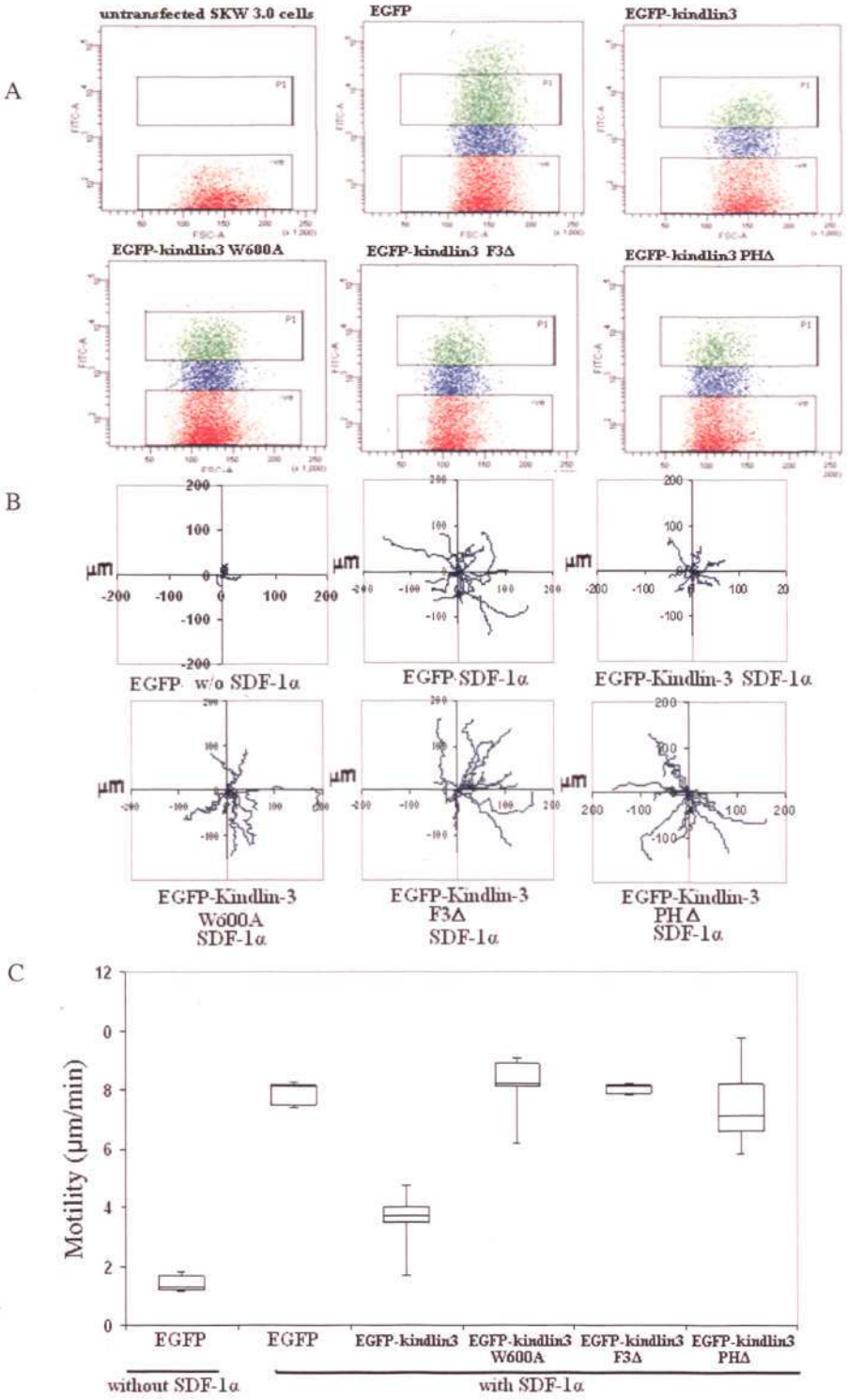

Fig. 4.5 Migration of SKW 3.0 transfectants (EGFP, EGFP-kndlin3, EGFP-kndlin3 W600A, EGFP-kndlin3 F3Δ, or EGFP-kndlin3 PHΔ) on ICAM-1 and SDF-1α. (A) Transfected cells were sorted based on the EGFP emission signal gated P1. (B) The sorted cells were allowed to migrate on ICAM-1 with or without SDF-1α. The representative migratory tracks of 15 transfected cells (based on EGFP emission signal) were generated using Metamorph®, and the trajectories were presented on an X-Y (microns) plot with the origin of each recorded cell positioned at X = 0 μm, Y = 0 μm. (C) Box plot presentation of motility (μm/min) out of 80 cells examined for each sample.

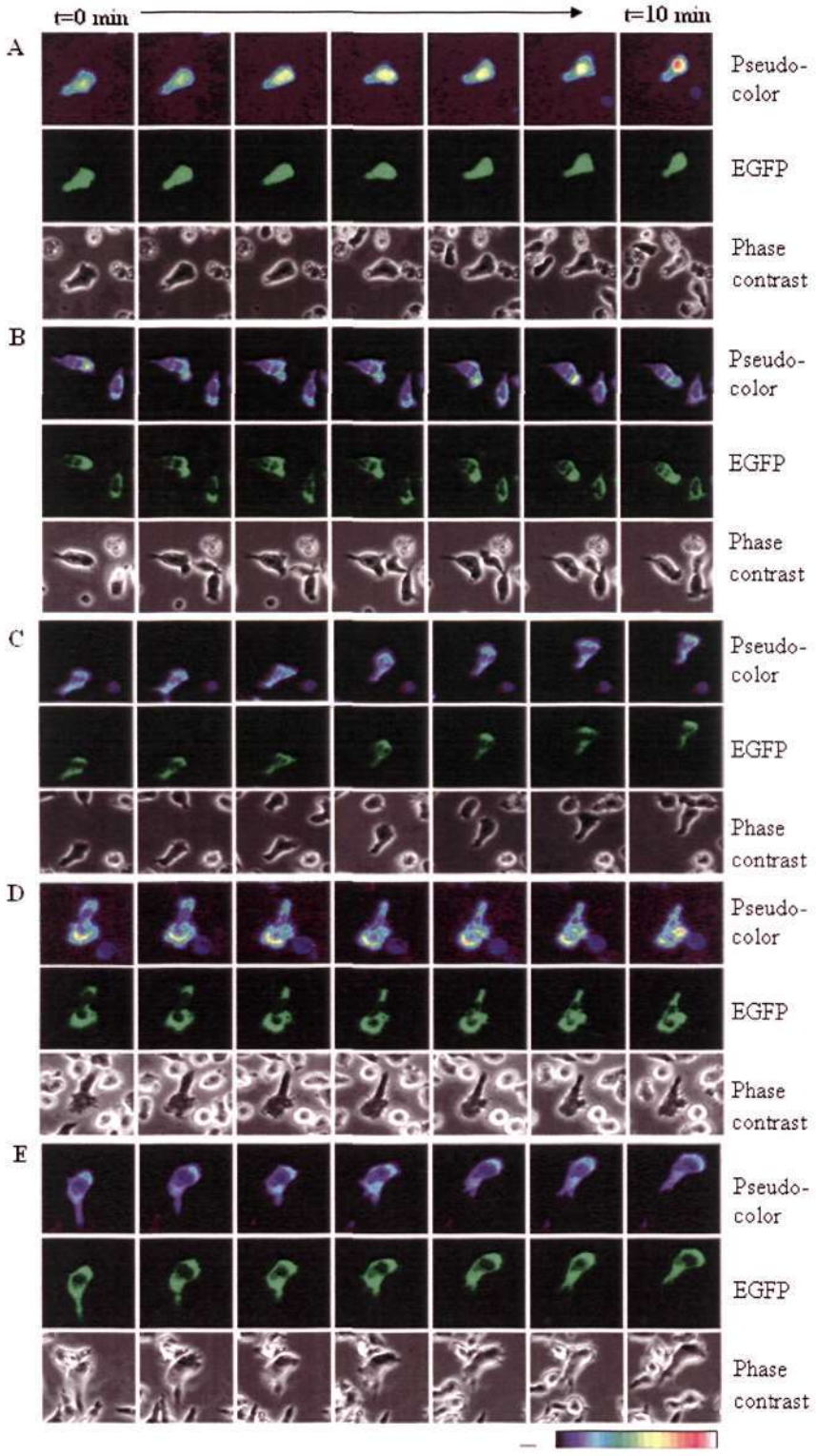

Fig. 4.6 Live cell images of SKW 3.0 transfectants on ICAM-1 and SDF-1α. EGFP pheudocolor, EGFP, and Phase-contrast microscopy images of transfectants, bearing (A) EGFP, (B) EGFP-kindlin3, (C) EGFP-kindlin3 W600A, (D) EGFP-kindlin3 F3Δ, or (E) EGFP-kindlin3 PHΔ, migrating on ICAM-1 and SDF-1α with time (7 images are shown for an interval of 10 min). Rainbow showing white and black represent high and low intensities of EGFP signal, respectively. Scale bar: 10 μm.

4.2.3 Kindlin3, talin and αLβ2 co-localize at the leading edge of migratory T cells

Transfection of immature dendritic cells with EGFP-kindlin3 revealed kindlin3 localization to the actin surrounding ring of podosomes (Ussar et al., 2006). However, kindlin3 localization in polarized T cells has not been reported. In the previous section, we observed possible localization of kindlin3 at the pseudopodia of polarized SKW 3.0 cells migrating on ICAM-1 on a live-cell imaging system. Here, we extended the study by analyzing the localization of kindlin3, talin, and αLβ2 in these cells. SKW 3.0 cells transfected with EGFP-kindlin3 were allowed to adhere to ICAM-1 and SDF-1α-coated slides at 37 ºC for 30 min. Therafter, cells were fixed, permeabilized, and stained with anti-talin antibody (8d4) or anti-αLβ2 (7E4) antibody followed by Alexa594-fluorophore conjugated secondary antibody as decribed in materials and methods. Cells were then examined on a confocal laser-scanning microscope. Z-sectioned images of the cells were acquired, processed with a LSM image examiner, and the images at the bottom of the z-stack where the cells bound ligand ICAM-1 were presented in Fig. 4.7.

Overlay of the images of EGFP-kindlin3 (green) and endogenous talin (red) showed overlapping signals predominantly at the migratory front of the cell (Fig. 4.7A & B). This can also be observed in the intensity plot along the indicated axis in line with the direction of migration of the cell. Similarly, co-localization of αLβ2 with kindlin3 was observed predominantly at the migrating front of the cell (Fig. 4.7C & D). The control sample in which cells were transfected with empty EGFP vector showed an even distribution of EGFP, suggesting that the high intensity of kindlin3 at the migrating front was not attributed to the volume of the membrane ruffles (Fig. 4.8A & B). Similarly, the staining of talin at the migratory front of the cell was verified by the lack of signal in cells staining

with an irrelevant antibody followed by Alexa594-conjugated secondary antibody (Fig. 4.8C & D).

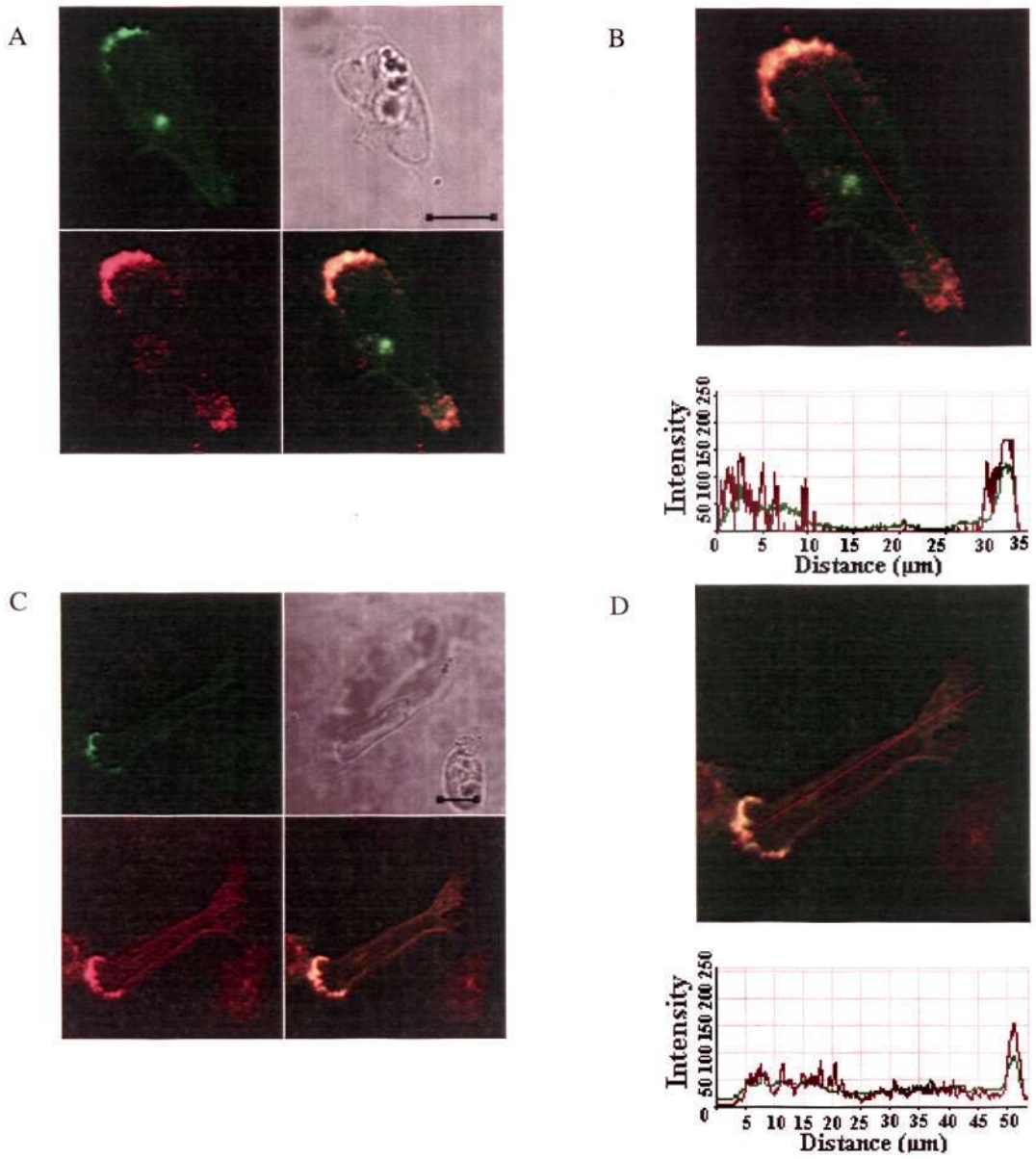

Fig. 4.7 Co-localization of kindlin3 with talin and αLβ2 on migrating T cells. (A) Confocal image of a representative SKW 3.0 cell transfected with EGFP-kindlin3 (green) and stained with 8d4 (red) followed by Alexa594 secondary antibody to detect talin (red) following fixation. (B) The fluorescence intensity of EGFP-kindlin3 expression (green trace) and 8d4 staining (red trace) along the length of the polarized SKW 3.0 T cell (indicated by red arrow on merged image) is recorded. (C) EGFP-kindlin3 (green) transfected SKW 3.0 cells were stained with 7E4 followed by Alexa594 secondary antibody to detect integrin αLβ2 (red). (D) Merged image of EGFP-kindlin3 (green) and 7E4 staining (red). Respresentative image was shown out of 15 images aquired. Scale bar: 10 μm.

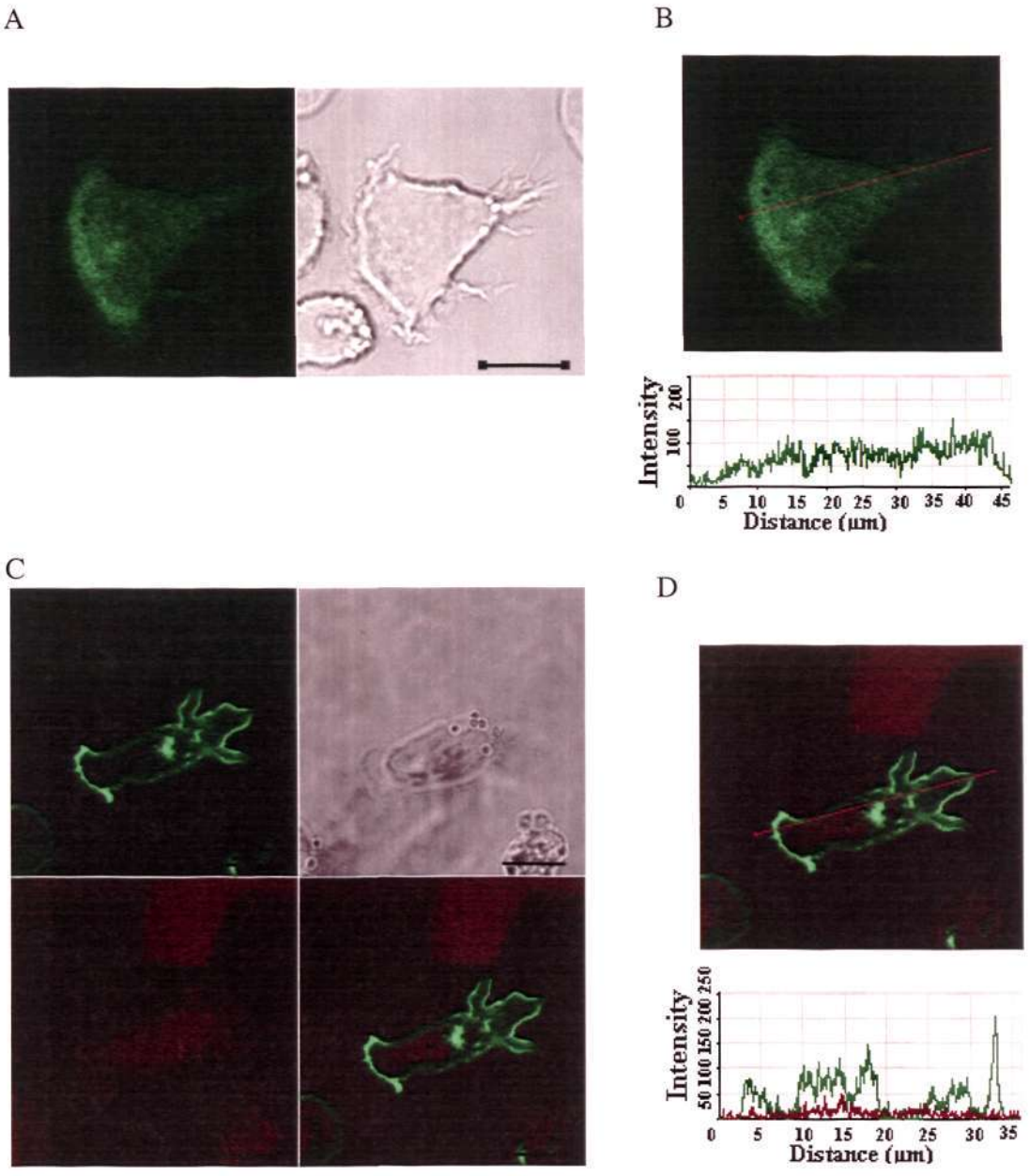

Fig. 4.8 Images of control cells. (A) Confocal images of EGFP (green) in migrating SKW 3.0 cells. (B) The expression level of EGFP (green trace) along the length of the polarized SKW 3.0 T cell (indicated by red arrow) is recorded. (C) Image of SKW 3.0 cells transfected with EGFP-kindlin3 (green) and stained with an irrelevant antibody (red) followed by Alexa594 secondary antibody. (D) The fluorescence intensity of EGFP-kindlin3 expression (green trace) and control antibody staining (red) along the length of the polarized SKW 3.0 T cell (indicated by red arrow on merged image) is shown. Scale bar: 10 µm.

4.2.4 Possible interaction between kindlin3 and RACK1

Other than the F3 subdomain in kindlins that binds integrin β subunit cytoplasmic tails, the kindlins also contain a PH domain. PH domain is known to interact with a number of proteins including the Receptor for Activated C Kinases (RACK1), a 36 kD cytoplasmic protein having seven Trp-Asp (WD) repeats that fold into a seven-bladed propeller structure (McCahill et al., 2002). RACK1 expression is ubiquitous, and as its name indicates, it binds to activated PKCs, in particular the conventional PKC isoform PKCβII (Ron et al., 1995; Stebbins and Mochly-Rosen, 2001). Apart from PKCs, RACK1 is a scaffolding protein important in various signaling events (McCahill et al., 2002). Proteins reported to associate with RACK1 include FAK (Kiely et al., 2009), Src (Cox et al., 2003), and the cytoplasmic tail of integrin β subunit (Kiely et al., 2006). The structure of RACK1 allows docking of different proteins to its different blades, thus fulfilling its role as an adapter molecule that serves as a hub for cell signaling. RACK1 was shown to bind to several PH-domain containing molecules (Rodriguez et al., 1999). Our group detected interaction between kindlin3 and RACK1 in 293-T transfectants by co-immunoprecipitation, and the association is dependent on the kindlin3 PH domain (this was a study made by another student in the lab and data not shown). Thus, we examined the localization of EGFP-kindlin3 and endogenous RACK1 in SKW 3.0 cells migrating on ICAM-1 and SDF-1α-coated slide (Fig. 4.9). RACK1 was detected with anti-RACK1 antibody followed by staining with Alex594-fluorophore conjugated secondary antibody. Overlay of the images of EGFP-kindlin3 (green) and endogenous RACK1 (red) indicated overlapping signals, suggesting co-localization of these molecules. However, RACK1 was also observed to localize in the uropod of a number of cells. This need not be unexpected because RACK1 is known to interact with many other cellular proteins. The observation could suggest that the association of RACK1 with kindlin3 is a

dynamic process because of competition for RACK1 binding sites in the migrating cell (McCahill et al., 2002). Further studies will be required to address the regulatory mechanism of kindlin3 and RACK1 interaction, and the biological relevance of such association.

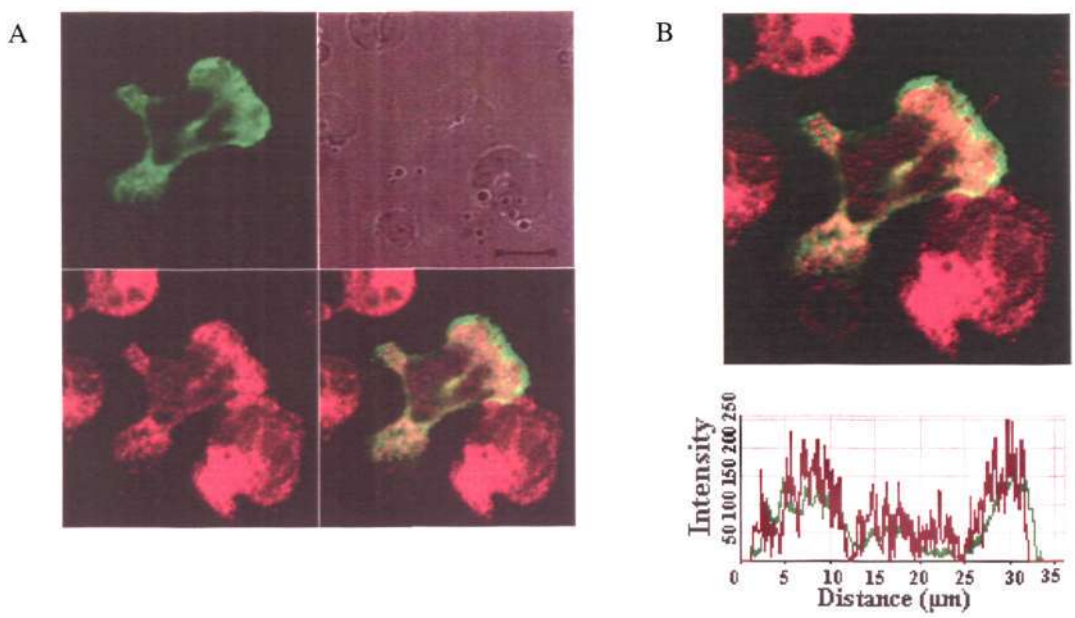

Fig. 4.9 Co-localization of kindlin3 with RACK1 in migrating T cells. (A) Confocal image of a representative SKW 3.0 cell transfected with EGFP-kindlin3 (green) and stained with anti-RACK1 antibody followed by Alexa594 secondary antibody (red) following fixation. (B) The fluorescence intensity of EGFP-kindlin3 expression (green trace) and RACK1 staining (red trace) along the length of the polarized SKW 3.0 T cell (indicated by red arrow on merged image) is shown. Scale bar: 10 μm.

4.3 Discussion

In this chapter, we have investigated the role of kindlin3 in the regulation of αLβ2 activation and αLβ2-mediated T cell migration. In line with the reported co-activator status of kindlins (Ma et al., 2008; Moser et al., 2008), we showed that kindlin3 alone failed to promote αLβ2 activation without the presence of talin HD in 293-T transfectants. By domain deletion, we observed that both the F3 subdomain and the PH domain of kindlin3 are important for its role as an integrin co-activator. Despite similar negative effect of these domain deletions on the function of kindlin3, it appears that the effect is more pronounced in F3 subdomain deleted as compared to PH domain deleted mutants. Whereas the F3 subdomain binds to the cytoplasmic tail of the integrin β subunit, the PH domain of kindlin3 could bind to phosphatidylinositol phosphates. The lesser effect of PH domain deleted mutant as compared to F3 subdomain deleted mutant could be attributed to the different roles of these individual domains.

In all kindlin studies thus far reported, co-immunoprecipitation data of kindlins with integrins are lacking. Many of the studies made use of pull-down assays with GST-tagged integrin cytoplasmic tail as the bait to probe for kindlin association in cell lysates (Ma et al., 2008; Moser et al., 2009a; Moser et al., 2008). We have attempted co-immunoprecipitation assays of kindlin3 with αLβ2 in 293-T transfectants and cell lines, but were not successful in detecting significant interaction. It is possible that the association of kindlin3 with the integrin cytoplasmic tail is weak or the interaction is sensitive to detergent used in the immunoprecipitation protocols. Alternatively, an adapter molecule is required for the association of kindlins with the integrin cytoplasmic tails.

In the immunofluoresence analyses, we observed co-localization of kindlin3 with integrin αLβ2 in the T cell line SKW 3.0 that was allowed to attach, polarize, and migrate on ICAM-1 in the presence of chemokine SDF-1α. We also detected co-localization of kindlin3 with talin in these cells. Considering the synergistic action of kindlin and talin on integrin activation, we have performed co-immunoprecipitation assay to check whether talin HD interacts with kindlin3 (data not shown). We could not detect any significant association of these molecules. Thus it is unlikely that talin serves as an adaptor for the docking of kindlin to the integrin cytoplasmic tail. However, this may need further verification by studies that demonstrate direct interaction. We have previously expressed talin HD in *E. coli* for isothermal calorimetry assays with recombinant integrin cytoplasmic tail peptide (Bhunia et al., 2009). Thus we have also attempted to express kindlin3 similarly; however, the expression of full-length kindlin3 or kindlin3 F3 subdomain in *E. coli* system was poor. Harburger et al. also reported similar observation (Harburger et al., 2009). We have not explored using insect cell or mammalian cell expression systems, but these are possible future studies to be conducted.

Notably, we detected possible co-localization of kindlin3 with RACK1 at the migratory front of the SKW 3.0 T cells. Taking into consideration that kindlin3 and RACK1 co-precipitated from cell lysates of 293-T transfectants as demonstrated by my colleague in the lab, and that the PH domain of kindlin3 is required for this association, these data suggest possible role of kindlin3 in downstream signaling other than its co-activator status in integrin activation. RACK1 is shown to bind to activated PKCs, in particular PKCβII (Ron et al., 1995; Stebbins and Mochly-Rosen, 2001). PKCs are well established to play important roles in cell migration, proliferation, differentiation, and apoptosis (Ghayur et al., 1996; Humphries et al., 2006; Li et al., 2003a; Mischak et al., 1993; Watanabe et al., 1992). In T cells, PKCβI (note: PKCβI and PKCβII are splice variants) is shown to be

crucial for the αLβ2-mediated migration, and PKCβI is preferentially localized at the microtubule organizing centre (MTOC) with diffused localization in the trailing portion of the T cell (Volkov et al., 2001). Whether there is any functional correlation amongst kindlin3, RACK1, and PKCβ isoforms remains to be clarified. Kindlin can also regulate the connectivity between integrins and the cytoskeleton. Kindlin2 is shown to associate with migfilin which links focal adhesions to filamin and the actin cytoskeleton (Tu et al., 2003) although no cytoskeleton binding sites have been identified in kindlin3 at present.

The aforementioned studies made use of overexpressed EGFP-tagged kindlin3. We have attempted to study endogenous kindlin3, but were met with difficulties. Most of the kindlin3 studies made use of polyclonal kindlin3 antibodies raised against kindlin3 peptide Glu^{156}-Ala^{170} from Fässler's group (Moser et al., 2008; Ussar et al., 2006). The antibody was not accessible to us, and commercial sources of antibodies were purchased and tested, but were all very poor in reactivities to endogenous kindlin3. Subsequently, we have generated polyclonal antibodies to kindlin3 using the same strategy as Fässler's group, but the antibody reacts poorly with endogenous kindlin3 tested in many different leukocyte cell lines. We acknowledged that studies analyzing endogenous kindlin3 are essential for future work along this direction, and we are still optimizing the immunization procedures to obtain suitable anti-kindlin3 antibodies.

Chapter 5 Discussion and future work

The importance of integrins in cell adhesion and migration is well established and described in many reviews (Abram and Lowell, 2009a; Hynes, 2002; Vicente-Manzanares et al., 2009). Three decades earlier, the seminal report by Hynes et al. suggested a family of molecules that linked the cytoskeleton to the extracellular matrix fibronectin (Hynes, 1976). Subsequently, identification of mutations that disrupt integrins expressions and/or expression of defective integrins in diseases, such as leukocyte adhesion deficiency type I (Arnaout, 1990; Hogg and Bates, 2000), Glanzmann's thrombasthenia (Morel-Kopp et al., 1997; Nurden, 2007), and junctional epidermolysis bullosa (Vidal et al., 1995), provided strong evidence of integrins playing major roles in cell adhesion and migration. Like many other molecules, the need to explain the mechanism(s) of integrin regulation requires knowledge of the integrin structure. During the period 1980-2000, many groups had attempted to resolve the complete integrin structure. Electron microscopy (EM) images of integrins suggest a molecule with a large globular head and two stalks (Xiong et al., 2001; Zhu et al., 2008). However, these EM images did not provide finer details of integrin domain organization and folding. X-ray crystallography studies provided detailed information on the structure of the isolated integrin I domains that allow good explanation of the divalent cation dependency of ligand-binding for integrins containing an I domain (Lee et al., 1995a; Lee et al., 1995b). The breakthrough came in year 2001 when the first full-length ectodomain structure of an integrin was reported despite the fact that certain regions of the the integrin $\alpha V\beta 3$ were not solved (Xiong et al., 2001). Nonetheless, the obtuse bent conformation of $\alpha V\beta 3$ seen in these structures along with many subsequent studies on integrin conformations led to the development of an integrin activation paradigm (Beglova et al., 2002). In this activation model, resting integrin adopts a bent conformation that upon activation

consequently flips into an extended conformation that allows easy access of its ligand-binding site(s) to ligand presented on substratum or on another cell. Following additional refinements of this model, three activation (affinity) states of integrin were proposed (Takagi et al., 2002b). This was verified by functional and structural studies with different integrins (Nishida et al., 2006; Tang et al., 2008b; Xiao et al., 2004).

With the resolution of the integrin structures, the cytoplasmic proteins that interact with the integrin cytoplasmic tails received much attention because of their possible involvement in integrin inside-out signaling. The cytoplasmic protein talin was shown to associate with a highly conserved region in all integrin β cytoplasmic tails, and more importantly it is critical for the activation of many integrins (Calderwood et al., 1999; Tadokoro et al., 2003). The mechanism of talin activation of an integrin involves forced-separation of the integrin α/β cytoplasmic tails as determined by FRET analyses of integrin αLβ2 (Kim et al., 2003). NMR studies of talin-integrin tail interactions provided direct evidence of the importance of talin F3 subdomain in interacting with the membrane proximal NPxY/F sequence of the integrin β cytoplasmic tail. However, the contribution of other regions of the talin HD, for example F0, F1, and F2, are still being investigated, and there is increasing evidence suggesting the importance of these subdomains in talin function (Bouaouina et al., 2008; Ulmer et al., 2003). For example, the F0 and F1 subdomains are essential for the activating property of talin on integrin α5β1, but less so for integrin αIIbβ3 (Bouaouina et al., 2008), suggesting that there may be subtle but important integrin-specific differences in the activating property of talin. In the same vein, the extent of conformational change of a talin-activated integrin requires clarification. In the three activation states model that involves three integrin conformers (i) bent conformer with low ligand-binding affinity, (ii) extended conformer with closed

headpiece having intermediate ligand-binding affinity, and (iii) extended conformer with open headpiece having high ligand-binding affinity, it was previously unknown which activation state, (ii) or (iii), is induced in an integrin activated by talin. In our study, we have shown that talin induces an intermediate affinity αLβ2 (Li et al., 2007). Together with another study from our group investigating αLβ2 conformational transitions based on mutations and conformation-sensitive reporter antibodies (Tang et al., 2008b), we gather that talin induces an extended αLβ2 conformer with a closed headpiece. Our conclusion is in line with the conformation transitions of an integrin when activated and finally ligand-engaged as proposed by others (Hynes, 1992, 2002; Tadokoro et al., 2003). When activated by talin, the integrin converts from a bent conformation to one that is extended with a closed headpiece. This allows effective engagement of the ligand-binding site(s) in the headpiece to ligand. Once ligand is engaged, the headpiece undergoes additional conformational changes culminating in the swing-out of the integrin hybrid domain that ultimately transforms the integrin into an extended open headpiece conformation (Arnaout et al., 2005; Takagi et al., 2003).

In the physiological setting of an integrin-mediated migrating cell, it is conceivable that integrin conformers exist in a state of dynamic equilibrium in which physiological stimuli shift the integrin from one activation state to another, from resting to activated (unliganded) at the migratory front of the cell, activated to de-activated followed by recycling at the rear of the cell (Morin et al., 2008). The extended conformation with an open headpiece induced by ligand-engagement may require stabilization by concomitant cytoskeletal remodeling and tension. In a recent report making use of molecular dynamic (MD) simulations of integrin αIIbβ3 with applied forces in the pN range at different regions of the integrin, it was shown that applied forces at the headpiece mimicking

ligand-engagement and at the C-terminal stalks of the integrin, in particular the β subunit, are required to stabilize an extended and open structure (Gaillard et al., 2009; Provasi et al., 2009). This agrees well in the context of talin activated integrin because the rod region of talin is known to interact with the actin cytoskeleton (Moes et al., 2007). Clearly, the regulation of integrin ligand-binding couples both biochemical reactions and mechanical forces (Puklin-Faucher and Sheetz, 2009). In the classical example of leukocytes in blood capillaries, the shear force exerted on these cells play an important role in regulating the rate of integrin conformational change, that is shifting of the integrin from one conformation to the next, as demonstrated using isolated αLβ2 I domain displayed on surrogate cells subjected to shear force (Astrof et al., 2006). In fact, mechanical force is also important for talin conformational changes to expose its vinculin binding sites in its rod domain (Hytönen and Vogel, 2008).

Apart from talin, the identification of another family of molecules kindlins that interact directly with integrin cytoplasmic tails and have co-activating property adds yet another level of complexity in the regulation of integrin function (Moser et al., 2009b). Unlike talin, kindlins appear to possess minimal integrin-activating capacity in the absence of talin (Harburger et al., 2009; Ma et al., 2008; Montanez et al., 2008). Kindlin3 expression was reported to be restricted to hematopoietic cells and to play crucial roles in β2 integrins mediated-adhesion of leukocytes (Moser et al., 2009a; Ussar et al., 2006). In this study, we showed that the F3 subdomain and PH domain of kindlin3 are both required for its capacity to act as a co-activator, and overexpressed kindlin3 co-localized with endogenous talin or αLβ2 in T cell line SKW 3.0 migrating on ICAM-1. Perhaps most surprising was the observation that overexpressed kindlin3 in SKW 3.0 had an inhibitory effect on cell migration. Removal of the PH domain, F3 subdomain or mutation of the integrin-tail binding site in the F3 subdomain of overexpressed kindlin3 completely

restored the migratory capacity of these cells. In fact, overexpression of kindlin2 was reported to have a suppressive effect on the metastasis of mesenchymal cells (Shi and Wu, 2008). Overexpressed kindlin3 may sequester molecules that are required for effective cell migration. One of these candidate molecules that may be sequestered by the overexpressed kindlin3 is PIP3. PIP3 is produced by phosphorylation of PIP2 by phosphatidylinositol 3-kinases (PI3K), and PIP2 is a substrate of PH domain (Czech, 2000; Harlan et al., 1994; Harlan et al., 1995). Although PIP3 accumulates at the leading edge of *Dictyostelium* and mammalian cells undergoing directional chemotaxis (Kolsch et al., 2008; Van Haastert and Veltman, 2007), *Dictyostelium* amoeboid cells that are PIP3 null as a result of gene ablation of all five type I PI3Ks in these cells had miminal effect on their directional responses toward a chemokine gradient and were able to polarize effectively, rather these cells showed slower chemotaxis speed and random movement (Hoeller and Kay, 2007). It is possible that the sequestering of PIP2 by excess kindlin3 as in this case of an overexpression system diminished PIP3 production that leads to a reduction in migratory speed of SDF-1α stimulated SKW 3.0 cells on ICAM-1. It is therefore interesting in future studies to first establish the PIP2-binding capacity of kindlin3. One possible strategy is to express recombinant PH domain of kindlin3 and examine its PIP2 binding properties. Despite the poor expression of full-length kindlin3 as described in previous chapter, the expression of isolated kindlin3 PH domain is feasible because NMR structural determination of kindlin3 PH domain has been performed (PDB code: 2YS3).

Finally, another interesting direction to pursue is the interaction of kindlin3 with RACK1. As mentioned in previous chapter, RACK1 associates with several signaling proteins that are important for cell adhesion and migration (Chen et al., 2008; Cox et al., 2003; Liliental and Chang, 1998). There are however conflicting reports on whether RACK1

promotes (Kiely et al., 2006) or inhibits cell migration (Buensuceso et al., 2001; Chen et al., 2008; Cox et al., 2003). At this juncture, despite the observed co-localization of RACK1 with kindlin3 in SKW 3.0 cells and the association of RACK1 with kindlin3 as determined by others in the lab, more studies are required to clarify the physiological implications of this interaction.

Publications and conferences

Publication from this study:

Li, Y.-F., Tang, R.-H., Puan, K.-J., Law, S.K.A., and Tan, S.-M. (2007). The cytosolic protein talin induces an intermediate affinity integrin αLβ2. J Biol Chem *282*, 24310-24319.

Publications from other studies:

Tang, X.-Y., Li, Y.-F., and Tan, S.-M. (2008). Intercellular adhesion molecule-3 binding of integrin αLβ2 requires both extension and opening of the integrin headpiece. J Immunol *180*, 4793-4804.

Domadia, P.N., Li, Y.-F., Bhunia, A., Mohanram, H., Tan, S.-M., and Bhattacharjya, S. (2010). Functional and structural characterization of the talin F0F1 domain. Biochem Biophys Res Commun *391*, 159-165.

International conferences attended:

Mechanisms Of Cell Signalling
September 16-21, 2007. Magdalen College, Oxford, United Kingdom

The 9th International Congress on Cell Biology (ICCB)
October 7-10, 2008. COEX, Seoul, Korea (South)

References

Abram, C.L., and Lowell, C.A. (2009a). The ins and outs of leukocyte integrin signaling. Annu Rev Immunol *27*, 339-362.

Abram, C.L., and Lowell, C.A. (2009b). Leukocyte adhesion deficiency syndrome: a controversy solved. Immunol Cell Biol *87*, 440-442.

Acevedo, A., del Pozo, M.A., Arroyo, A.G., Sánchez-Mateos, P., González-Amaro, R., and Sánchez-Madrid, F. (1993). Distribution of ICAM-3-bearing cells in normal human tissues. Expression of a novel counter-receptor for LFA-1 in epidermal Langerhans cells. Am J Pathol *143*, 774-783.

Anderson, D.C., Miller, L.J., Schmalstieg, F.C., Rothlein, R., and Springer, T.A. (1986). Contributions of the Mac-1 glycoprotein family to adherence-dependent granulocyte functions: structure-function assessments employing subunit-specific monoclonal antibodies. J Immunol *137*, 15-27.

Anderson, M.E., and Siahaan, T.J. (2003). Mechanism of binding and internalization of ICAM-1-derived cyclic peptides by LFA-1 on the surface of T cells: A potential method for targeted drug delivery. Pharm Res *20*, 1523-1532.

Andrew, D., Shock, A., Bali, E., Ortlepp, S., Bell, J., and Robinson, M. (1993). KIM185, a monoclonal antibody to CD18 which induces a change in the conformation of CD18 and promotes both LFA-1- and CR3-dependent adhesion. Eur J Immunol *23*, 2217-2222.

Armulik, A., Nilsson, I., von Heijne, G., and Johansson, S. (1999). Determination of the border between the transmembrane and cytoplasmic domains of human integrin subunits. J Biol Chem *274*, 37030-37034.

Arnaout, M.A. (1990). Leukocyte adhesion molecules deficiency: its structural basis, pathophysiology and implications for modulating the inflammatory response. Immunol Rev *114*, 145-180.

Arnaout, M.A., Mahalingam, B., and Xiong, J.P. (2005). Integrin structure, allostery, and bidirectional signaling. Annu Rev Cell Dev Biol *21*, 381-410.

Astrof, N.S., Salas, A., Shimaoka, M., Chen, J., and Springer, T.A. (2006). Importance of force linkage in mechanochemistry of adhesion receptors. Biochemistry *45*, 15020-15028.

Bailly, P., Tontti, E., Hermand, P., Cartron, J.-P., and Gahmberg, C.G. (1995). The red cell LW blood group protein is an intercellular adhesion molecule which binds to CD11/CD18 leukocyte integrins. Eur J Immunol *25*, 3316-3320.

Barclay, A.N., Brown, M.H., Law, S.K.A., McKnight, A.J., Tomlinson, M.G., and van der Merwe, P.A. (1997). The Leukocyte Antigen FactsBook, Second Edition edn (Academic

Press).

Beglova, N., Blacklow, S.C., Takagi, J., and Springer, T.A. (2002). Cysteine-rich module structure reveals a fulcrum for integrin rearrangement upon activation. Nat Struct Mol Biol *9*, 282-287.

Bhunia, A., Tang, X.-Y., Mohanram, H., Tan, S.-M., and Bhattacharjya, S. (2009). NMR solution conformations and interactions of integrin αLβ2 cytoplasmic tails. J Biol Chem *284*, 3873-3884.

Bilsland, C.A., Diamond, M.S., and Springer, T.A. (1994). The leukocyte integrin p150,95 (CD11c/CD18) as a receptor for iC3b. Activation by a heterologous β subunit and localization of a ligand recognition site to the I domain. J Immunol *152*, 4582-4589.

Blackford, J., Reid, H., Pappin, D., Bowers, F., and Wilkinson, J. (1996). A monoclonal antibody, 3/22, to rabbit CD11c which induces homotypic T cell aggregation: evidence that ICAM-1 is a ligand for CD11c/CD18. Eur J Immunol *26*, 525-531.

Bork, P., Doerks, T., Springer, T.A., and Snel, B. (1999). Domains in plexins: links to integrins and transcription factors. Trends Biochem Sci *24*, 261-263.

Bouaouina, M., Lad, Y., and Calderwood, D.A. (2008). The N-terminal domains of talin cooperate with the phosphotyrosine binding-like domain to activate β1 and β3 integrins. J Biol Chem *283*, 6118-6125.

Buensuceso, C.S., Woodside, D., Huff, J.L., Plopper, G.E., and O'Toole, T.E. (2001). The WD protein Rack1 mediates protein kinase C and integrin-dependent cell migration. J Cell Sci *114*, 1691-1698.

Bullard, D., Hu, X., Adams, J., Schoeb, T., and Barnum, S. (2007). p150/95 (CD11c/CD18) expression is required for the development of experimental autoimmune encephalomyelitis. Am J Pathol *170*, 2001-2008.

Butta, N., Arias-Salgado, E.G., Gonzalez-Manchon, C., Ferrer, M., Larrucea, S., Ayuso, M.S., and Parrilla, R. (2003). Disruption of the β3 663-687 disulfide bridge confers constitutive activity to β3 integrins. Blood *102*, 2491-2497.

Calderwood, D.A. (2004). Integrin activation. J Cell Sci *117*, 657-666.

Calderwood, D.A., Huttenlocher, A., Kiosses, W.B., Rose, D.M., Woodside, D.G., Schwartz, M.A., and Ginsberg, M.H. (2001). Increased filamin binding to β-integrin cytoplasmic domains inhibits cell migration. Nat Cell Biol *3*, 1060-1068.

Calderwood, D.A., Zent, R., Grant, R., Rees, D.J.G., Hynes, R.O., and Ginsberg, M.H. (1999). The talin head domain binds to integrin β subunit cytoplasmic tails and regulates integrin activation. J Biol Chem *274*, 28071-28074.

Campbell, J.J., Hedrick, J., Zlotnik, A., Siani, M.A., Thompson, D.A., and Butcher, E.C. (1998). Chemokines and the arrest of lymphocytes rolling under flow conditions. Science *279*, 381-384.

Casasnovas, J.M., Stehle, T., Liu, J.H., Wang, J.H., and Springer, T.A. (1998). A dimeric crystal structure for the N-terminal two domains of intercellular adhesion molecule-1. Proc Natl Acad Sci U S A *95*, 4134-4139.

Chen, J., Salas, A., and Springer, T.A. (2003). Bistable regulation of integrin adhesiveness by a bipolar metal ion cluster. Nat Struct Biol *10*, 995-1001.

Chen, S., Lin, F., Shin, M.E., Wang, F., Shen, L., and Hamm, H.E. (2008). RACK1 regulates directional cell migration by acting on Gβγ at the interface with its effectors PLCβ and PI3Kγ. Mol Biol Cell *19*, 3909-3922.

Cheng, M., Foo, S.-Y., Shi, M.-L., Tang, R.-H., Kong, L.-S., Law, S.K.A., and Tan, S.-M. (2007). Mutation of a conserved Asparagine in the I-like domain promotes constitutively active integrins αLβ2 and αIIbβ3. J Biol Chem *282*, 18225-18232.

Cox, E.A., Bennin, D., Doan, A.T., O'Toole, T., and Huttenlocher, A. (2003). RACK1 regulates integrin-mediated adhesion, protrusion, and chemotactic cell migration via its Src-binding site. Mol Biol Cell *14*, 658-669.

Critchley, D.R. (2000). Focal adhesions-the cytoskeletal connection. Curr Opin Cell Biol *12*, 133-139.

Critchley, D.R., and Gingras, A.R. (2008). Talin at a glance. J Cell Sci *121*, 1345-1347.

Czech, M.P. (2000). PIP2 and PIP3: complex roles at the cell surface. Cell *100*, 603-606.

Czuchra, A., Meyer, H., Legate, K.R., Brakebusch, C., and Fässler, R. (2006). Genetic analysis of β1 integrin "activation motifs" in mice. J Cell Biol *174*, 889-899.

Davignon, D., Martz, E., Reynolds, T., Kurzinger, K., and Springer, T.A. (1981). Lymphocyte function-associated antigen 1 (LFA-1): a surface antigen distinct from Lyt-2,3 that participates in T lymphocyte-mediated killing. Proc Natl Acad Sci U S A *78*, 4535-4539.

de Fougerolles, A., Diamond, M., and Springer, T. (1995). Heterogenous glycosylation of ICAM-3 and lack of interaction with Mac-1 and p150,95. Eur J Immunol *25*, 1008-1012.

de Fougerolles, A.R., and Springer, T.A. (1992). Intercellular adhesion molecule 3, a third adhesion counter-receptor for lymphocyte function-associated molecule 1 on resting lymphocytes. J Exp Med *175*, 185-190.

de Pereda, J.M., Wiche, G., and Liddington, R.C. (1999). Crystal structure of a tandem pair of fibronectin type III domains from the cytoplasmic tail of integrin α6β4. EMBO J

18, 4087-4095.

Dransfield, I., and Hogg, N. (1989). Regulated expression of Mg^{2+} binding epitope on leukocyte integrin α subunits. EMBO J *8*, 3759-3765.

Dunker, A.K., Cortese, M.S., Romero, P., Iakoucheva, L.M., and Uversky, V.N. (2005). Flexible nets. The roles of intrinsic disorder in protein interaction networks. FEBS J *272*, 5129-5148.

Ebnet, K., Suzuki, A., Ohno, S., and Vestweber, D. (2004). Junctional adhesion molecules (JAMs): more molecules with dual functions? J Cell Sci *117*, 19-29.

Ehlers, M.R. (2000). CR3: a general purpose adhesion-recognition receptor essential for innate immunity. Microbes Infect *2*, 289-294.

Emsley, J., King, S.L., Bergelson, J.M., and Liddington, R.C. (1997). Crystal structure of the I domain from integrin α2β1. J Biol Chem *272*, 28512-28517.

Emsley, J., Knight, C.G., Farndale, R.W., Barnes, M.J., and Liddington, R.C. (2000). Structural basis of collagen recognition by integrin α2β1. Cell *101*, 47-56.

Fagerholm, S.C., Hilden, T.J., Nurmi, S.M., and Gahmberg, C.G. (2005). Specific integrin α and β chain phosphorylations regulate LFA-1 activation through affinity-dependent and -independent mechanisms. J Cell Biol *171*, 705-715.

Fernandez-Calotti, P.X., Salamone, G., Gamberale, R., Trevani, A., Vermeulen, M., Geffner, J., and Giordano, M. (2003). Downregulation of mac-1 expression in monocytes by surface-bound IgG. Scand J Immunol *57*, 35-44.

Gahmberg, C.G., Fagerholm, S.C., Nurmi, S.M., Chavakis, T., Marchesan, S., and Grönholm, M. (2009). Regulation of integrin activity and signalling. Biochim Biophys Acta *1790*, 431-444.

Gahmberg, C.G., Tolvanen, M., and Kotovuori, P. (1997). Leukocyte adhesion-structure and function of human leukocyte β2-integrins and their cellular ligands. Eur J Biochem *245*, 215-232.

Gaillard, T., Dejaegere, A., and Stote, R.H. (2009). Dynamics of β3 integrin I-like and hybrid domains: insight from simulations on the mechanism of transition between open and closed forms. Proteins *76*, 977-994.

Geiger, C., Nagel, W., Boehm, T., van Kooyk, Y., Figdor, C.G., Kremmer, E., Hogg, N., Zeitlmann, L., Dierks, H., Weber, K.S., *et al.* (2000). Cytohesin-1 regulates β-2 integrin-mediated adhesion through both ARF-GEF function and interaction with LFA-1. EMBO J *19*, 2525-2536.

Ghayur, T., Hugunin, M., Talanian, R.V., Ratnofsky, S., Quinlan, C., Emoto, Y., Pandey, P.,

Datta, R., Huang, Y., Kharbanda, S., *et al.* (1996). Proteolytic activation of protein kinase C δ by an ICE/CED 3-like protease induces characteristics of apoptosis. J Exp Med *184*, 2399-2404.

Ginsberg, M.H., Partridge, A., and Shattil, S.J. (2005). Integrin regulation. Curr Opin Cell Biol *17*, 509-516.

Goult, B.T., Bate, N., Anthis, N.J., Wegener, K.L., Gingras, A.R., Patel, B., Barsukov, I.L., Campbell, I.D., Roberts, G.C.K., and Critchley, D.R. (2009). The structure of an interdomain complex that regulates talin activity. J Biol Chem *284*, 15097-15106.

Gupta, V., Gylling, A., Alonso, J.L., Sugimori, T., Ianakiev, P., Xiong, J.-P., and Amin Arnaout, M. (2007). The β-tail domain (βTD) regulates physiologic ligand binding to integrin CD11b/CD18. Blood *109*, 3513-3520.

Hajishengallis, G., and Harokopakis, E. (2007). Porphyromonas gingivalis interactions with complement receptor 3 (CR3): innate immunity or immune evasion? Front Biosci *12*, 4547-4557.

Harburger, D.S., Bouaouina, M., and Calderwood, D.A. (2009). Kindlin-1 and -2 directly bind the C-terminal region of β integrin cytoplasmic tails and exert integrin-specific activation effects. J Biol Chem *284*, 11485-11497.

Harlan, J.E., Hajduk, P.J., Yoon, H.S., and Fesik, S.W. (1994). Pleckstrin homology domains bind to phosphatidylinositol-4,5-bisphosphate. Nature *371*, 168-170.

Harlan, J.E., Yoon, H.S., Hajduk, P.J., and Fesik, S.W. (1995). Structural characterization of the interaction between a pleckstrin homology domain and phosphatidylinositol 4,5-bisphosphate. Biochemistry *34*, 9859-9864.

Hayflick, J.S., Kilgannon, P., and Gallatin, W.M. (1998). The intercellular adhesion molecule (ICAM) family of proteins: new members and novel functions. Immunol Res *17*, 313-327.

Hersmann, G.H.W., Kriegsmann, J., Simon, J., Huettich, C., and Brauer, R. (1998). Expression of cell adhesion molecules and cytokines in Murine antigen-induced Arthritis. Cell Adhes Commun *6*, 69-82.

Hildreth, J.E., Gotch, F.M., Hildreth, P.D., and McMichael, A.J. (1983). A human lymphocyte-associated antigen involved in cell-mediated lympholysis. Eur J Immunol *13*, 202-208.

Hoeller, O., and Kay, R.R. (2007). Chemotaxis in the absence of PIP3 gradients. Curr Biol *17*, 813-817.

Hogg, N., and Bates, P.A. (2000). Genetic analysis of integrin function in man: LAD-1 and other syndromes. Matrix Biology *19*, 211-222.

Hubbard, A.K., and Rothlein, R. (2000). Intercellular adhesion molecule-1 (ICAM-1) expression and cell signaling cascades. Free Radic Biol Med *28*, 1379-1386.

Hughes, P.E., Diaz-Gonzalez, F., Leong, L., Wu, C., McDonald, J.A., Shattil, S.J., and Ginsberg, M.H. (1996). Breaking the integrin hinge. A defined structural constraint regulates integrin signaling. J Biol Chem *271*, 6571-6574.

Hughes, P.E., O'Toole, T.E., Ylänne, J., Shattil, S.J., and Ginsberg, M.H. (1995). The conserved membrane-proximal region of an integrin cytoplasmic domain specifies ligand binding affinity. J Biol Chem *270*, 12411-12417.

Humphries, M.J. (2000). Integrin structure. Biochem Soc Trans *28*, 311-339.

Humphries, M.J., Limesand, K.H., Schneider, J.C., Nakayama, K.I., Anderson, S.M., and Reyland, M.E. (2006). Suppression of apoptosis in the protein kinase Cδ null mouse in vivo. J Biol Chem *281*, 9728-9737.

Huth, J.R., Olejniczak, E.T., Mendoza, R., Liang, H., Harris, E.A., Lupher, M.L., Jr., Wilson, A.E., Fesik, S.W., and Staunton, D.E. (2000). NMR and mutagenesis evidence for an I domain allosteric site that regulates lymphocyte function-associated antigen 1 ligand binding. Proc Natl Acad Sci U S A *97*, 5231-5236.

Hynes, R.O. (1976). Cell surface proteins and malignant transformation. Biochim Biophys Acta *458*, 73-107.

Hynes, R.O. (1992). Integrins: versatility, modulation, and signaling in cell adhesion. Cell *69*, 11-25.

Hynes, R.O. (2002). Integrins: bidirectional, allosteric signaling machines. Cell *110*, 673-687.

Hytönen, V.P., and Vogel, V. (2008). How force might activate talin's vinculin binding sites: SMD reveals a structural mechanism. PLoS Comput Biol *4*, e24.

Ingalls, R., and Golenbock, D. (1995). CD11c/CD18, a transmembrane signaling receptor for lipopolysaccharide. J Exp Med *181*, 1473-1479.

Katagiri, K., Maeda, A., Shimonaka, M., and Kinashi, T. (2003). RAPL, a Rap1-binding molecule that mediates Rap1-induced adhesion through spatial regulation of LFA-1. Nat Immunol *4*, 741-748.

Keizer, G., Te Velde, A., Schwarting, R., Figdor, C., and De Vries, J. (1987a). Role of p150,95 in adhesion, migration, chemotaxis and phagocytosis of human monocytes. Eur J Immunol *17*, 1317-1322.

Keizer, G.D., Borst, J., Visser, W., Schwarting, R., de Vries, J.E., and Figdor, C.G. (1987b). Membrane glycoprotein p150,95 of human cytotoxic T cell clone is involved in conjugate

formation with target cells. J Immunol *138*, 3130-3136.

Kiely, P.A., Baillie, G.S., Barrett, R., Buckley, D.A., Adams, D.R., Houslay, M.D., and O'Connor, R. (2009). Phosphorylation of RACK1 on tyrosine 52 by c-Abl is required for IGF-I-mediated regulation of focal adhesion kinase (FAK). J Biol Chem, M109.017640.

Kiely, P.A., O'Gorman, D., Luong, K., Ron, D., and O'Connor, R. (2006). Insulin-like growth factor I controls a mutually exclusive association of RACK1 with protein phosphatase 2A and β1 integrin to promote cell migration. Mol Cell Biol *26*, 4041-4051.

Kiema, T., Lad, Y., Jiang, P., Oxley, C.L., Baldassarre, M., Wegener, K.L., Campbell, I.D., Ylänne, J., and Calderwood, D.A. (2006). The molecular basis of filamin binding to integrins and competition with talin. Mol Cell *21*, 337-347.

Kim, M., Carman, C.V., and Springer, T.A. (2003). Bidirectional transmembrane signaling by cytoplasmic domain separation in integrins. Science *301*, 1720-1725.

Kolsch, V., Charest, P.G., and Firtel, R.A. (2008). The regulation of cell motility and chemotaxis by phospholipid signaling. J Cell Sci *121*, 551-559.

Krawczyk, C., Oliveira-dos-Santos, A., Sasaki, T., Griffiths, E., Ohashi, P.S., Snapper, S., Alt, F., and Penninger, J.M. (2002). Vav1 controls integrin clustering and MHC/peptide-specific cell adhesion to antigen-presenting cells. Immunity *16*, 331-343.

Lad, Y., Jiang, P., Ruskamo, S., Harburger, D.S., Ylänne, J., Campbell, I.D., and Calderwood, D.A. (2008). Structural basis of the migfilin-filamin interaction and competition with integrin β tails. J Biol Chem *283*, 35154-35163.

Larjava, H., Plow, E.F., and Wu, C. (2008). Kindlins: essential regulators of integrin signalling and cell-matrix adhesion. EMBO rep *9*, 1203-1208.

Larson, R.S., and Springer, T.A. (1990). Structure and function of leukocyte integrins. Immunol Rev *114*, 181-217.

Lau, T.-L., Kim, C., Ginsberg, M.H., and Ulmer, T.S. (2009). The structure of the integrin αIIbβ3 transmembrane complex explains integrin transmembrane signalling. EMBO J *28*, 1351-1361.

Lau, T.-L., Partridge, A.W., Ginsberg, M.H., and Ulmer, T.S. (2008). Structure of the integrin β3 transmembrane segment in phospholipid bicelles and detergent micelles. Biochemistry *47*, 4008-4016.

Le Clainche, C., and Carlier, M.-F. (2008). Regulation of actin assembly associated with protrusion and adhesion in cell migration. Physiol Rev *88*, 489–513.

Lee, J.-O., Bankston, L.A., Arnaout, M.A., and Liddington, R. (1995a). Two conformations of the integrin A-domain (I-domain): a pathway for activation? Structure *3*,

1333-1340.

Lee, J.-O., Rieu, P., Arnaout, M.A., and Liddington, R. (1995b). Crystal structure of the A domain from the α subunit of integrin CR3 (CD11 b/CD18). Cell *80*, 631-638.

Legge, G.B., Kriwacki, R.W., Chung, J., Hommel, U., Ramage, P., Case, D.A., Dyson, H.J., and Wright, P.E. (2000). NMR solution structure of the inserted domain of human leukocyte function associated antigen-1. J Mol Biol *295*, 1251-1264.

Leitinger, B., and Hogg, N. (2000). Effects of I domain deletion on the function of the β2 integrin lymphocyte function-associated antigen-1. Mol Biol Cell *11*, 677-690.

Ley, K., Laudanna, C., Cybulsky, M.I., and Nourshargh, S. (2007). Getting to the site of inflammation: the leukocyte adhesion cascade updated. Nat Rev Immunol *7*, 678-689.

Li, C., Wernig, F., Leitges, M., Hu, Y., and Xu, Q. (2003a). Mechanical stress-activated PKCδ regulates smooth muscle cell migration. FASEB J *17*, 2106-2108.

Li, R., Babu, C.R., Lear, J.D., Wand, A.J., Bennett, J.S., and DeGrado, W.F. (2001). Oligomerization of the integrin αIIbβ3: Roles of the transmembrane and cytoplasmic domains. Proc Natl Acad Sci U S A *98*, 12462-12467.

Li, R., Gorelik, R., Nanda, V., Law, P.B., Lear, J.D., DeGrado, W.F., and Bennett, J.S. (2004). Dimerization of the transmembrane domain of integrin αIIb subunit in cell membranes. J Biol Chem *279*, 26666-26673.

Li, R., Mitra, N., Gratkowski, H., Vilaire, G., Litvinov, R., Nagasami, C., Weisel, J.W., Lear, J.D., DeGrado, W.F., and Bennett, J.S. (2003b). Activation of integrin αIIbβ3 by modulation of transmembrane helix associations. Science *300*, 795-798.

Li, Y.-F., Tang, R.-H., Puan, K.-J., Law, S.K.A., and Tan, S.-M. (2007). The cytosolic protein talin induces an intermediate affinity integrin αLβ2. J Biol Chem *282*, 24310-24319.

Liliental, J., and Chang, D.D. (1998). Rack1, a receptor for activated protein kinase C, interacts with integrin β subunit. J Biol Chem *273*, 2379-2383.

Liu, S., Calderwood, D.A., and Ginsberg, M.H. (2000). Integrin cytoplasmic domain-binding proteins. J Cell Sci *113*, 3563-3571.

Loike, J.D., Sodeik, B., Cao, L., Leucona, S., Weitz, J.I., Detmers, P.A., Wright, S.D., and Silverstein, S.C. (1991). CD11c/CD18 on neutrophils recognizes a domain at the N terminus of the Aα chain of fibrinogen. Proc Natl Acad Sci U S A *88*, 1044-1048.

Long, A., Mitchell, S., Kashanin, D., Williams, V., Mello, A.P., Shvets, I., Kelleher, D., and Volkov, Y. (2004). A multidisciplinary approach to the study of T cell migration. Annals of the New York Academy of Sciences *1028*, 313-319.

Lu, C., Shimaoka, M., Ferzly, M., Oxvig, C., Takagi, J., and Springer, T.A. (2001a). An isolated, surface-expressed I domain of the integrin αLβ2 is sufficient for strong adhesive function when locked in the open conformation with a disulfide bond. Proc Natl Acad Sci U S A *98*, 2387-2392.

Lu, C., and Springer, T.A. (1997). The α subunit cytoplasmic domain regulates the assembly and adhesiveness of integrin lymphocyte function-associated antigen-1. J Immunol *159*, 268-278.

Lu, C., Takagi, J., and Springer, T.A. (2001b). Association of the membrane proximal regions of the α and β subunit cytoplasmic domains constrains an integrin in the inactive state. J Biol Chem *276*, 14642-14648.

Luo, B., Carman, C., Takagi, J., and Springer, T. (2005). Disrupting integrin transmembrane domain heterodimerization increases ligand binding affinity, not valency or clustering. Proc Natl Acad Sci U S A *102*, 3679-3684.

Luo, B., Carman, C.V., and springer, T.A. (2007). Structural basis of integrin regulation and signaling. Annu Rev Immunol, 619-647.

Luo, B.H., Springer, T.A., and Takagi, J. (2003). Stabilizing the open conformation of the integrin headpiece with a glycan wedge increases affinity for ligand. Proc Natl Acad Sci U S A *100*, 2403-2408.

Ma, Y.-Q., Qin, J., Wu, C., and Plow, E.F. (2008). Kindlin-2 (Mig-2): a co-activator of β3 integrins. J Cell Biol *181*, 439-446.

Mabon, P.J., Weaver, L.C., and Dekaban, G.A. (2000). Inhibition of monocyte/macrophage migration to a spinal cord injury site by an antibody to the integrin αD: a potential new anti-inflammatory treatment. Exp Neurol *166*, 52-64.

Malhotra, V., Hogg, N., and Sim, R. (1986). Ligand binding by the p150,95 antigen of U937 monocytic cells: properties in common with complement receptor type 3 (CR3). Eur J Immunol *16*, 1117-1123.

Malinin, N.L., Zhang, L., Choi, J., Ciocea, A., Razorenova, O., Ma, Y.-Q., Podrez, E.A., Tosi, M., Lennon, D.P., Caplan, A.I., *et al.* (2009). A point mutation in KINDLIN3 ablates activation of three integrin subfamilies in humans. Nat Med *15*, 313-318.

Manser, E., Huang, H.Y., Loo, T.H., Chen, X.Q., Dong, J.M., Leung, T., and Lim, L. (1997). Expression of constitutively active α-PAK reveals effects of the kinase on actin and focal complexes. Mol Cell Biol *17*, 1129-1143.

Marlin, S.D., and Springer, T.A. (1987). Purified intercellular adhesion molecule-1 (ICAM-1) is a ligand for lymphocyte function-associated antigen 1 (LFA-1). Cell *51*, 813-819.

Mayadas, T.N., and Cullere, X. (2005). Neutrophil β2 integrins: moderators of life or death decisions. Trends Immunol *26*, 388-395.

McCahill, A., Warwicker, J., Bolger, G.B., Houslay, M.D., and Yarwood, S.J. (2002). The RACK1 scaffold protein: a dynamic cog in cell response mechanisms. Mol Pharmacol *62*, 1261-1273.

Micklem, K., and Sim, R. (1985). Isolation of complement-fragment-iC3b-binding proteins by affinity chromatography. The identification of p150,95 as an iC3b-binding protein. Biochem J *231*, 233–236.

Miller, J., Knorr, R., Ferrone, M., Houdei, R., Carron, C.P., and Dustin, M.L. (1995). Intercellular adhesion molecule-1 dimerization and its consequences for adhesion mediated by lymphocyte function associated-1. J Exp Med *182*, 1231-1241.

Mischak, H., Pierce, J.H., Goodnight, J., Kazanietz, M.G., Blumberg, P.M., and Mushinski, J.F. (1993). Phorbol ester-induced myeloid differentiation is mediated by protein kinase C-α and -δ and not by protein kinase C-βII, -ε, -ζ, and -η. J Biol Chem *268*, 20110-20115.

Moes, M., Rodius, S., Coleman, S.J., Monkley, S.J., Goormaghtigh, E., Tremuth, L., Kox, C., van der Holst, P.P.G., Critchley, D.R., and Kieffer, N. (2007). The integrin binding site 2 (IBS2) in the talin rod domain is essential for linking integrin β subunits to the cytoskeleton. J Biol Chem *282*, 17280-17288.

Monkley, S.J., Zhou, X.-H., Kinston, S.J., Giblett, S.M., Hemmings, L., Priddle, H., Brown, J.E., Pritchard, C.A., Critchley, D.R., and Fässler, R. (2000). Disruption of the talin gene arrests mouse development at the gastrulation stage. Dev Dyn *219*, 560-574.

Montanez, E., Ussar, S., Schifferer, M., Bösl, M., Zent, R., Moser, M., and Fässler, R. (2008). Kindlin-2 controls bidirectional signaling of integrins. Genes Dev *22*, 1325-1330.

Morel-Kopp, M.C., Kaplan, C., Proulle, V., Jallu, V., Melchior, C., Peyruchaud, O., Aurousseau, M.H., and Kieffer, N. (1997). A three amino acid deletion in glycoprotein IIIa is responsible for type I Glanzmann's thrombasthenia: importance of residues Ile325Pro326Gly327 for β3 integrin subunit association. Blood *90*, 669-677.

Morin, N.A., Oakes, P.W., Hyun, Y.-M., Lee, D., Chin, Y.E., King, M.R., Springer, T.A., Shimaoka, M., Tang, J.X., Reichner, J.S., *et al.* (2008). Nonmuscle myosin heavy chain IIA mediates integrin LFA-1 de-adhesion during T lymphocyte migration. J Exp Med *205*, 195-205.

Moser, M., Bauer, M., Schmid, S., Ruppert, R., Schmidt, S., Sixt, M., Wang, H.-V., Sperandio, M., and Fässler, R. (2009a). Kindlin-3 is required for β2 integrin-mediated leukocyte adhesion to endothelial cells. Nat Med *15*, 300-305.

Moser, M., Legate, K.R., Zent, R., and Fässler, R. (2009b). The tail of integrins, talin, and

kindlins. Science *324*, 895-899.

Moser, M., Nieswandt, B., Ussar, S., Pozgajova, M., and Fässler, R. (2008). Kindlin-3 is essential for integrin activation and platelet aggregation. Nat Med *14*, 325-330.

Mould, A.P., Barton, S.J., Askari, J.A., Craig, S.E., and Humphries, M.J. (2003a). Role of ADMIDAS cation-binding site in ligand recognition by integrin α5β1. J Biol Chem *278*, 51622-51629.

Mould, A.P., Barton, S.J., Askari, J.A., McEwan, P.A., Buckley, P.A., Craig, S.E., and Humphries, M.J. (2003b). Conformational changes in the integrin βA domain provide a mechanism for signal transduction via hybrid domain movement. J Biol Chem *278*, 17028-17035.

Mould, A.P., Symonds, E.J.H., Buckley, P.A., Grossmann, J.G., McEwan, P.A., Barton, S.J., Askari, J.A., Craig, S.E., Bella, J., and Humphries, M.J. (2003c). Structure of an integrin-ligand complex deduced from solution x-ray scattering and site-directed mutagenesis. J Biol Chem *278*, 39993-39999.

Naik, U.P., and Eckfeld, K. (2003). Junctional adhesion molecule 1 (JAM-1). J Biol Regul Homeost Agents *17*, 341-347.

Nishida, N., Xie, C., Shimaoka, M., Cheng, Y., Walz, T., and Springer, T.A. (2006). Activation of leukocyte β2 integrins by conversion from bent to extended conformations. Immunity *25*, 583-594.

Noti, J.D. (2002). Expression of the myeloid-specific leukocyte integrin gene CD11d during macrophage foam cell differentiation and exposure to lipoproteins. Int J Mol Med *10*, 721-727.

Nurden, A.T. (2007). Interesting variations on how a disease is defined: comparisons of von Willebrand disease and Glanzmann thrombasthenia. J Thromb Haemost *5*, 647-649.

Nurmi, S.M., Autero, M., Raunio, A.K., Gahmberg, C.G., and Fagerholm, S.C. (2007). Phosphorylation of the LFA-1 integrin β2-chain on Thr-758 leads to adhesion, Rac-1/Cdc42 activation, and stimulation of CD69 expression in human T cells. J Biol Chem *282*, 968-975.

O'Toole, T.E., Katagiri, Y., Faull, R.J., Peter, K., Tamura, R., Quaranta, V., Loftus, J.C., Shattil, S.J., and Ginsberg, M.H. (1994). Integrin cytoplasmic domains mediate inside-out signal transduction. J Cell Biol *124*, 1047.

O'Toole, T.E., Mandelman, D., Forsyth, J., Shattil, S.J., Plow, E.F., and Ginsberg, M.H. (1991). Modulation of the affinity of integrin αIIbβ3 (GPIIb-IIIa) by the cytoplasmic domain of αIIb. Science *254*, 845-847.

Ostermann, G., Weber, K., Zernecke, A., Schröder, A., and Weber, C. (2002). JAM-1 is a

ligand of the β2 integrin LFA-1 involved in transendothelial migration of leukocytes. Nat Immunol *3*, 151-158.

Pasvolsky, R., Feigelson, S.W., Kilic, S.S., Simon, A.J., Tal-Lapidot, G., Grabovsky, V., Crittenden, J.R., Amariglio, N., Safran, M., Graybiel, A.M., *et al.* (2007). A LAD-III syndrome is associated with defective expression of the Rap-1 activator CalDAG-GEFI in lymphocytes, neutrophils, and platelets. J Exp Med *204*, 1571-1582.

Pearson, M.A., Reczek, D., Bretscher, A., and Karplus, P.A. (2000). Structure of the ERM protein moesin reveals the FERM domain fold masked by an extended actin binding tail domain. Cell *101*, 259-270.

Perez, O.D., Mitchell, D., Jager, G.C., South, S., Murriel, C., McBride, J., Herzenberg, L.A., Kinoshita, S., and Nolan, G.P. (2003). Leukocyte functional antigen 1 lowers T cell activation thresholds and signaling through cytohesin-1 and Jun-activating binding protein 1. Nat Immunol *4*, 1083-1092.

Peterson, E.J., Woods, M.L., Dmowski, S.A., Derimanov, G., Jordan, M.S., Wu, J.N., Myung, P.S., Liu, Q.-H., Pribila, J.T., Freedman, B.D., *et al.* (2001). Coupling of the TCR to integrin activation by Slap-130/Fyb. Science *293*, 2263-2265.

Peterson, J.A., Visentin, G.P., Newman, P.J., and Aster, R.H. (1998). A recombinant soluble form of the integrin αIIbβ3 (GPIIb-IIIa) assumes an active, ligand-binding conformation and is recognized by GPIIb-IIIa-specific monoclonal, allo-, auto-, and drug-dependent platelet antibodies. Blood *92*, 2053-2063.

Plow, E.F., Haas, T.A., Zhang, L., Loftus, J., and Smith, J.W. (2000). Ligand binding to integrins. J Biol Chem *275*, 21785-21788.

Postigo, A., Corbí, A., Sánchez-Madrid, F., and de Landázuri, M. (1991). Regulated expression and function of CD11c/CD18 integrin on human B lymphocytes. Relation between attachment to fibrinogen and triggering of proliferation through CD11c/CD18. J Exp Med *174*, 1313-1322.

Priddle, H., Hemmings, L., Monkley, S., Woods, A., Patel, B., Sutton, D., Dunn, G.A., Zicha, D., and Critchley, D.R. (1998). Disruption of the talin gene compromises focal adhesion assembly in undifferentiated but not differentiated embryonic stem cells. J Cell Biol *142*, 1121-1133.

Provasi, D., Murcia, M., Coller, B.S., and Filizola, M. (2009). Targeted molecular dynamics reveals overall common conformational changes upon hybrid domain swing-out in beta3 integrins. Proteins *Epub ahead of print*.

Puklin-Faucher, E., and Sheetz, M.P. (2009). The mechanical integrin cycle. J Cell Sci *122*, 179-186.

Rees, D.J.G., Ades, S.E., Singer, S.J., and Hynes, R.O. (1990). Sequence and domain

structure of talin. Nature *347*, 685-689.

Ridley, A.J., Schwartz, M.A., Burridge, K., Firtel, R.A., Ginsberg, M.H., Borisy, G., Parsons, J.T., and Horwitz, A.R. (2003). Cell migration: integrating signals from front to back. Science *302*, 1704-1709.

Rodius, S., Chaloin, O., Moes, M., Schaffner-Reckinger, E., Landrieu, I., Lippens, G., Lin, M., Zhang, J., and Kieffer, N. (2008). The talin rod IBS2 α-helix interacts with the β3 integrin cytoplasmic tail membrane-proximal helix by establishing charge complementary salt bridges. J Biol Chem *283*, 24212-24223.

Rodriguez, M.M., Ron, D., Touhara, K., Chen, C.-H., and Mochly-Rosen, D. (1999). RACK1, a protein kinase C anchoring protein, coordinates the binding of activated protein kinase C and select pleckstrin homology domains in vitro. Biochemistry *38*, 13787-13794.

Ron, D., Luo, J., and Mochly-Rosen, D. (1995). C2 region-derived peptides inhibit translocation and function of β protein kinase C in vivo. J Biol Chem *270*, 24180-24187.

Sánchez-Madrid, F., and Del Pozo, M.A. (1999). Leukocyte polarization in cell migration and immune interactions. EMBO J *18*, 501-511.

Salas, A., Shimaoka, M., Kogan, A.N., Harwood, C., von Andrian, U.H., and Springer, T.A. (2004). Rolling adhesion through an extended conformation of integrin αLβ2 and relation to α I and β I-like domain interaction. Immunity *20*, 393-406.

Savage, B., and Ruggeri, Z.M. (1991). Selective recognition of adhesive sites in surface-bound fibrinogen by glycoprotein IIb-IIIa on nonactivated platelets. J Biol Chem *266*, 11227-11233.

Savage, B., Shattil, S.J., and Ruggeri, Z.M. (1992). Modulation of platelet function through adhesion receptors. A dual role for glycoprotein IIb-IIIa (integrin αIIbβ3) mediated by fibrinogen and glycoprotein Ib-von Willebrand factor. J Biol Chem *267*, 11300-11306.

Shamri, R., Grabovsky, V., Gauguet, J.-M., Feigelson, S., Manevich, E., Kolanus, W., Robinson, M.K., Staunton, D.E., Von Andrian, U.H., and Alon, R. (2005). Lymphocyte arrest requires instantaneous induction of an extended LFA-1 conformation mediated by endothelium-bound chemokines. Nat Immunol *6*, 497-506.

Shi, M., Foo, S.Y., Tan, S.-M., Mitchell, E.P., Law, S.K.A., and Lescar, J. (2007a). A structural hypothesis for the transition between bent and extended conformations of the Leukocyte β2 Integrins. J Biol Chem *282*, 30198-30206.

Shi, M., Sundramurthy, K., Liu, B., Tan, S.-M., Law, S.K.A., and Lescar, J. (2005). The crystal structure of the plexin-semaphorin-integrin domain/hybrid domain/I-EGF1 segment from the human integrin β2 subunit at 1.8-A resolution. J Biol Chem *280*,

30586-30593.

Shi, X., Ma, Y.-Q., Tu, Y., Chen, K., Wu, S., Fukuda, K., Qin, J., Plow, E.F., and Wu, C. (2007b). The MIG-2/integrin interaction strengthens cell-matrix adhesion and modulates cell motility. J Biol Chem *282*, 20455-20466.

Shi, X., and Wu, C. (2008). A suppressive role of Mitogen Inducible Gene-2 in Mesenchymal cancer cell invasion. Mol Cancer Res *6*, 715-724.

Shimaoka, M., Lu, C., Palframan, R.T., von Andrian, U.H., McCormack, A., Takagi, J., and Springer, T.A. (2001). Reversibly locking a protein fold in an active conformation with a disulfide bond: integrin αL I domains with high affinity and antagonist activity in vivo. Proc Natl Acad Sci U S A *98*, 6009-6014.

Shimaoka, M., Takagi, J., and Springer, T.A. (2002). Conformational regulation of integrin structure and function. Annu Rev Biophys Biomol Struct *31*, 485-516.

Shimaoka, M., Xiao, T., Liu, J.-H., Yang, Y., Dong, Y., Jun, C.-D., McCormack, A., Zhang, R., Joachimiak, A., Takagi, J., *et al.* (2003). Structures of the αL I domain and its complex with ICAM-1 reveal a shape-shifting pathway for integrin regulation. Cell *112*, 99-111.

Siegelman, M. (2001). More than the sum of the parts: cooperation between leukocyte adhesion receptors during extravasation. J Clin Invest *107*, 159-160.

Simon, D.I., Ezratty, A.M., Francis, S.A., Rennke, H., and Loscalzo, J. (1993). Fibrin(ogen) is internalized and degraded by activated human monocytoid cells via Mac-1 (CD11b/CD18): a nonplasmin fibrinolytic pathway. Blood *82*, 2414-2422.

Simonson, W.T.N., Franco, S.J., and Huttenlocher, A. (2006). Talin1 regulates TCR-mediated LFA-1 function. J Immunol *177*, 7707-7714.

Sligh, J.E., Jr., , Ballantyne, C.M., Rich, S.S., Hawkins, H.K., Smith, C.W., Bradley, A., and Beaudet, A.L. (1993). Inflammatory and immune responses are impaired in mice deficient in intercellular adhesion molecule 1. Proc Natl Acad Sci U S A *90*, 8529-8533.

Smith, A., Carrasco, Y.R., Stanley, P., Kieffer, N., Batista, F.D., and Hogg, N. (2005). A talin-dependent LFA-1 focal zone is formed by rapidly migrating T lymphocytes. J Cell Biol *170*, 141-151.

Springer, T.A. (1994). Traffic signals for lymphocyte recirculation and leukocyte emigration: The multistep paradigm. Cell *76*, 301-314.

Springer, T.A. (1997). Folding of the N-terminal, ligand-binding region of integrin α-subunits into a β-propeller domain. Proc Natl Acad Sci U S A *94*, 65-72.

Springer, T.A., Jing, H., and Takagi, J. (2000). A novel Ca^{2+} binding β hairpin loop better

resembles integrin sequence motifs than the EF hand. Cell *102*, 275-277.

Springer, T.A., and Wang, J.-H. (2004). The three-dimensional structure of integrins and their ligands, and conformational regulation of cell adhesion. Adv Protein Chem *68*, 29-63.

Stacker, S.A., and Springer, T.A. (1991). Leukocyte integrin P150,95 (CD11c/CD18) functions as an adhesion molecule binding to a counter-receptor on stimulated endothelium. J Immunol *146*, 648-655.

Staunton, D.E., Dustin, M.L., and Springer, T.A. (1989). Functional cloning of ICAM-2, a cell adhesion ligand for LFA-1 homologous to ICAM-1. Nature *339*, 61-64.

Stebbins, E.G., and Mochly-Rosen, D. (2001). Binding specificity for RACK1 resides in the V5 region of βII protein kinase C. J Biol Chem *276*, 29644-29650.

Stossel, T.P., Condeelis, J., Cooley, L., Hartwig, J.H., Noegel, A., Schleicher, M., and Shapiro, S.S. (2001). Filamins as integrators of cell mechanics and signalling. Nat Rev Mol Cell Biol *2*, 138-145.

Stossel, T.P., and Hartwig, J.H. (2003). Filling gaps in signaling to actin cytoskeletal remodeling. Dev Cell *4*, 444-445.

Streuli, C.H. (2009). Integrins and cell-fate determination. J Cell Sci *122*, 171-177.

Tadokoro, S., Shattil, S.J., Eto, K., Tai, V., Liddington, R.C., de Pereda, J.M., Ginsberg, M.H., and Calderwood, D.A. (2003). Talin binding to integrin β tails: a final common step in integrin activation. Science *302*, 103-106.

Takagi, J., Beglova, N., Yalamanchili, P., Blacklow, S.C., and Springer, T.A. (2001a). Definition of EGF-like, closely interacting modules that bear activation epitopes in integrin β subunits. Proc Natl Acad Sci U S A *98*, 11175-11180.

Takagi, J., DeBottis, D.P., Erickson, H.P., and Springer, T.A. (2002a). The role of the specificity-determining loop of the integrin β subunit I-like domain in autonomous expression, association with the α subunit, and ligand binding. Biochemistry *41*, 4339-4347.

Takagi, J., Erickson, H.P., and Springer, T.A. (2001b). C-terminal opening mimics 'inside-out' activation of integrin α5β1. Nat Struct Biol *8*, 412 - 416.

Takagi, J., Petre, B.M., Walz, T., and Springer, T.A. (2002b). Global conformational rearrangements in integrin extracellular domains in outside-in and inside-out signaling. Cell *110*, 599-611.

Takagi, J., and Springer, T.A. (2002). Integrin activation and structural rearrangement. Immunol Rev *186*, 141-163.

Takagi, J., Strokovich, K., Springer, T.A., and Walz, T. (2003). Structure of integrin α5β1 in complex with fibronectin. EMBO J *22*, 4607-4615.

Takala, H., Nurminen, E., Nurmi, S.M., Aatonen, M., Strandin, T., Takatalo, M., Kiema, T., Gahmberg, C.G., Ylänne, J., and Fagerholm, S.C. (2008). β2 integrin phosphorylation on Thr758 acts as a molecular switch to regulate 14-3-3 and filamin binding. Blood *112*, 1853-1862.

Tan, S.-M., Hyland, R.H., Al-Shamkhani, A., Douglass, W.A., Shaw, J.M., and Law, S.K.A. (2000). Effect of integrin β2 subunit truncations on LFA-1 (CD11a/CD18) and Mac-1 (CD11b/CD18) assembly, surface expression, and function. J Immunol *165*, 2574-2581.

Tan, S.-M., Walters, S.E., Mathew, E.C., Robinson, M.K., Drbal, K., Shaw, J.M., and Law, S.K.A. (2001). Defining the repeating elements in the cysteine-rich region (CRR) of the CD18 integrin β2 subunit. FEBS Lett *505*, 27-30.

Tang, M.-L., Kong, L.-S., Law, S.K.A., and Tan, S.-M. (2006). Down-regulation of integrin αMβ2 ligand-binding function by the urokinase-type plasminogen activator receptor. Biochem Biophys Res Commun *348*, 1184-1193.

Tang, M.-L., Vararattanavech, A., and Tan, S.-M. (2008a). Urokinase-type plasminogen activator receptor induces conformational changes in the integrin αMβ2 headpiece and reorientation of its transmembrane domains. J Biol Chem *283*, 25392-25403.

Tang, R.-H., Tng, E., Law, S.K.A., and Tan, S.-M. (2005). Epitope mapping of monoclonal antibody to integrin αLβ2 hybrid domain suggests different requirements of affinity states for Intercellular Adhesion Molecules (ICAM)-1 and ICAM-3 binding. J Biol Chem *280*, 29208-29216.

Tang, X.-Y., Li, Y.-F., and Tan, S.-M. (2008b). Intercellular adhesion molecule-3 binding of integrin αLβ2 requires both extension and opening of the integrin headpiece. J Immunol *180*, 4793-4804.

te Velde, A., Keizer, G., and Figdor, C. (1987). Differential function of LFA-1 family molecules (CD11 and CD18) in adhesion of human monocytes to melanoma and endothelial cells. Immunology *61*, 261-267.

Tian, L., Yoshihara, Y., Mizuno, T., Mori, K., and Gahmberg, C.G. (1997). The neuronal glycoprotein telencephalin is a cellular ligand for the CD11a/CD18 leukocyte integrin. J Immunol *158*, 928-936.

Tng, E., Tan, S.-M., Ranganathan, S., Cheng, M., and Law, S.K.A. (2004). The Integrin αLβ2 hybrid domain serves as a link for the propagation of activation signal from its stalk regions to the I-like domain. J Biol Chem *279*, 54334-54339.

Tu, Y., Wu, S., Shi, X., Chen, K., and Wu, C. (2003). Migfilin and Mig-2 link focal

adhesions to Filamin and the actin cytoskeleton and function in cell shape modulation. Cell *113*, 37-47.

Tzivion, G., and Avruch, J. (2002). 14-3-3 proteins: active cofactors in cellular regulation by serine/threonine phosphorylation. J Biol Chem *277*, 3061-3064.

Ulmer, T.S., Calderwood, D.A., Ginsberg, M.H., and Campbell, I.D. (2003). Domain-specific interactions of talin with the membrane-proximal region of the integrin β3 subunit. Biochemistry *42*, 8307-8312.

Ussar, S., Wang, H.-V., Linder, S., Fässler, R., and Moser, M. (2006). The Kindlins: subcellular localization and expression during murine development. Exp Cell Res *312*, 3142-3151.

Van der Vieren, M., Crowe, D.T., Hoekstra, D., Vazeux, R., Hoffman, P.A., Grayson, M.H., Bochner, B.S., Gallatin, W.M., and Staunton, D.E. (1999). The leukocyte integrin αDβ2 binds VCAM-1: evidence for a binding interface between I domain and VCAM-1. J Immunol *163*, 1984-1990.

Van der Vieren, M., Le Trong, H., Wood, C.L., Moore, P.F., St John, T., Staunton, D.E., and Gallatin, W.M. (1995). A novel leukointegrin, αDβ2, binds preferentially to ICAM-3. Immunity *3*, 683-690.

Van Haastert, P.J.M., and Veltman, D.M. (2007). Chemotaxis: navigating by multiple signaling pathways. Sci STKE *2007*, pe40.

van Kooyk, Y., and Figdor, C.G. (2000). Avidity regulation of integrins: the driving force in leukocyte adhesion. Curr Opin Cell Bio *12*, 542-547.

Vararattanavech, A., Lin, X., Torres, J., and Tan, S.-M. (2009). Disruption of the integrin αLβ2 transmembrane domain interface by β2 Thr-686 mutation activates αLβ2 and promotes micro-clustering of the αL subunits. J Biol Chem *284*, 3239-3249.

Vicente-Manzanares, M., Choi, C.K., and Horwitz, A.R. (2009). Integrins in cell migration-the actin connection. J Cell Sci *122*, 199-206.

Vidal, F., Baudoin, C., Miquel, C., Galliano, M.F., Christiano, A.M., Uitto, J., Ortonne, J.P., and Meneguzzi, G. (1995). Cloning of the laminin α3 chain gene (LAMA3) and identification of a homozygous deletion in a patient with Herlitz junctional epidermolysis bullosa. Genomics *30*, 273-280.

Vinogradova, O., Vaynberg, J., Kong, X., Haas, T.A., Plow, E.F., and Qin, J. (2004). Membrane-mediated structural transitions at the cytoplasmic face during integrin activation. Proc Natl Acad Sci U S A *101*, 4094-4099.

Vinogradova, O., Velyvis, A., Velyviene, A., Hu, B., Haas, T.A., Plow, E.F., and Qin, J. (2002). A structural mechanism of integrin αIIbβ3 "inside-out" activation as regulated by

its cytoplasmic face. Cell *110*, 587-597.

Volkov, Y., Long, A., McGrath, S., Eidhin, D.N., and Kelleher, D. (2001). Crucial importance of PKC-β(I) in LFA-1-mediated locomotion of activated T cells. Nat Immunol *2*, 508-514.

Watanabe, T., Ono, Y., Taniyama, Y., Hazama, K., Igarashi, K., Ogita, K., Kikkawa, U., and Nishizuka, Y. (1992). Cell division arrest induced by phorbol ester in CHO cells overexpressing protein kinase Cδ subspecies. Proc Natl Acad Sci U S A *89*, 10159-10163.

Wegener, K.L., and Campbell, I.D. (2008). Transmembrane and cytoplasmic domains in integrin activation and protein-protein interactions. Mol Membr Biol *25*, 376-387.

Wegener, K.L., Partridge, A.W., Han, J., Pickford, A.R., Liddington, R.C., Ginsberg, M.H., and Campbell, I.D. (2007). Structural basis of integrin activation by talin. Cell *128*, 171-182.

Williams, M.J., Hughes, P.E., O'Toole, T.E., and Ginsberg, M.H. (1994). The inner world of cell adhesion: integrin cytoplasmic domains. Trends in Cell Biology *4*, 109-112.

Xiao, J.H., Davidson, I., Matthes, H., Garnier, J.-M., and Chambon, P. (1991). Cloning, expression, and transcriptional properties of the human enhancer factor TEF-1. Cell *65*, 551-568.

Xiao, T., Takagi, J., Coller, B.S., Wang, J.H., and Springer, T.A. (2004). Structural basis for allostery in integrins and binding to fibrinogen-mimetic therapeutics. Nature *432*, 59-67.

Xie, C., Shimaoka, M., Xiao, T., Schwab, P., Klickstein, L.B., and Springer, T.A. (2004). The integrin α-subunit leg extends at a Ca^{2+}-dependent epitope in the thigh/genu interface upon activation. Proc Natl Acad Sci U S A *101*, 15422–15427.

Xiong, J.-P., Stehle, T., Diefenbach, B., Zhang, R., Dunker, R., Scott, D.L., Joachimiak, A., Goodman, S.L., and Arnaout, M.A. (2001). Crystal structure of the extracellular segment of integrin αVβ3. Science *294*, 339-345.

Xiong, J.P., Stehle, T., Goodman, S.L., and Arnaout, M.A. (2004). A novel adaptation of the integrin PSI domain revealed from its crystal structure. J Biol Chem *279*, 40252-40254.

Xiong, J.P., Stehle, T., Zhang, R., Joachimiak, A., Frech, M., Goodman, S.L., and Arnaout, M.A. (2002). Crystal structure of the extracellular segment of integrin αVβ3 in complex with an Arg-Gly-Asp ligand. Science *296*, 151-155.

Yalamanchili, P., Lu, C., Oxvig, C., and Springer, T.A. (2000). Folding and function of I domain-deleted Mac-1 and lymphocyte function-associated antigen-1. J Biol Chem *275*, 21877-21882.

Yan, B., Calderwood, D.A., Yaspan, B., and Ginsberg, M.H. (2001). Calpain cleavage promotes talin binding to the β3 integrin cytoplasmic domain. J Biol Chem *276*, 28164-28170.

Zhu, J., Boylan, B., Luo, B.-H., Newman, P.J., and Springer, T.A. (2007). Tests of the extension and deadbolt models of integrin activation. J Biol Chem *282*, 11914-11920.

Zhu, J., Luo, B.-H., Barth, P., Schonbrun, J., Baker, D., and Springer, T.A. (2009). The structure of a receptor with two associating transmembrane domains on the cell surface: integrin αIIbβ3. Mol Cell *34*, 234-249.

Zhu, J., Luo, B.-H., Xiao, T., Zhang, C., Nishida, N., and Springer, T.A. (2008). Structure of a complete integrin ectodomain in a physiologic resting state and activation and deactivation by applied forces. Mol Cell *32*, 849-861.